STATISTICAL TECHNIQUES FOR DESIGNING
A DECOUPLED CONTROLLER TO BE
ROBUST TO MODEL AND SENSOR NOISE

THESIS

Jeb Ewell Brewer
Captain, USAF

AFIT/GA/ENY/90M-1

DTIC
ELECTE
APR 16 1990
S
B
D

DEPARTMENT OF THE AIR FORCE
AIR UNIVERSITY
AIR FORCE INSTITUTE OF TECHNOLOGY

Wright-Patterson Air Force Base, Ohio

90 04 13 194

STATISTICAL TECHNIQUES FOR DESIGNING
A DECOUPLED CONTROLLER TO BE
ROBUST TO MODEL AND SENSOR NOISE

THESIS
Jeb Ewell Brewer
Captain, USAF

AFIT/GA/ENY/90M-1

**DTIC
ELECTE
APR 16 1990
S
B
D**

Approved for public release; distribution unlimited

STATISTICAL TECHNIQUES FOR DESIGNING A DECOUPLED

CONTROLLER TO BE ROBUST TO MODEL AND SENSOR NOISE

THESIS

Presented to the Faculty of the School of Engineering

of the Air Force Institute of Technology

Air University

In Partial Fulfillment of the

Requirements for the Degree of

Master of Science in Astronautical Engineering

Jeb Ewell Brewer, B.S.

Captain, USAF

March 1990

Accession For

NTIS GRA&I	☑
DTIC TAB	☐
Unannounced	☐
Justification	

By

Distribution/

Availability Codes

Dist	Avail and/or Special
A-1	

QUALITY INSPECTED 1

Preface

The engineering design process involves a mixture of theortical facts and experience. This experience allows many design parameters to be set at acceptable levels without detailed exploration. This experience factor is necessary since any design problem involves almost unlimited possible configurations. This investigation focused on developing anaylitical, statistical design tools to help specify design parameters for a robust decoupled controller, an area with alimited pool of engineering experience. While significant progress was made in applying these statistical tools some judgements were still necessary on such items as ranges of parameters, and scope of investigaiton. I myself don't have a large pool of experience to draw upon. This factor should be kept in mind. While this inexperience may have reduced my effectiveness in judgemental decisions, my fresh look should be of benefit especially in developing unbasised techniques.

I would like thank my family, friends and church for their support and encouragement. I would like to thank my advisor Major David G. Robinson, Ph. and my committe members Robert A. Calico, Jr, PhD, and Major Kenneth W. Bauer, PhD for imbuing me with knowledge and assisting me in this effort.

Jeb Ewell Brewer

ii

Table of Contents

iii

List of Figures

List of Tables

Notation

Symbol	Description
A	state-space plant matrix
Ac	cross-section area of element
Ae	state-space closed-loop plant matrix (error states)
B	state-space input matrix
Be	state-space input matrix with error states
B_i^*	decoupled state-space input matrix
C	state-space output matrix
Ce	state-space output matrix with error states
Cp	position sensors, submatrix of C
Cv	velocity sensors, submatrix of C
C_i^*	decoupled state-space output matrix
D	global coordinate input matrix
$\underline{e}$	state-space error states
E	damping matrix
Ey	Young's Modulus
$\underline{f}$	local coordinate force vector
F_p	F statistic for variable p
F_ℓ	F statistic for lack of fit
h	truss element length
$\underline{i}$	local coordinate frame
I	identity matrix
K	stiffness matrix
Kc	feedback control gains
Kf	estimator control gains

Symbol	Description
L	global to local transformation matrix
LOS	line of sight
m	mass
m_p	number of design points in experiment matrix Z
M	mass matrix
MS_e	mean sum of squares for pure error
MS_ℓ	mean sum of squares for lack of fit
MS_p	mean sum of squares for variable p
N	number of subcontrollers
n_a	number of actuators
n_i	number of modes in ith subcontroller
n_n	number of noise settings
n_p	total number of data points
n_s	number of sensors
p	number of parameters in regression model
P	Riccati solution
Q_o	state weighting matrix
R_i	direction cosine matrices
R_o	control weighting matrix
$\underline{r}$	local coordinate displacement vector
r_p	number of replications at one design point
$\underline{s}$	global coordinate frame
$S(\theta)$	sum of squares function
T_i	input transform to orthogonal subspace
t_r	response time
$\underline{u}$	control input vector

Symbol	Description
U	modal transformation matrix
$\underline{w}_i$	decoupled output vector
$\underline{x}$	state-space vector
$\hat{\underline{x}}$	estimated state-space vector
y	data vector in regression equation
$\underline{y}$	state-space output vector
$\hat{\underline{y}}$	estimated state-space output vector
Z	experiment design matrix
$\underline{z}$	augmentation state vector (error states)
ϵ	experimental error
ϕ	rotation angle about i_3 axis
γ	rotation angle about i_2 axis
Γ_i	output transform to orthogonal subspace
$\underline{\eta}$	modal coordinate frame
λ	eigenvalue
θ	parameter vector in regression equation
φ	rotation angle about i_1 axis
ω	natural frequency
ξ	set of uncoded input variables in regression eqn
ξ_c	set of coded input variables in regression eqn
$\underline{\vartheta}$	decoupled control vector
ζ	modal damping value

Abstract

This investigation developed and tested statistical design methods for configuring a robust decoupled controller on a lightly damped structure. The test model used was a lumped mass finite element representation of the Charles Stark Draper Laboratory Model I (CSDL-I). The decoupled control methods consisted of a system of three individual subcontrollers designed on the basis of a subset of plant dynamics with control authority enacted through the total system of structural actuators. Transforms were applied to the subcontrollers to insure that dynamic coupling, called observation spillover and control spillover, didn't destabilize the global system. The decoupled controller system was designed based on only the first eight of the twelve natural frequencies (modes) for the CSDL-I. The remaining four high frequency modes were modeled as residuals.

This investigation used signal-to-noise ratios, orthogonal numerical experiments, and linear regression to efficiently probe the design space and to produce a robust control system. The measure of system performance was the structural alignment of a particular node referred to as line-of-sight (LOS). This LOS requirement simulated space vehicle requirements associated with aligning antennas, LASER beams, solar arrays, etc. The first major design parameters were the elements in diagonal state weighting matrices.

These state weighting matrices were used in Linear Quadratic Regulator and Linear Quadratic Estimator Theory to compute control gains for the subcontrollers. The second major design parameters were the groupings of modes within the individual subcontrollers. A heuristic was developed to select these groupings so that the total system was robust to certain noises. The noise variables investigated included error readings in position sensors, and the error associated with only designing the system based on eight of the possible twelve modes.

It was concluded that the techniques were efficient in configuring a decoupled controller to be robust to sensor noise and modal truncation while still maintaining adequate LOS performance. The techniques reduced the CPU time required from a possible 76,354 years for a global search to only 16.5 hours. It was also found that the robust controller used a significant amount of actuator authority and it was recommended that further work be done to expand the statistical design techniques to include actuator authority as an output metric.

STATISTICAL TECHNIQUES FOR DESIGNING A DECOUPLED
CONTROLLER TO BE ROBUST TO MODEL AND SENSOR NOISE

I. Introduction

In the future exploration of space, larger more complex structures will be placed in orbit. Whether these structures will be manned space stations or unmanned satellites they most probably will be extremely light-weight, flexible structures requiring accurate structural alignment. High precision structural alignment requirements for LASER beams, solar arrays, antennas, etc will necessitate active structural control of the orbiting vehicles. Light-weight flexible structures possess many closely spaced low frequency vibrational modes that make active feedback control computationally burdensome. In an effort to actively control such structures while minimizing on-line computational loads two design approaches have been used; simplifying the dynamic model representation, and using decentralized control methods. Mercadal (8:1-20) provides a good summary of the many simplification and decentralized control methods currently being explored. One particular type of decentralized control of interest in this investigation is the decoupled control as presented by Calico (1). This type of control is a system of individual subcontrollers designed on the basis of a subset of system dynamics with control

authority enacted through the total system of structural actuators. Transforms are applied to the subcontrollers to insure the dynamic coupling called observation spillover and control spillover is not destabilizing to the global system.

In space a structure is required to perform its mission for long durations of time with no maintenance. Even if future orbital transportation becomes more available, the costs associated with periodic maintenance of active control systems will dictate the need for highly reliable control systems. Recently, work has been directed towards designing the control system to be fundamentally more reliable based upon its configuration. The design of space power systems has traditionally used redundant components in parallel as a means to increase reliability through system configuration. A control system could in a similar manner use redundant actuators, sensors, etc to build a more reliable system, but it could also use more subtle methods. Carignan (4:12) demonstrates that a control system's total reliability will change based upon the number and the location of sensors and actuators. While Carignan's global searching methods were generally applied to centralized controllers it leads to another type of reliability issue associated with decoupled controllers. An individual subcontroller observes a structure and enforces control on the structure differently for different modal arrangements. It is possible to smartly arrange the decoupled controller so that it is more robust to certain types of environmental noises, specifically sensor

1-2

errors. The basic errors in sensor measurements will increase over time as the equipment degrades due to the harsh space environment. A decoupled controller with a basic configuration, robust to sensor noise will enact adequate control over the structure for a longer period of time as the sensors degrade and input incorrect information. This is a subtle way of increasing the overall reliability of the system.

The techniques used to design decoupled controllers can't be classified as rigid or even as well defined, but there exists some basic procedures for selecting design parameters. One of the major design parameters of a decoupled controller is the arrangement of modes between individual subcontrollers. Sumner (11:sec 8-2) investigated selecting the arrangement using modal cost analysis techniques, modal internal balancing techniques, and ascending order ranking. He concluded that the ascending order ranking provided the simplest, yet best performing system. He selected the performance criteria as time to dampen the structure to a disturbance and didn't consider sensor noise robustness. The major thrust of this investigation was to try and develop design techniques to select parameters of a decoupled controller so that the system is robust to sensor noise and delivers adequate performance. The main design parameters investigated were subcontroller modal arrangement and controller gain.

This report first describes the structural model that

was used to demonstrate the design techniques. Next, the decoupled control theory is developed. A chapter is then devoted to explaining the basic statistical tools used. The Investigation Chapter then demonstates the actual design techniques used by incorporating the theory developed in the previous three chapters. A Results Chapter then evaluates the new controller design against a traditional controller design. The final chapter summarizes the investigation and recommends areas of further study.

II. <u>System Model</u>

All new structural control design techniques developed and refined in this thesis were applied to a single model that simply, but adequately, represents large space structures. The Charles Stark Draper Laboratory Inc. of Cambridge Massachusetts test model one (CSDL-I) was selected as the test system model because of its simplicity, lightly damped 3-dimensional characteristics, and its general familiarity. The CSDL-II model is a different, more complicated structure, than the CSDL-I consisting of 59 nodes, numerous truss elements, mirrors and solar panels. The CSDL-II is often used in current control studies, but was not chosen here because of its complexity. The smaller CSDL-I allowed verification of the fractional experiment techniques through full factorial experiments. Obviously the objective of developing adequate fractional design techniques becomes paramount if any of this thesis is to be applied to actual structures with large number of vibrational modes like the CSDL-II.

The following sections will first describe the CSDL-I structure, then develop the necessary equations of motion. The CSDL-I is modeled using finite element techniques and then transformed into modal coordinates. The modal coordinate representation is then transformed to a state-space form suitable for control law implementation.

Description of CSDL-I

The CSDL-I is a lumped mass tetrahedral truss shown in Figure 2-1. The four one unit masses lumped at each vertex of the tetrahedral were modeled as having three translational degrees of freedom. To enforce only translational motion each truss member was modeled as a pin connected member capable of carrying only axial loading. The truss members were considered as massless springs (the nodes containing all of the mass). The nodes and truss members are labeled in Figure 2-1.
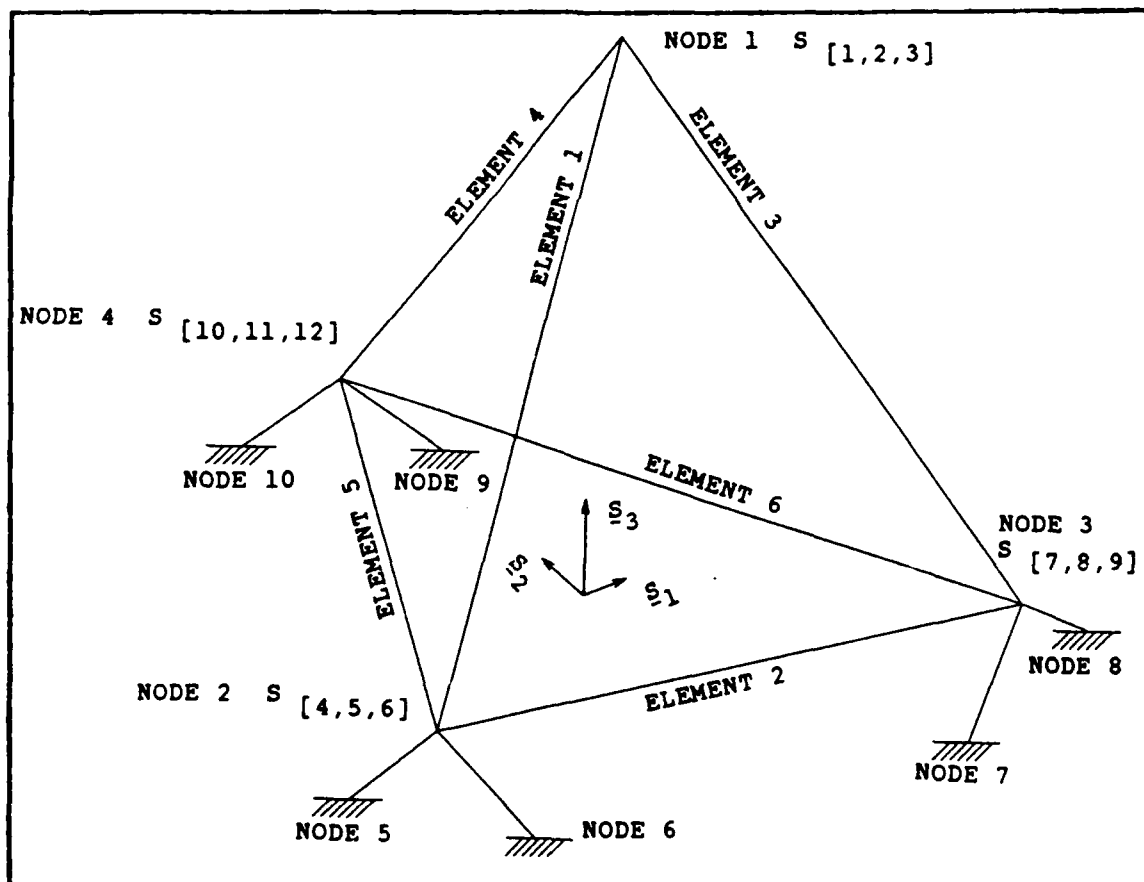
Figure 2-1 CSDL-I

The coordinates of each node are tabulated in global coordinate frame $\underline{s}$ in Table 2-1.

Table 2-1
CSDL-I Node Coordinates

Node	$\underline{s}_1$	$\underline{s}_2$	$\underline{s}_3$
1	0.0	0.0	10.165
2	-5.0	-2.887	2.0
3	5.0	-2.887	2.0
4	0.0	5.774	2.0
5	-6.0	-1.155	0.0
6	-4.0	-4.619	0.0
7	4.0	-4.619	0.0
8	6.0	-1.155	0.0
9	-2.0	5.774	0.0
10	2.0	5.774	0.0

The three lower mass nodes 2,3,4 are supported by two truss legs each, which are then, in turn, anchored. The nodes 5 through 10 were modeled as perfectly fixed. The cross-sectional area's (Ac), length (h) and the ratio Ey(Ac)/h for each element are listed in Table 2-2. Ey is defined as Young's Modulus and was assumed to be unity throughout the investigation to simplify computations.

Table 2-2
CSDL-I Element Properties

Element	Node 1	Node 2	Cross-Section Ac	Length h	(Ey·Ac)/h
1	1	2	1000	10.00	100.00
2	2	3	1000	10.00	100.00
3	1	3	100	10.00	10.00
4	1	4	100	10.00	10.00
5	2	4	1000	10.00	100.00
6	3	4	1000	10.00	100.00
7	2	5	100	2.83	35.36
8	2	6	100	2.83	35.36
9	3	7	100	2.83	35.36
10	3	8	100	2.83	35.36
11	4	9	100	2.83	35.36
12	4	10	100	2.83	35.36

The system was observed by six position sensors mounted on the six support legs 7 through 12. The sensors measure axial displacement along their respective leg axis in the local coordinate frame $\underline{i}$. The system was controlled by six actuators collocated with the six position sensors. The actuators also exerted their force along the respective leg axes. There was no requirement to locate the sensors and actuators in such a configuration, however, the collocated arrangement had been used in previous studies and allows easier verification of computer programs. It would be of benefit to examine the effects of differing configurations since this would have a dramatic impact on performance; this was not investigated in this project due to time constraints. There is a specific requirement as to the number of sensors and actuators required depending on the particular controller arrangement selected as discussed in the next chapter.

The objective of the control system was to maintain a "line of sight" or LOS. The LOS criteria is defined as the deviation of node 1 from the undisturbed position in the global plane s_1, s_2. This objective simulates requirements necessary for aligning solar panels, antennas, LASER beams, or many other uses associated with orbiting vehicle operations. A number of metrics were investigated as applicable to represent the LOS requirement are discussed in later chapters.

The following sections develop the equations of motion necessary to model the CSDL-I and to enact active feedback

control. The different coordinate/vector spaces should be noted carefully in the development. The development starts in a local coordinate system $\underline{i}$ then proceeds to a global coordinate system $\underline{s}$, then a modal vector space $\underline{\eta}$, and finally orthogonal spaces for each subcontroller's feedback.

Development of the CSDL-I Model Equations

Finite Element Model. The basic finite element vibrational model was constructed using the assumptions in the previous sections and the methodology outlined by Meirovitch (7:300). A detailed development is presented here since the transformations necessary to apply noise to the sensors in local coordinates are the same as those contained in the finite element model. Often the program NASTRAN is used to calculate the equations of motions, but its use was precluded due to problems associated with applying the noise in a repetitive computational scheme. The development starts with the system stiffness matrix, then the mass matrix, then damping matrix and finally ends with the force input location matrix.

By examining a basic truss element in a local coordinate frame, Figure 2-2, a relationship is developed relating nodal displacement vector $\underline{r}$ to nodal force vector $\underline{f}$.
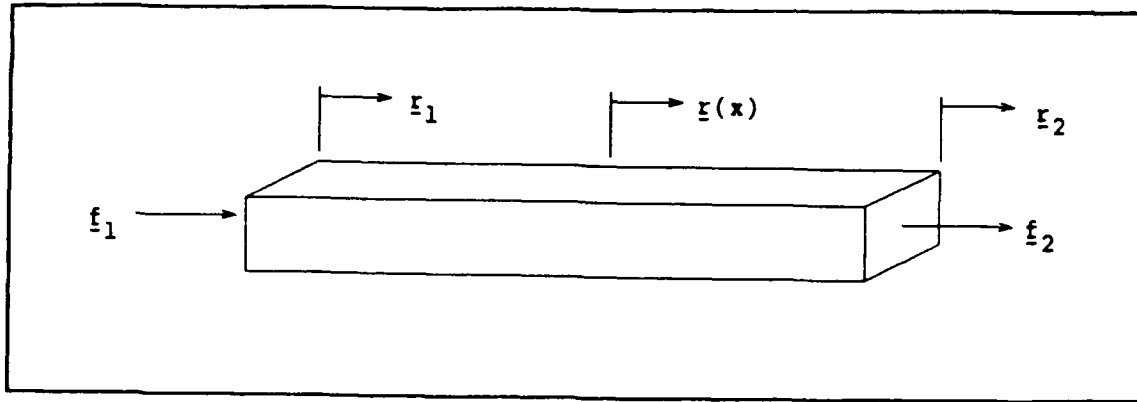
Figure 2-2 Element Truss Member

By assuming constant cross-sectional area and Young's Modulus the axial displacement has an equation of the following form

$$Ey(Ac)\frac{d^2\underline{r}(x)}{dx^2} = 0 \qquad\qquad 0 \leq x \leq h \quad (2.1)$$

where

Ey   = Young's Modulus

Ac   = cross-sectional area

$\underline{r}(x)$ =   axial displacement

h   = length of truss member

Integrating Eq (2.1) and using the fact that the displacement at x=0 is $\underline{r}_1$ and the displacement at x=h is $\underline{r}_2$ to solve for the constants of integration, the following expression results:

$$\underline{r}(x) = (1-x/h)\underline{r}_1 + (x/h)\underline{r}_2 \qquad\qquad (2.2)$$

where

$\underline{r}_1$ = displacement at node 1

$\underline{r}_2$ = displacement at node 2

The displacement equation, Eq (2.2), can be differentiated and substituted into the following boundary conditions:

2-6

$$Ey(Ac) \frac{d\underline{r}(x)}{dx} \Bigg|_{x=0} = -\underline{f}_1 \qquad (2.3)$$

$$Ey(Ac) \frac{d\underline{r}(x)}{dx} \Bigg|_{x=h} = \underline{f}_2 \qquad (2.4)$$

where

$\underline{f}_1$ = force at node 1

$\underline{f}_2$ = force at node 2

The resulting equations are:

$$Ey(Ac) \frac{\underline{r}_2 - \underline{r}_1}{h} = -\underline{f}_1 \qquad (2.5)$$

$$Ey(Ac) \frac{\underline{r}_2 - \underline{r}_1}{h} = \underline{f}_2 \qquad (2.6)$$

Eqs (2.5) and (2.6) may be written in a matrix form as:

$$K\underline{r} = \underline{f} \qquad (2.7)$$

where

$$K = Ey(Ac) \begin{bmatrix} 1 & 0 & 0 & -1 & 0 & 0 \\ 0 & 0 & 0 & 0 & 0 & 0 \\ 0 & 0 & 0 & 0 & 0 & 0 \\ -1 & 0 & 0 & 1 & 0 & 0 \\ 0 & 0 & 0 & 0 & 0 & 0 \\ 0 & 0 & 0 & 0 & 0 & 0 \end{bmatrix} \qquad (2.8)$$

$$\underline{r} = \begin{Bmatrix} \underline{r}_1 \\ \underline{r}_2 \end{Bmatrix} \qquad (2.9)$$

$$\underline{f} = \begin{Bmatrix} \underline{f}_1 \\ \underline{f}_2 \end{Bmatrix} \qquad (2.10)$$

The stiffness matrix K for an individual element can be assembled with the other element stiffness matrices to form the overall system stiffness matrix. The combining of the matrices must be done in a global coordinate frame; e.g. reference frame $\underline{s}$ already introduced in Figure 2-1. For development purposes let $\underline{i}$ be the local coordinate frames for each element. As shown in Figure 2-3, the i_1 direction vector is always aligned along the axial direction pointing from the lower node number to the higher node number.
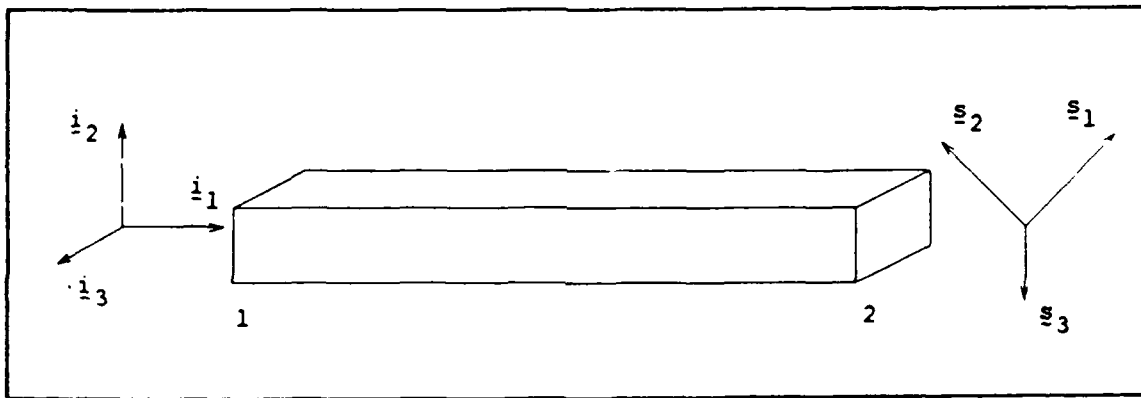
Figure 2-3 Local Coordinate Frame

Define a transform matrix L such that

$$\underline{r}_i = L\underline{r}_s \qquad (2.11)$$

where

$\underline{r}_i$ = the displacement vector in local coordinate frame $\underline{i}$

$\underline{r}_s$ = the displacement vector in global coordinate frame $\underline{s}$

$$L = \begin{bmatrix} L_{11} & 0 \\ 0 & L_{22} \end{bmatrix} \qquad \text{(transform matrix)}$$

It should be observed that $L_{11}=L_{12}$ and is the rotation matrix of the global coordinate frame to the local frame. That is

$$\underline{i} = L_{11}\underline{s} \qquad (2.12)$$

Rotation matrix L_{11} can be constructed by taking the product of the direction cosines matrices for each axis of rotation necessary to align the element axis up with the s_1 direction vector. By defining the following matrices the appropriate rotations for the CSDL-I can be tabulated as is done in Table 2-3:

$$R_1 = \begin{bmatrix} 1 & 0 & 0 \\ 0 & \cos\varphi & -\sin\varphi \\ 1 & \sin\varphi & \cos\varphi \end{bmatrix} \qquad (2.13)$$

$$R_2 = \begin{bmatrix} \cos\gamma & 0 & \sin\gamma \\ 0 & 1 & 0 \\ -\sin\gamma & 0 & \cos\gamma \end{bmatrix} \qquad (2.14)$$

$$R_3 = \begin{bmatrix} \cos\phi & -\sin\phi & 0 \\ \sin\phi & \cos\phi & 0 \\ 0 & 0 & 1 \end{bmatrix} \qquad (2.15)$$

where

φ = rotation angle about axis i_1

γ = rotation angle about axis i_2

ϕ = rotation angle about axis i_3

Table 2-3
Summary of Rotation Matrices

Element	Rotation Matrix
1	$R_3(150°)R_2(-54.73°)$
2	I
3	$R_3(30°)R_2(-54.73°)$
4	$R_3(-90°)R_2(-54.73°)$
5	$R_3(-60°)$
6	$R_3(120°)$
7	$R_3(-120°)R_2(-45°)$
8	$R_3(60°)R_2(-45°)$
9	$R_3(120°)R_2(-45°)$
10	$R_3(-60°)R_2(-45°)$
11	$R_2(-45°)$
12	$R_3(180°)R_2(-45°)$

The stiffness matrix K and the force vector $\underline{f}$ can be converted to the global coordinate frame by the following transformations developed in the discussion by Meirovitch (7:315).

$$K_s = L^T K_i L \qquad (2.16)$$

$$\underline{f}_s = L^T \underline{f}_i \qquad (2.17)$$

where

K_s = stiffness in global coordinate frame $\underline{s}$

K_i = stiffness in local coordinate frame $\underline{i}$

$\underline{f}_s$ = force in global coordinate frame $\underline{s}$

$\underline{f}_i$ = force in local coordinate frame $\underline{i}$

After transforming each of the 12 stiffness matrices associated with the 12 truss elements to the global coordinate frame $\underline{s}$ they are summed together in their extended

form. The extended form is a 30×30 matrix where zero rows and zero columns have been inserted in the original 6×6 K_s matrices for those generalized nodal displacements that are not represented in the original K_s. An example extended matrix for element 3 is listed in Appendix A. After summing the extended K_s matrices, the boundary conditions are applied. The boundary conditions are enforced by deleting the rows and columns associated with the fixed nodal displacements (i.e. nodes 5-10) since reaction forces are not of interest. The final stiffness matrix associated with the equation of motion is also included in Appendix A. The remainder of this report shall refer to the total 12×12 stiffness as simply K unless noted otherwise. A computer program to calculate K called STIFF.M written in Pro-MATLAB script language is listed in Appendix B.

The mass matrix M is simply an identity matrix I since the original assumption was 1 unit lumped masses at each of the nodes. It should be noted that if the assumption of lumped masses was not enforced the mass matrix should be developed. The mass matrix can be constructed as outlined in Meirovitch (7:306) using the same interpolation function (i.e. Eq (2.2)) as the stiffness matrix. The method is not discussed here since it was not used.

The general form of the system equation of motion may be written in the generalized global coordinate frame as:

$$M\ddot{\underline{s}} + E\dot{\underline{s}} + K\underline{s} = D\underline{u} \qquad (2.18)$$

where

       M = n×n mass matrix

       E = n×n damping matrix

       K = n×n stiffness matrix

       D = n×m input location matrix (actuator locations)

       $\underline{s}$ = n×1 global coordinate vector

       $\underline{u}$ = n×1 control input vector

Matrix E contains all of the viscous damping terms. The CSDL-I model does not incorporate any assumptions about the damping. The viscous terms could be modeled in the global coordinate frame and transformed into modal coordinates, much like the stiffness terms. The disadvantage is that the E matrix will not be decoupled; it is more convenient to assume a representative viscous damping term which can be modeled directly in modal coordinates. An assumed value of .005 for each mode was use to represent a lightly damped system.

The input location matrix D converts the force applied from any one actuator to the global coordinate frame. It should be noted that $\underline{u}$ isn't in the global coordinate frame, but represents a vector of actuator gains along their own local coordinate axis. The D matrix is constructed by transforming the actuator's i_1 direction vector to global coordinate frame using the relationships in Eqs (2.12) and (2.17). The matrix is then assembled like the K matrix using an extended form. A program to calculate D called SENSOR.M written in Pro-MATLAB script language is listed in Appendix C. This code is used extensively to calculate the final

state-space matrices after applying perturbations to the actuators in the local coordinate frame. The final D matrix is listed in Appendix A.

Modal Coordinate Transformation. The modal coordinate system is a vector space which utilizes the natural mode shapes as a basis. These natural modes are orthogonal to each other and therefore will decouple the equations of motion. This decoupling will allow each individual second order differential equation to be represented as two coupled first order differential equations. The two coupled first order differential equations allow for conversion to state-space form, useful for applying structural control techniques.

The natural mode shapes and their associated frequencies can be computed by solving the characteristic eigenvalue problem.

$$[K - \lambda_j M]\{U_j\} = 0 \qquad (2.19)$$

where

λ_j = eigenvalue

U_j = eigenvector

It can also be shown that the natural frequencies of the system are:

$$\lambda_j = \omega_j^2 \qquad (2.20)$$

where

ω_j^2 = natural frequency

A complete description is provided in Mierovitch (7:107).

Table 2-4 lists the natural frequencies for the CSDL-I model.

<div align="center">

Table 2-4

CSDL-I Natural Frequencies

Assigned Mode Number	Natural Frequency ω in Rad/sec
1	1.34
2	1.66
3	2.89
4	2.96
5	3.40
6	4.20
7	4.66
8	4.75
9	8.54
10	9.25
11	10.28
12	12.90

</div>

Once the eigenvalue problem is solved, U becomes a matrix whose columns are the U_j eigenvectors associated with the λ_j eigenvalues. It should be noted that the amplitudes of U_j are not unique, only the shape. A unique amplitude can be enforced by requiring orthonormality of U with the mass matrix M.

$$U^T M U = I \qquad (2.21)$$

The equations of motion can then be transformed to modal coordinates through the relationship

$$\underline{s} = U \eta \qquad (2.22)$$

where

η = the vector of modal coordinates

Substituting Eq (2.22) into Eq (2.18) yields

$$U^T M \ddot{\eta} + U^T E U \dot{\eta} + U^T K \eta = U^T D \underline{u} \qquad (2.23)$$

By first recognizing U is a matrix of orthogonal

eigenvectors, M is an identity matrix, and using the relationship in Eq (2.19), Eq (2.23) can be rewritten as:

$$I\ddot{\underline{\eta}} + U^T E U \dot{\underline{\eta}} + \left[\begin{array}{c} \diagdown \\ \qquad \omega_j^2 \\ \qquad\qquad \diagdown \end{array} \right] \underline{\eta} = U^T D \underline{u} \qquad (2.24)$$

Recalling that the viscous damping is modeled only in the modal coordinates, Eq (2.24) can be expressed as:

$$I\ddot{\underline{\eta}} + \left[\begin{array}{c} \diagdown \\ 2\zeta\omega_j^2 \\ \qquad \diagdown \end{array} \right] \dot{\underline{\eta}} + \left[\begin{array}{c} \diagdown \\ \qquad \omega_j^2 \\ \qquad\qquad \diagdown \end{array} \right] \underline{\eta} = U^T D \underline{u} \qquad (2.25)$$

where

ζ = modal damping (assumed as .005)

State-space Transformation. After obtaining the equations of motion in modal coordinates, Eq (2.25), a transformation to a state space representation is possible. As presented in Sumner (11:Sec 3,1) the objective is to arrange the equations into the form:

$$\dot{\underline{x}} = A\underline{x} + B\underline{u} \qquad (2.26)$$

$$\underline{y} = C\underline{x} \qquad (2.27)$$

where

A = 2n×2n plant matrix

B = 2n×m control input matrix

C = 2n×1 output matrix

$\underline{x}$ = 2n×1 state vector

$\underline{u}$ = m×1 control input vector

This conversion is implemented by defining the state vector as:

$$\underline{x} = \left[\begin{array}{c} \eta \\ \hline \dot{\eta} \end{array} \right] \tag{2.28}$$

This in turn requires the other matrices to be of the form

$$A = \left[\begin{array}{c|c} 0 & I \\ \hline \diagdown -\omega_j^2 & \diagdown -2\zeta\omega_j^2 \\ \diagdown & \diagdown \end{array} \right] \tag{2.29}$$

$$B = \left[\begin{array}{c} 0 \\ \hline U^T D \end{array} \right] \tag{2.30}$$

$$C = [C_p U \mid C_v U] \tag{2.31}$$

where

$C_p = n_p \times n$ displacement sensor output matrix

$C_v = n_v \times n$ velocity sensor output matrix

In the particular arrangement of the CSDL-I model used in this report there are no velocity sensors, so C_v is simply a matrix of zeros. Also, the sensors are collocated with actuators so that the C_p matrix is simply the transpose of the D matrix.

$$C_p = D^T U \quad \text{or} \quad [U^T D]^T \tag{2.32}$$

The final output matrix for the CSDL-I is then

$$C = [(U^T D)^T \mid 0] \tag{2.33}$$

The relationship in Eq (2.33) is used to invoked noise in the sensors during feedback. As shown in later sections perturbations are applied in local $\underline{i}$ coordinates, then a new D matrix is calculated, and then finally a new C matrix is

formed to be used in the control methodology. The nominal A, B, and C matrices are listed in Appendix D. The next chapter develops the control methodology applied to the state-space Eqs (2.28),(2.29),(2.30),and (2.33).

III. Control Law Development

Decoupled control can be implemented with a variety of different dynamic feedback control laws. The decoupled methodology uses orthogonal transforms to decompose the original single state-space representation into a number of separate representations. These separate state-space representation can have their own individual dynamic feedback control laws applied to them without destabilizing the other individual systems. It should be noted that any unmodeled dynamics (i.e. modes) may or may not be destabilized by applying dynamic feedback control to the separate subcontrollers. This fact is true for any dynamic feedback system, decoupled or not, that has only partial knowledge of the plant dynamics within the bandwidth of the control system.

The first of the following sections introduces the fundamentals of linear quadratic feedback theory. This particular type of dynamic feedback was implemented on a complete fullstate representation of the CSDL-I as a benchmark for decoupled controller performance. The linear quadratic regulator(LQR) and linear quadratic estimator(LQE) theories were also applied to the separate decoupled state-space systems. The LQR/LQE theory is developed separately to emphasize that other types of dynamic feedback control laws could be implemented. The second section outlines the theory necessary to decouple the original

state-space representation into separate decoupled systems. The third section then applies the theory of the first two sections to the CSDL-I.

Fullstate Linear Quadratic Theory

As presented more thoroughly in Franklin (6:312-405), Sumner (11:sec 3,6-9) and Ridgley (9:sec 6,1-15), a state-space system of the form

$$\dot{\underline{x}} = A\underline{x} + B\underline{u} \qquad (3.1)$$

$$\underline{y} = C\underline{x} \qquad (3.2)$$

may be actively controlled by "feeding back" a set of control forces based upon the current state of the system, or mathematically let

$$\underline{u} = Kc\underline{x} \qquad (3.3)$$

where

Kc = matrix of control gains

Eq (3.3) assumes complete knowledge of the state vector $\underline{x}$. Since this is not the case with the given six position sensors ($\underline{x}$ is rarely known completely), a method to estimate $\underline{x}$ is constructed. The $\underline{x}$ vector can be estimated by taking information from the sensors $\underline{y}$ and forming an "estimator" or sometimes called "observer" of the form

$$\dot{\hat{\underline{x}}} = A\hat{\underline{x}} + B\underline{u} + Kf\{\underline{y}-\hat{\underline{y}}\} \qquad (3.4)$$

$$\hat{\underline{y}} = C\hat{\underline{x}} \qquad (3.5)$$

where

$\hat{\underline{x}}$ = estimated state vector

$\hat{\underline{y}}$ = estimated output vector

Kf = matrix of estimator gains

The feedback is then accomplished using the estimated states.

$$\underline{u} = Kc\hat{\underline{x}} \tag{3.6}$$

The Kc and Kf matrices are formed using LQR/LQE theory. The Kf matrix must also be of a form to insure the error state defined as:

$$\underline{e} = \hat{\underline{x}} - \underline{x} \tag{3.7}$$

where

$\underline{e}$ = state error vector

goes asymptotically to zero in steady state.

The LQR theory determines Kc by minimizing a cost function J that represents a compromise between obtaining minimum deviation of the present state from the final desired value (tracking error) and control input effort necessary to obtain the desired value.

$$J = \int_0^\infty (\underline{x}^T Q_o \underline{x} + \underline{u}^T R_o \underline{u}) dt \tag{3.8}$$

where

Q_o = a positive semidefinite square state weighting matrix

R_o = a positive definite square control weighting matrix

The solution to the minimization of Eq (3.8) can be found to be:

$$Kc = R_o^{-1} B^T P \tag{3.9}$$

where

P = positive definite solution to the following Riccati
Equation:

$$A^T P + PA - PBR_o^{-1}B^T P + Q_o = 0 \qquad (3.10)$$

Using the principle of duality, the gain matrix Kf is also
obtained by the solution method outlined in Eqs (3.8) (3.9)
and (3.10) by substituting C^T for B and A^T for A. The
weighting matrices Q_o and R_o are not necessarily the same for
the Kf calculation. The Q_o and R_o used in the estimator
calculations contain assumptions about how the process noise
and measurement noise are distributed across the state-space
model. To insure stable feedback for fullstate control
matrices A and B must be a controllable pair along with the
conditions on Q_o and R_o stated in Eq (3.8). A more detailed
discussion is given in Ridgely (9:sec 6,5-8). This
investigation used diagonal matrices for Q_o and R_o, thus
insuring a stable LQR/LQE compensator.

Now that the components have been developed the complete
compensator design can be formed. By substituting Eq (3.6)
into Eq (3.1):

$$\dot{\underline{x}} = A\underline{x} + BKc\underline{\hat{x}} \qquad (3.11)$$

Substituting Eq (3.2), (3.5) and (3.6) into Eq (3.4) yields:

$$\dot{\underline{\hat{x}}} = A\underline{\hat{x}} + BKc\underline{\hat{x}} + Kf(C\underline{x}-C\underline{\hat{x}}) \qquad (3.12)$$

Differentiating Eq (3.7) yields:

$$\dot{\underline{e}} = \dot{\underline{\hat{x}}} - \dot{\underline{x}} \qquad (3.13)$$

Substituting Eq (3.11), (3.12) into (3.13) collecting terms and using Eq (3.7) to define $\underline{e}$ yields:

$$\dot{\underline{e}} = (A - KfC)\underline{e} \tag{3.14}$$

Taking Eq (3.7) and reforming as:

$$\hat{\underline{x}} = \underline{e} + \underline{x} \tag{3.15}$$

and substituting into Eq (3.11) results in:

$$\dot{\underline{x}} = (A + BKc)\underline{x} + BKc\underline{e} \tag{3.16}$$

Now Eqs (3.16) and (3.14) can be written in matrix form as

$$\begin{bmatrix} \dot{\underline{x}} \\ \dot{\underline{e}} \end{bmatrix} = \begin{bmatrix} A + BKc & BKc \\ 0 & A - KfC \end{bmatrix} \begin{bmatrix} \underline{x} \\ \underline{e} \end{bmatrix} \tag{3.17}$$

or more compactly

$$\begin{bmatrix} \dot{\underline{x}} \\ \dot{\underline{e}} \end{bmatrix} = Ae \begin{bmatrix} \underline{x} \\ \underline{e} \end{bmatrix} \tag{3.18}$$

where

Ae = the state-space closed loop plant matrix with error states

The compensator, Eq (3.17), doesn't have an error state reference input matrix, Be. Franklin (6:372) develops various methods of forming the error state input reference matrix, Be, based on whether the error states are to be excited or not. This investigation looked only at a reference impulse as the test input, where an impulse can be thought of as a set of initial displacements. The original B matrix can then be used to convert the set of initial

displacements along the actuator's local coordinate frame $\underline{i}$ into the state-space frame, by defining an error state input matrix in the form shown in Eq (3.19). However, using the original B matrix to form the Be matrix does restrict applying the initial displacement conditions to combinations of displacements along the actuator axes, but this presented little problem in the investigation. A typographical mistake in the program DECOUPLE.M, Appendix F, was noticed late in this investigation and prevented implementation of Be as previously defined. Further comments on the necessary changes required in the code to implement the defined Be are included in the program documentation. For the purposes of this investigation the exact form of Be was of little consequence since the reference inputs used were exactly the same for all design configurations considered. The main objective was to compare different design's relative performance, but not to predict actual performance of a real structure to a specific input. The error state output matrix Ce is simply the original C matrix augmented with zeros as shown below since the sensor locations have not changed. The final compensator design with LQR/LQE control can be represented as:

$$\begin{bmatrix} \dot{\underline{x}} \\ \dot{\underline{e}} \end{bmatrix} = Ae \begin{bmatrix} \underline{x} \\ \underline{e} \end{bmatrix} + Be\underline{u} \qquad (3.19)$$

$$\underline{y} = Ce \begin{bmatrix} \underline{x} \\ \underline{e} \end{bmatrix} \qquad (3.20)$$

where

Ae = defined in Eq (3.17)

$$Be = \begin{bmatrix} B \\ \hline 0 \end{bmatrix}$$

Ce = [C ┆ 0]

Decoupled Controller Theory

The basic concept of decoupled control is to break an entire structural model Eqs (3.1) and (3.2) into partitions that can be actively controlled separately without destabilizing any other partition. This decoupled controller theory section also addresses a partition of residual structural modes that are not considered in the control development, but are modeled in the time response of controller performance. These residuals mathematically represent the partition of the physical model that is unknown for control law development, yet ever so present in application.

As presented in Calico (2:10-11) the state-space vector can be partitioned into separate subcontroller and a residual components.

$$\underline{x} = \begin{bmatrix} \underline{x}_1 \\ \underline{x}_2 \\ \vdots \\ \underline{x}_N \\ \underline{x}_r \end{bmatrix} \qquad (3.21)$$

where

$\underline{x}_N$ = a vector of modes grouped into the Nth subcontroller

$\underline{x}_r$ = the residual modes that will not be actively controlled

The decision of which structural modes to group into which subcontroller group $\underline{x}_N$ is one of the main thrusts of this investigation. It will be shown later the decoupling transform enforces different restrictions on subcontroller $\underline{x}_1$ than $\underline{x}_N$, so that the performance of the total system will be different for different arrangements. Each subcontroller can be written as a partition of the total plant.

$$\dot{\underline{x}} = A_i \underline{x} + B_i \underline{u} \qquad\qquad i=1,\ldots.N \qquad (3.22)$$

and

$$\dot{\underline{x}}_r = A_r \underline{x} + B_r \underline{u} \qquad\qquad (3.23)$$

where A_i , B_i , A_r and B_r are defined as the partitions of Eqs (2.29) (2.30) and (2.31).

$$A_i = \begin{bmatrix} 0 & I \\ \searrow & \searrow \\ (-\omega_j^2)_i & (-2\zeta\omega_j^2)_i \\ \searrow & \searrow \end{bmatrix} \qquad (3.24)$$

$$B_i = \begin{bmatrix} 0 \\ (U^T D_j)_i \end{bmatrix} \qquad (3.25)$$

$$C_i = [(C_p U)_i \mid (C_v U)_i] \qquad (3.26)$$

where

j = the individual mode assigned to the ith controller

i = the ith partition of residual partition

The dimensions of the partitioned matrices are $2n_i \times 2n_i$ for A_i , $2n_i \times n_a$ for B_i ,and $n_s \times 2n_i$ for C_i where n_i is the number of modes in the ith subcontroller, n_a is the total number of actuators for the structure, and n_s is the number of sensors for the structure.

To apply control to the N individual systems defined as:

$$\dot{\underline{x}}_i = A_i \underline{x}_i + B_i \underline{u} \tag{3.27}$$

$$\underline{y} = C\underline{x} \tag{3.28}$$

requires that the controllers don't interact with each other. In the form of Eqs (3.27) and (3.28) interaction is present in that the control input $\underline{u}$ and the output vector $\underline{y}$ are the same for all N subcontrollers. This interaction is called control spillover and observation spillover respectively and may be eliminated by enforcing certain constraints on the Kc and Kf matrices. Consider a new control variable $\underline{\vartheta}_i$ and output variable $\underline{w}_i$ defined as:

$$\underline{u} = \sum_{i=1}^{N} T_i \underline{\vartheta}_i \tag{3.29}$$

$$\underline{w}_i = \Gamma_i \underline{y} \tag{3.30}$$

By substituting Eq (3.29) into Eq (3.27) and Eq (3.28) into Eq (3.30):

$$\dot{\underline{x}}_i = A_i \underline{x}_i + B_i \sum_{j=1}^{N} T_j \underline{\vartheta}_j \tag{3.31}$$

$$\underline{w}_i = \Gamma_i \sum_{j=1}^{N} C_j \underline{x}_j \tag{3.32}$$

To completely remove all spillover effects T_i and Γ_i form the null space of the other separate partitions, B_j and C_j matrices, or symbolically,

$$\begin{aligned} B_i T_j &= 0 \\ \Gamma_i C_j &= 0 \end{aligned} \quad \text{for} \quad \begin{aligned} i &= 1 \ldots N \\ j &= 1 \ldots N \end{aligned} \quad i \neq j \tag{3.33}$$

It is also possible to enforce less restrictive conditions on T_i and Γ_i that allow coupled but stable subcontrollers. They are:

$$\begin{aligned} B_i T_j &= 0 \\ \Gamma_i C_j &= 0 \end{aligned} \quad \text{for} \quad \begin{aligned} i &= 1 \ldots N-1 \\ j &= 1+1 \ldots N \end{aligned} \quad i \neq j \tag{3.34}$$

The conditions in Eq (3.34) were used in this investigation to enforce a stable set of subcontrollers. Now noticing that by substituting conditions in Eq (3.34) into Eqs (3.31) and (3.32) the following maybe formed.

$$\dot{\underline{x}}_i = A_i \underline{x}_i + B_i^* \underline{\vartheta}_i \tag{3.35}$$

$$\underline{w}_i = C_i^* \underline{x}_i \tag{3.36}$$

where

$$\begin{aligned} B_i^* &= B_i T_i \\ C_i^* &= \Gamma_i C_i \end{aligned}$$

Any type of dynamic feedback control can be implemented on the N set of equations Eq (3.35) and Eq (3.36) without destabilizing each other. The LQR/LQE theory as presented in the previous section was implemented on Eqs (3.35) and (3.36) resulting in N controller gain matrices Kc and N estimator

gain matrices Kf. The notation of Kc_i and Kf_i will be used
to denote controller and estimator gain matrices for the ith
individual subcontroller. The resulting form of the
estimator for each subcontroller as defined in Eqs (3.35) and
(3.36) is:

$$\dot{\hat{\underline{x}}}_i = A_i \hat{\underline{x}} + B_i^* \underline{\vartheta}_i + Kf_i(\underline{w}_i - \hat{\underline{w}}_i) \tag{3.37}$$

where

$$\hat{\underline{w}}_i = C_i^* \hat{\underline{x}}_i$$

and for feedback control

$$\underline{\vartheta}_i = Kc_i \hat{\underline{x}}_i \tag{3.38}$$

To implement the subcontrollers, the compensator system as
defined in Eqs (3.37) and (3.38) are transformed back to a
form containing the actual input vector $\underline{u}$. The vector $\underline{u}$
defines the set of actuators that may physically be invoked
to perform control. Substituting Eq (3.38) into (3.39) yields
feedback control equations:

$$\dot{\underline{x}}_i = A_i \underline{x}_i + B_i \underline{u} \tag{3.39}$$

$$\underline{u} = \sum_{i=1}^{N} T_i Kc_i \hat{\underline{x}}_i \tag{3.40}$$

The above is another expression of Eq (3.31) that indicates
that $\underline{u}$ will be the input control vector instead of $\underline{\vartheta}$. A new
closed loop plant matrix Ae can be formed by applying the
steps outlined for a fullstate controller Eqs (3.11) through
(3.17) to each of the N subcontrollers and then augmenting
the individual Ae_i into a single Ae that also includes

residuals. Instead of developing the general form which , slightly messy the procedure will be applied directly to the CSDL-I model in the the following section.

Before developing the actual model the number of sensors and actuators required to enforce decoupled control are examined. The conditions in Eq (3.34) to enforce orthogonal subcontrollers require the column of T_N to be orthogonal to the rows of B_1 through B_{N-1}. Calico (2:11) shows that for T_N to exist there must be enough actuators to make B_i be of sufficient rank to ensure a null space of at least one vector exists. The exact requirement is

$$n_a > \sum_{i=1}^{N-1} n_i \qquad (3.41)$$

In words this says the number of modes grouped in the first N-1 subcontrollers must be less than the available actuators. Similarly in order for Γ_i to exist there must be enough sensors to make C_i be of sufficient rank. That is:

$$n_s > \sum_{i=1}^{N-1} n_i \qquad (3.42)$$

Again, in words, this states the number of sensors must exceed the number of modes grouped in the last N-1 subcontrollers.

Controller Model for CSDL-I

The particular arrangement of subcontrollers used in this investigation involved three modes grouped in subcontroller one, two modes grouped into subcontroller two, and three modes grouped into subcontroller three, with the highest four modes always assigned to the residuals. With an

arrangement of six sensors and six actuators the requirements of Eqs (3.41) and (3.42) are satisfied. The variation in size of the groupings was not investigated, only the assignment of modes 1-8 to the 3-2-3 subcontroller arrangement. It would be desirable to limit the number of subcontrollers in an actual implementation so as to minimize energy input necessary to keep subcontrollers orthogonal. Therefore, a realistic design would choose subcontrollers as large as possible based on computational capabilities, thus making the size variation an unimportant variable. This decision was part of the original outscoping and downscoping of the problem.

The $\underline{x}$ vector is first partitioned into its components and augmented with the error states to form the augmented state vector $\underline{z}$.

$$\underline{z} = \{\underline{x}_1^T , \underline{e}_1^T , \underline{x}_2^T , \underline{e}_2^T , \underline{x}_3^T , \underline{e}_3^T , \underline{x}_r^T \}^T \tag{3.43}$$

The subcontroller's states and feedback are formed using Eqs (3.39) and (3.40).

$$\underline{\dot{x}}_1 = A_1 \underline{x}_1 + B_1 \underline{u} \tag{3.44}$$

$$\underline{\dot{x}}_2 = A_2 \underline{x}_2 + B_2 \underline{u} \tag{3.45}$$

$$\underline{\dot{x}}_3 = A_3 \underline{x}_3 + B_3 \underline{u} \tag{3.46}$$

$$\underline{\dot{x}}_r = A_r \underline{x}_r + B_r \underline{u} \tag{3.47}$$

and

$$\underline{u} = T_1 Kc_1 \underline{\hat{x}}_1 + T_2 Kc_2 + T_3 Kc_3 \underline{\hat{x}}_3 \tag{3.48}$$

The estimators are formed by applying Eq (3.37) written in input vector $\underline{u}$ notation, and also Eq (3.32).

$$\dot{\underline{\hat{x}}}_1 = A_1\underline{\hat{x}}_1 + B_1\underline{u} + Kf_1(\underline{w}_1-\underline{\hat{w}}_1) \tag{3.49}$$

$$\dot{\underline{\hat{x}}}_2 = A_2\underline{\hat{x}}_2 + B_2\underline{u} + Kf_2(\underline{w}_2-\underline{\hat{w}}_2) \tag{3.50}$$

$$\dot{\underline{\hat{x}}}_3 = A_3\underline{\hat{x}}_3 + B_3\underline{u} + Kf_3(\underline{w}_3-\underline{\hat{w}}_3) \tag{3.51}$$

and

$$\underline{w}_1 = \Gamma_1C_1\underline{x}_1 + \Gamma_1C_2\underline{x}_2 + \Gamma_1C_3\underline{x}_3 + \Gamma_1Cr\underline{x}_r \tag{3.52}$$

$$\underline{w}_2 = \Gamma_2C_1\underline{x}_1 + \Gamma_2C_2\underline{x}_2 + \Gamma_2C_3\underline{x}_3 + \Gamma_2Cr\underline{x}_r \tag{3.53}$$

$$\underline{w}_3 = \Gamma_3C_1\underline{x}_1 + \Gamma_3C_2\underline{x}_2 + \Gamma_3C_3\underline{x}_3 + \Gamma_3Cr\underline{x}_r \tag{3.54}$$

and

$$\underline{\hat{w}}_1 = \Gamma_1C_1\underline{\hat{x}}_1 \tag{3.55}$$

$$\underline{\hat{w}}_2 = \Gamma_2C_2\underline{\hat{x}}_2 \tag{3.56}$$

$$\underline{\hat{w}}_3 = \Gamma_3C_3\underline{\hat{x}}_3 \tag{3.57}$$

By substituting Eq (3.48) into Eq (3.44) and Eqs (3.52) and (3.55) into Eq (3.49) and then recalling $\dot{\underline{e}}_i = \dot{\underline{\hat{x}}}_i - \dot{\underline{x}}_i$ yields the error state equations:

$$\dot{\underline{e}}_1 = (A_1 - Kf_1\Gamma_1C_1)\underline{e}_1 + Kf_1\Gamma_1C_2\underline{x}_2 + Kf_1\Gamma_1C_3\underline{x}_3 \\ + Kf_1\Gamma_1Cr\underline{x}_r \tag{3.58}$$

$$\dot{\underline{e}}_2 = (A_2 - Kf_2\Gamma_2C_2)\underline{e}_2 + Kf_2\Gamma_2C_1\underline{x}_1 + Kf_2\Gamma_2C_3\underline{x}_3 \\ + Kf_2\Gamma_2Cr\underline{x}_r \tag{3.59}$$

$$\dot{\underline{e}}_3 = (A_3 - Kf_3\Gamma_3C_3)\underline{e}_3 + Kf_3\Gamma_3C_1\underline{x}_1 + Kf_3\Gamma_3C_2\underline{x}_2 \\ + Kf_3\Gamma_3Cr\underline{x}_r \tag{3.60}$$

Substituting $\hat{\underline{x}}_i = \underline{e}_i + \underline{x}_i$ into Eq (3.48) and then combining Eq (3.48) with Eqs (3.44), (3.45), (3.46) and (3.47) yields the state variable portion of $\dot{\underline{z}}$:

$$\dot{\underline{x}}_1 = (A_1 + B_1T_1Kc_1)\underline{x}_1 + B_1T_1Kc_1\underline{e}_1 + B_1T_2Kc_2(\underline{e}_2 + \underline{x}_2) + B_1T_3Kc_3(\underline{e}_3 + \underline{x}_3) \qquad (3.61)$$

$$\dot{\underline{x}}_2 = (A_2 + B_2T_2Kc_2)\underline{x}_2 + B_2T_2Kc_2\underline{e}_2 + B_2T_1Kc_1(\underline{e}_1 + \underline{x}_1) + B_2T_3Kc_3(\underline{e}_3 + \underline{x}_3) \qquad (3.62)$$

$$\dot{\underline{x}}_3 = (A_3 + B_3T_3Kc_3)\underline{x}_3 + B_3T_3Kc_3\underline{e}_3 + B_3T_1Kc_1(\underline{e}_1 + \underline{x}_1) + B_3T_2Kc_2(\underline{e}_2 + \underline{x}_2) \qquad (3.63)$$

$$\dot{\underline{x}}_r = A_r\underline{x}_r + BrT_1Kc_1(\underline{e}_1 + \underline{x}_1) + BrT_2Kc_2(\underline{e}_2 + \underline{x}_2) + BrT_3Kc_3(\underline{e}_3 + \underline{x}_3) \qquad (3.64)$$

Now Eqs (3.58), (3.59), (3.60), (3.61), (3.62), (3.63), and (3.64) may be assembled into the matrix form of Ae, the compensator closed loop plant matrix:

$$\dot{\underline{z}} = Ae\underline{z} \qquad (3.65)$$

where

$$Ae =$$

$$\begin{bmatrix}
A_1+B_1^*Kc_1 & B_1^*Kc_1 & B_1T_2Kc_2 & B_1T_2Kc_2 & B_1T_3Kc_3 & B_1T_3Kc_3 & 0 \\
0 & A_1-Kf_1C_1^* & Kf_1\Gamma_1C_2 & 0 & Kf_1\Gamma_1C_3 & 0 & Kf_1\Gamma_1Cr \\
B_2T_1Kc_1 & B_2T_1Kc_1 & A_2+B_2^*Kc_2 & B_2^*Kc_2 & B_2T_3Kc_3 & B_2T_3Kc_3 & 0 \\
Kf_2\Gamma_2C_1 & 0 & 0 & A_2-Kf_2C_2^* & Kf_2\Gamma_2C_3 & 0 & Kf_2\Gamma_2Cr \\
B_3T_1Kc_1 & B_3T_1Kc_1 & B_3T_1Kc_2 & B_3T_1Kc_2 & A_3+B_3^*Kc_3 & B_3^*Kc_3 & 0 \\
Kf_3\Gamma_3C_1 & 0 & Kf_3\Gamma_3C_2 & 0 & 0 & A_3-Kf_3C_3^* & Kf_3\Gamma_3Cr \\
BrT_1Kc_1 & BrT_1Kc_1 & BrT_2Kc_2 & BrT_2Kc_2 & BrT_3Kc_3 & BrT_3Kc_3 & Ar
\end{bmatrix}$$

and

$$B_i^* = B_i T_i$$
$$C_i^* = \Gamma_i C_i$$

It can easily be seen that by applying the requirements of Eq(3.34) that the Ae matrix becomes lower block triangular. This condition suppresses the spillover. An example Ae matrix for the CSDL-I is contained in Appendix E for modes 1,2,3 assigned to subcontroller one, modes 4,5 assigned to subcontroller two, and modes 6,7,8 assigned to subcontroller three. The controller and estimator gains where computed as previously explained both using a diagonal Q_o matrix of 20 and a unity matrix R_o.

The next chapter will depart from the equations of motion and develop the statistical techniques necessary to efficiently exercise these equations of motion. These techniques will be used to create a numerical experiment plan. The numerical experiment consisting of calculating the time history of the system to various applications of impulses to Eqs (3.19) and (3.20) using the definition of Ae as given in Eqs (3.17) and (3.65).

IV.   Response Surface Methodology

Box and Draper (1:1) explain, "Response surface methodology comprises a group of statistical techniques for empirical model building and model exploitation. By careful design and analysis of experiments, it seeks to relate a response, or output variable to the levels of a number of predictors, or input variables, that effect it." Usually response surface methodology (RSM) is applied to experimental data or simulation models, but can be applied to a deterministic type model such as the mathematical representation of the CSDL-I previously developed. The portions of RSM used in this investigation were principally regression techniques, fractional designs and signal-to-noise concepts. These tools allowed intelligent probing of the large number of design possibilities and identification of important design variables. They three tools, regression techniques, fractional designs and signal-to-noise concepts, will be developed in the following separate sections in the order mentioned.

Linear Regression

By investigating a complicated relationship over a sufficiently restricted region any function can be approximated by a polynomial. This approach involves the Taylor's series expansion of the true function over the region of interest. Let the proposed polynomial approximation be represented as:

$$y = f(\xi, \theta) + \varepsilon \tag{4.1}$$

where

y = output (i.e. response time, etc)

f = polynomial function

ξ = set of input variables

θ = set of parameters or coefficients in equation

ε = experimental error

The method of least-squares estimates θ by choosing a value of θ such that the sum of squares is minimized. The sum of squares $S(\theta)$ being

$$S(\theta) = \sum \{y_u - f(\xi_u, \theta)\}^2 \tag{4.2}$$

where

y_u = actual output value at design point u

ξ_u = particular setting of inputs for design point u

The least-squares estimate depends upon experimental errors being statically independent, constant variance and normally distributed. This is often verified by examining a plot of the residuals.

Eq (4.1) can be rewritten in a matrix form assuming a linear function f.

$$y = Z\theta + \varepsilon \tag{4.3}$$

where

$$y = \begin{bmatrix} y_1 \\ y_2 \\ \vdots \\ y_{n_p} \end{bmatrix}$$

$$Z = \begin{bmatrix} z_{11} & z_{21} & \cdots z_{p1} \\ z_{12} & z_{22} & \cdots z_{p2} \\ \vdots & \vdots & \vdots \\ z_{1n_p} & z_{2n_p} & \cdots z_{pn_p} \end{bmatrix}$$

$$\theta = \begin{bmatrix} \theta_1 \\ \theta_2 \\ \vdots \\ \theta_p \end{bmatrix}$$

$$\epsilon = \begin{bmatrix} \epsilon_1 \\ \epsilon_2 \\ \vdots \\ \epsilon_p \end{bmatrix}$$

n_p = number of data points

p = number of parameters in assumed model

Z = experimental design matrix

Using the form of Eq (4.3) it can be shown, Box and Draper (1:40-42), that the estimate of θ that minimizes $S(\theta)$ is

$$\hat{\theta} = (Z^\top Z)^{-1} Z^\top y \tag{4.4}$$

where

$\hat{\theta}$ = estimate of θ

To investigate a relationship using least-squares the form of f must be hypothesized. That is to say variables $\xi_1 \ldots \xi_p$ must initially be considered important. Each data point y_{n_p} is then generated from the physical or mathematical model for a unique combination of variables $\xi_1 \ldots \xi_p$. This unique combination is called a design point (i.e. a row of matrix Z). If the model is exercised twice(replication) at one design point another data point is generated, but the number

of design points remains constant. It is important to note the difference between design point and data point. A regression is then performed on the data using Eq (4.4). The statistical significance of each θ_p associated with a particular variable ξ_p and the overall model can be computed using an F statistic. This allows unimportant variables to be removed creating a parsimonious model capturing significant effects and interactions. The F statistic is defined as:

$$F_p = \frac{MS_p}{(MS_e \text{ or } MS_\ell)} \tag{4.5}$$

where

F_p = F statistic for parameter θ_p

MS_p = mean sum of squares for parameter θ_p

MS_e = mean sum of squares for pure error (only possible if a replication of a design point exists)

MS_ℓ = mean sum of squares for residuals (lack-of-fit when MS_e is zero)

and

$$F_\ell = \frac{MS_\ell}{MS_e} \tag{4.6}$$

where

F_ℓ = F statistic indicating appropiateness of model

MS_ℓ = mean sum of squares of lack-of-fit of model

The calculations of MS_e and MS_p are simplified greatly if the levels of each ξ_p are chosen so that the columns of Z are orthogonal to each other (each column of Z is associated with

a particular variable ξ_p). This is discussed in the next section. Assuming an orthogonal Z matrix the following can be shown, Box and Draper (1:34-62).

$$MS_p = (Z_p^T \psi)^2 / n_P \qquad (4.7)$$

where

Z_p = column of Z associated with variable ξ_p

and

$$MS_e = \frac{\sum_{i=1}^{m_P} \sum_{u=1}^{r_P} (\psi_{iu} - \bar{\psi}_i)^2}{(n_P - m_P)} \qquad (4.8)$$

where

m_P = number of design points (i.e. unique combinations of variables $\xi_1 - \xi_p$)

r_P = number of replications at design point i

$\bar{\psi}_i$ = mean across all replications at design point i

and

$$MS_\ell = \frac{\psi^T \psi - \left[\sum_{i=1}^{P} (Z_i^T \psi)^2 / n_P\right] - n_P \bar{\psi}^2 - MS_e(n_P - m_P)}{(m_P - p)} \qquad (4.9)$$

where

$\bar{\psi}$ = mean of all data points

By noticing that if there are no replications of design points ($r_P = 0$) Eq (4.9) can be simplified because MS_e reduces to zero.

$$MS_\ell = \frac{y^Ty - \left[\sum_{i=1}^{p} (z_i^Ty)^2/n_P\right] - n_P\bar{y}^2}{(m_P - p)} \qquad (4.10)$$

If no replications are performed then Eq (4.6) cannot be evaluated and Eq (4.5) must use MS_ℓ instead of MS_e.

The calculated F statistics (F_p and F_ℓ) are then compared to tabulated F values to test the hypothesis of significant variables and overall model. It should be noted that the hypothesis tested is whether the parameters of the variables are significant from zero. This is basically asking the question "Is the proposed function f better than no model at all?" Box and Draper (1:275-280) point out that more than this simple satistical significance of the parameters is required to ensure that the estimated model is reasonable. It must be validated that the change in the true function over the design region is larger than the error of the estimated model in the region. Box and Draper develop a conservative criteria to ensure that this condition is met. They assert that if the calculated F is 10 times larger than the tabulated F value the change in the true function is larger than the error of the estimated model. Some practitioners feel this is too conservative, but most all tests in this investigation met the 10 times F rule.

The final result of linear regression is that insignificant variables are removed in a screening type process and that a parsimonious polynomial is found that approximates the investigated relationship over the restricted

4-6

region of interest. The next section explains how to create the experimental design matrix, Z, used to calculate the equation parameters.

Fractional Designs

In order to generate the y vector in Eq (4.4) the mathematical model of the CSDL-I needs to be exercised at specific levels of the chosen input variables. The CSDL-I variables and levels chosen are described in the next chapter. Fractional factorial orthogonal designs were used in order to efficiently generate the data set. 2^{k-q} fractional designs were implemented on the input variables, and 3^{k-q} fractional designs were implemented on the noise factors. The noise factors or sensor errors are discussed further in the next section and the following chapter.

To simplify calculations and to remove variable scale effects the input variables are often coded to values of -1,0,1 for the low, medium, and high settings of the input variables. This coding is accomplished by a simple linear transformation.

$$\xi_c = \frac{\xi - \xi_{avg}}{1/2(\Delta\xi)} \tag{4.11}$$

where

ξ_c = coded values -1, 0, 1

ξ = uncoded values

$\xi_{avg} = (\xi_{max} - \xi_{min})/2$

$\Delta\xi = \xi_{max} - \xi_{min}$

To illustrate the concept of fractional designs consider a coded design matrix Z for two input variables. The design for investigating all possible combinations would require 2^2 runs and be of the following form.

$$Z = \begin{array}{cc} \xi_{c1} & \xi_{c2} \\ \begin{bmatrix} -1 & -1 \\ 1 & -1 \\ -1 & 1 \\ 1 & 1 \end{bmatrix} \end{array} \qquad (4.12)$$

If the proposed functional form was

$$y = \theta_0 + \theta_1 \xi_{c1} + \theta_2 \xi_{c2} + \theta_{12} \xi_{c1} \xi_{c2} \qquad (4.13)$$

the design matrix would need additional columns to estimate θ_0 and θ_{12} using Eq (4.4). The complete full factorial design would be

$$Z = \begin{array}{cccc} & \xi_{c1} & \xi_{c2} & \xi_{c1}\xi_{c2} \\ \begin{bmatrix} 1 & -1 & -1 & 1 \\ 1 & 1 & -1 & -1 \\ 1 & -1 & 1 & -1 \\ 1 & 1 & 1 & 1 \end{bmatrix} \end{array} \qquad (4.14)$$

noticing the mean, θ_0, is estimated by adding a column of ones. The design matrix in Eq (4.14) is composed of orthogonal columns. The dot product between each column is zero. This orthogonal property allows each θ_i to be estimated separately without affecting the values of the other parameters. If θ_2 was found to be statistically insignificant the proposed model would become

$$y = \theta_0 + \theta_1 \xi_{c1} + \theta_{12} \xi_{c1} \xi_{c2} \qquad (4.15)$$

The original values of θ_0, θ_1 and θ_{12} would remain unchanged after deleting θ_2. This is not true for nonorthogonal designs, and is a major benefit in screening variables. Another benefit of orthogonal designs is that the variance of the estimate of parameter θ is minimized. This is further explained in Box and Draper (1:76-80).

If the proposed function had three variables ξ_{c1}, ξ_{c2} and ξ_{c3} a full factorial design would require 2^3 or 8 runs. If is possible to reduce the number of runs in half by blocking or creating a fractional 2^{3-1} design. Again using the design matrix in Eq (4.13) the additional variable ξ_{c3} could be assigned to the interaction column $\xi_{c1}\xi_{c2}$. The actual experiment would have ξ_1 at the low level, ξ_2 at the low level, and ξ_3 at the high level for run number one. The price paid for decreasing the number of runs from 8 to 4 is that certain interaction terms are now aliased with other effects and can't be estimated separately. The most obvious alias is that interaction $\xi_{c1}\xi_{c2}$ is now aliased with main effect ξ_{c3}. The major assumption is that higher order effects (i.e. $\xi_{c1}\xi_{c2}$) are much smaller than main effects, and therefore affect the estimate of θ_3 very little. All aliasing patterns can be conveniently calculated using a generating function. In the given example the function is 3=12. By applying the rule that 3∘3=I, 1∘1=I, etc to the generating function all alias patterns can be found. For example the following are present: I=123 (mean is aliased with interaction 1,2,3), 13=2 (interaction 13 aliased with

main effect 2), and 23⊌1 (interaction 23 alasied with main effect 1). All fractional 2^{k-q} designs used in this investigation were standard designs listed in Box and Draper (1:164-165) of resolution III or higher. The resolution III simply refers to the fact that no main effects (ie ξ_{c1}, ξ_{c2}, etc) are aliased with other main effects. A resolution III design is the minimum required for estimating 1st order models. When estimating higher order models full factorial experiments were used so that aliasing was not a concern. The fractional 3^{k-q} design used in the noise matrix was a resolution III design taken from a National Bureau of Standards document (3a:13).

The next section develops the signal-to-noise ratio which was used in Eq (4.4) to investigate the system robustness to noise.

Signal-to-Noise Concepts

One of the main objectives of this investigation was to determine and demonstrate methods to design a decoupled controller to be robust to errors in specification of model parameters and sensor errors. Japanese manufacturing techniques have proven themselves to be very effective in designing systems to be robust to manufacturing variances. These Japanese statistical tools were used in this study to help design the decoupled controller to be robust to sensor errors. The specific tools used were the signal-to-noise ratios and parameter design techniques developed by Genichi Taguchi (10:167-205).

The first step in signal-to-noise analysis is the identification of design parameters that are easily regulated. The next step is to identify factors that are difficult or expensive to regulate,i.e. noise factors. In the CSDL-I example the fundamental design parameters that were easily regulated were controller gain and the arrangement of modes within the decoupled controller. The noise factors identified were model parameter errors and errors in the sensors. The actual factors selected could be numerous and more discussion on this is provided in the Choosing Metrics Section.

The next step is to construct efficient experiments (orthogonal) that investigate the effect of different design parameters on the output for a range of noise settings. The total experiment consists of orthogonal settings for the design parameters and orthogonal settings for the noise factors. For each design point associated with the design parameters there is a corresponding complete set of orthogonal noise factors. As a side point one should consider that this experiment requires the ability to enact some type of control over the noise factors. This controllability could tempt an experimenter to treat the noise factors as design parameters. If the noise factors were treated as design parameters they would have to be maintained at desirable levels throughout the life span of the system. The fundamental concept is that it is often easier and more economical to set other design parameters to such levels that the desired output is affected

4-11

little by changes in the noise factors. In the CSDL-I

experiment it maybe possible to build sensors accurate to

$\pm$ .0001 in displacement, but a sensor accurate only to $\pm$ .01

in maybe cheaper, lighter and more durable. If the control

gain and decoupled controller arrangement can be chosen so

that the $\pm$.01 sensor affects the output very little the new

design will be cheaper, lighter, more durable, yet with

similar output. This type of design is also beneficial for

space operation since the system degradation would occur in a

graceful manner. This is very important in the no

maintenance environment of space.

Once the experiment has been conceived and executed, the

best settings for the design parameters can be obtained by

maximizing a function derived through linear regression of

the observed response. The key in applying signal-to-noise

techniques is that the output variable to maximize should

reflect not only robustness to the noise setting, but also

reflect system performance. In the CSDL-I dynamic feedback

control the most robust system to senor noise would be a

controller with zero gain. The controller would not be

sending any signal to the actuators so the inputs to the

system would have no effect. Obviously this type of design

is of little use. This leads to the last step in

signal-to-noise concepts, the signal-to-noise ratio.

Taguchi (10:172) develops a loss function to describe how

deviations from a target value contribute to loss of the

final design's value. The loss function proposed by Taguchi

is a quadratic function.

$$\ell(\psi) = C(\psi - \tau)^2 \qquad (4.16)$$

where

C = constant

ψ = output

τ = target value of ψ (desired value)

$\ell(\circ)$ = loss function

The actual loss due to a particular design would be the expected value of Eq (4.16).

$$E(\ell(\psi)) = C \circ E[(\psi - \tau)^2] \qquad (4.17)$$

In the CSDL-I the performance was measured as a function of the response time required to dampen the system. The target value (τ) of the response time would be zero since the desired performance would be to immediately dampen the system (obviously impractical). In this case Eq (4.17) reduces to

$$E(\ell(\psi)) = C \circ E[(\psi)]^2 \qquad (4.18)$$

The maximum likelihood estimate of the loss is simply

$$E(\ell(\psi)) = \sum_{i=1}^{n_n} \psi_i^2/n_n \qquad (4.19)$$

where

n_n = number of noise settings (i.e. number of data points at one design setting)

Taguchi then recommends a transform of Eq (4.19) to the following:

$$SN = -10\log_{10}\left[\sum_{i=1}^{n_n} \psi_i^2/n_n\right] \qquad (4.20)$$

4-13

where

SN = signal-to-noise ratio

The negative sign allows the loss to be minimized when the SN ratio is the largest (i.e. less negative); a convention adopted in the literature. The actual SN ratio used in this investigation was:

$$SN = -10\log_{10}\left[\sum_{i=1}^{n_n} \psi_i^2\right] \qquad (4.21)$$

The $+10\log_{10}(n_n)$ constant was dropped for ease in calculation since all noise settings involved 27 runs. This would not be done if the number of noise settings changed within the experiment.

The next chapter utilizes these statistical tools to investigate the behavior of the CSDL-I model as developed in Chapters 2 and 3. These tools allow the decoupled controller's design parameters to be set at values so as to make the system robust to input noises.

V. <u>Investigation</u>

<u>Program Development</u>

In order to perform the numerical experiments necessary to design a robust decoupled controller a computer program was written. A script file program in Pro-MATLAB was written to enact the equation of motion described in Chapter 3. A documented listing is provided in Appendix F. The program reads in an input file consisting of the modal transform matrix U, a vector V of the natural frequencies squared, a matrix n consisting of possible decoupled controller arrangements, a matrix D representing the global coordinate input matrix, a matrix NOISE of sensor noise gains, a matrix Q_c of the Kalman filter state weighting values, and a matrix R_c of the Kalman filter control weighting values. The outputs are varied, but the main ones include a time history of the state vector $\underline{x}$ to an impulse input, and the response time to an impulse input for each unique setting of the input variables. The time history of motion for the CSDL-I was generated by applying an impulse in the equations of motion, Eqs (3.19) and (3.20). (The Ae matrix in Eq (3.19) being specified in Eq (3.65) for decoupled control and Eq (3.17) for full-order control.) The program calculates this time history using a Pro-MATLAB subroutine, impulse. The program was verified for accuracy by comparing the eigenvalues of the close loop state-space plant matrix Ae to output for a similar program developed by Robert Calico, PhD, Air Force

5-1

Institute of Technology, Wright- Patterson AFB, OH. The new program was written to allow easier external access to design parameters and more readily handle statistical analysis. The following sections will first discuss how the different types of metrics were choosen, then examine the actual numerical experiment.

Choosing Metrics

In choosing the proper performance metrics, three important questions raised by Box and Draper (1:4) should be answered. Which input variables should be studied and in what form? How should response be measured and in what form? What should the design region be? In trying to answer these questions it becomes apparent that the possible number of variables is almost unbounded. The possible number of variables can be better visualized by examining the outscoping diagram of the problem, Figure 5-1. It can be seen that even decoupled control becomes a variable when examining the more fundamental question of maintaining the alignment of a space structure. The problem was immediately narrowed down to the investigating of how modal arrangements within the decoupled controller and controller gain affect the system robustness. Once the problem was narrowed down to a size manageable for allotted resources specific inputs could be chosen. The following subsections will discuss noise inputs, then response measures and finally design parameters.

```
                    TYPE OF INPUT
           CONTROL ──┴── NO CONTROL
      PASSIVE ──┴── ACTIVE
VARY STRUCTURAL MEMBERS ──┴── CONSTANT CONFIGURATION
                DECOUPLED CONTROL ──┴── OTHER
             LQR/LQE ──┴── OTHER
   NUMBER OF SUBCONTROLLER ──┴── FIX 3 SUBCONTROLLER
                              │
                    ┌─────────────────────┐
                    │ ARRANGEMENT OF MODES │
                    └─────────────────────┘
                              │
        ESTIMATOR GAINS ──┴── │ CONTROLLER GAINS │
```
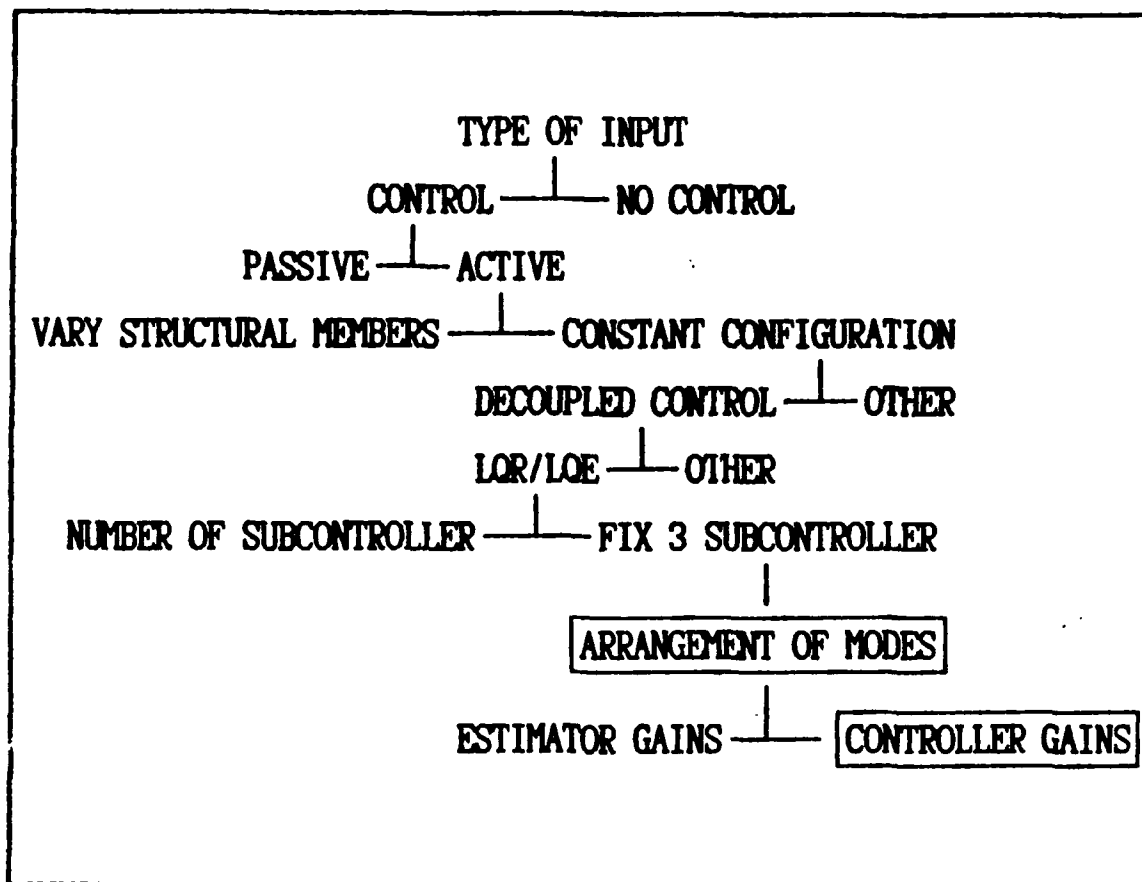
Figure 5-1 Outscoping of Problem

Input Noise Variables. Two types of noise inputs were
selected. The first type of noise was modelling error. Poor
specification of the model could take on many forms. A
structural model often contains error due to the
approximation of a continuous structure as a finite element
model. This type of error results in higher natural
frequencies being wrong and some completely missing. This
type of noise was simulated by only designing the controllers
based on the first eight natural frequencics. However, time
performance histories were based upon the total model of
twelve natural frequencies. A robust design should be able
to enact good control on a structure even though the design

was based on incomplete knowledge. This first type of noise was always present and was not varied in a signal-to-noise type experiment, but was treated as natural or pure experimental error.

The second type of noise input selected was incorrect sensor readings. A sensor may not be calibrated correctly and give incorrect information to the feedback system. A robust design should still be able to enact adequate control on a structure even with slightly wrong information. Since only position sensors were used, the errors could only be induced in position readings. Velocity or acceleration sensors would have different noise effects than position errors. The position errors should be a little more serious than velocity errors since the estimator differentiates the position readings to derive the other states. The errors were induced by multiplying the actual sensor readings by coefficients of .8, 1.0 and 1.2. The .8 coefficient causes the position sensor to always read low by 20%. It is important to note that the errors were supplied in the local coordinate frame $\underline{i}$ and then transformed into the appropriate perturbed C matrix using the rotation matrices in Eq (2.13) (2.14) and (2.15). The Kalman estimator gain design was based upon noise being decoupled in the state-space coordinate frame; a common assumption since the actual noise distribution is usually unknown. A robust design should be insensitive to real noises. This second type of noise was varied in a signal-to-noise type experiment using a 3_{III}^{6-3}

fractional design.

Response Measures. The final desired output was previously defined in Chapter 2 as maintaining the line of sight (LOS). The question is how to measure the LOS. This is a difficult question to answer. The CSDL-I model was small enough that it allowed performing various experiments on different output variables for various settings of input variables. The criterion for a good metric for LOS are; ability to measure the deviation of node one from it's undisplaced position, and ability to measure the time required to reduce deviation. Also the metric itself must have a large value spread for differing inputs.

The deviation of node one was measured by calculating the length and angle of a position vector from the undisplaced location for the time history of node one. A representative trace of the displacement is shown in Figure 5-2. The following derived metrics were investigated: average position vector length (radius) over a 20 second period, average angle over a 20 second period, standard deviation of radius, standard deviation of angle, a response time to a minimum moving average, and an average velocity of node one. The final performance metric based on the above mentioned criteria was the r onse time. The response time (t_r) is the time when the average radial displacement (using a 1.48 sec window) remained below .05 displacement units. A plot of 210 different subcontroller arrangements is shown in Figure 5-3. The plot shows a good spread of data from 6 to

20 seconds. The t_r metric is a direct measure of the amount of time to reduce node one displacement, and also provides a measure of the magnitude of node one displacement since it is a computed time based on an average radial displacement.
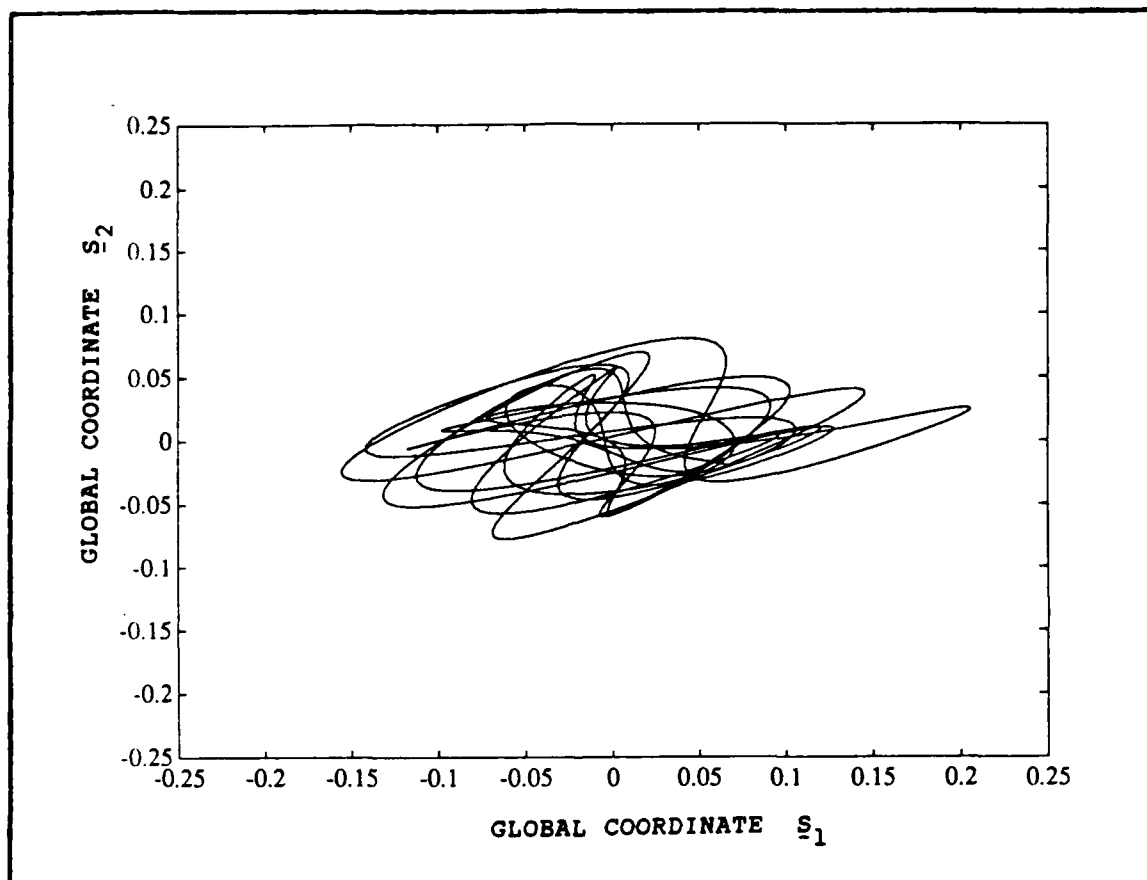
Figure 5-2 LOS Trace for Arrangement 123-45-678

The response time was determined as an appropriate output variable, but in order to design a robust controller a signal-to-noise (SN) ratio variable was necessary. By applying Eq (4.20) to t_r, a signal-to-noise ratio was calculated. All regressions in this investigation used both t_r and SN of t_r as output responses.

Design Parameters. In choosing design parameters it was decided to only investigate the gain associated with the
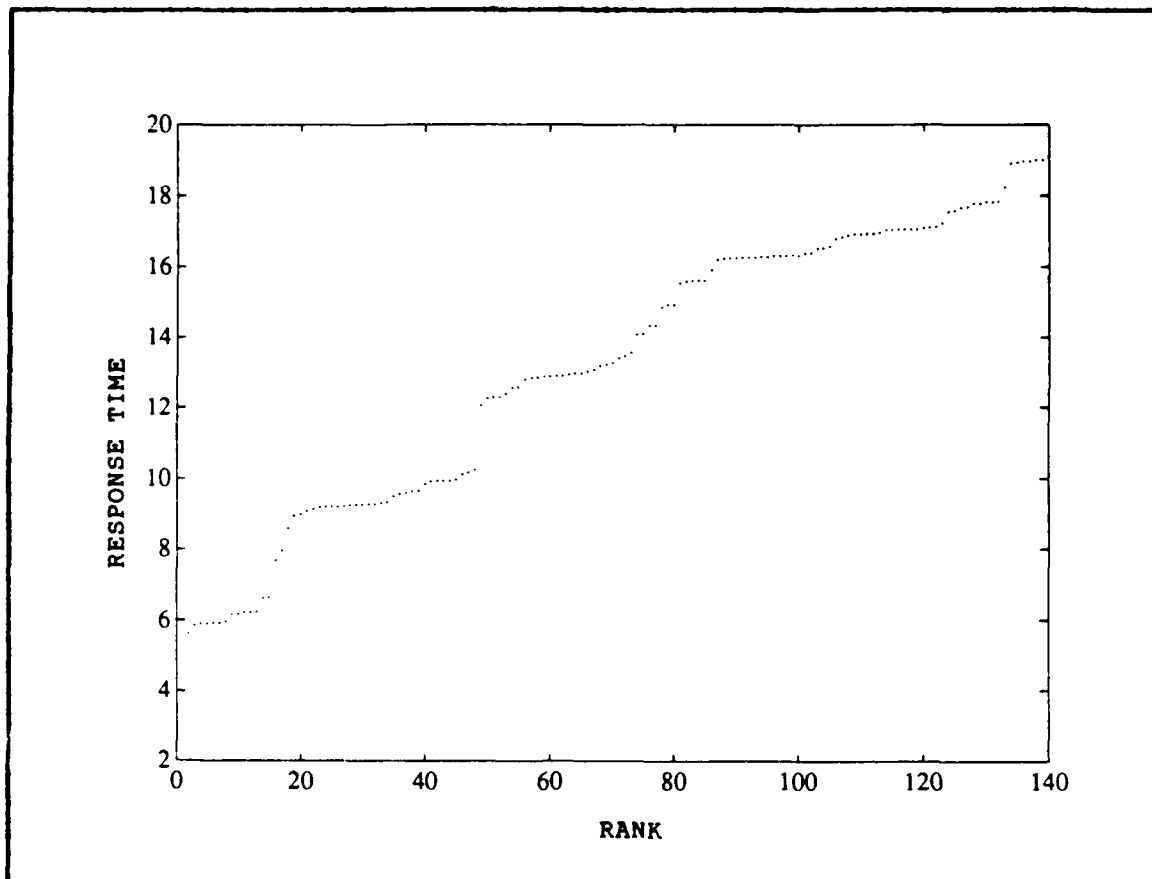
Figure 5-3 Response Time vs Rank

controller, Kc in Eq (3.3), and not the estimator, Kf in Eq
(3.4). In exploring the effects of controller and estimator
gains a small 3^2 design was performed on a few specific
subcontroller arrangements. The input variables were Q_o
matrix for the estimator, and the Q_o matrix for the
controller, Eq (3.8). As stated before the Q_o matrix was
always a diagonal matrix. In this initial exploratory
screening all the diagonal elements were changed
simultaneously for the estimator denoting this as a single
variable Q_{of}, and for the controller denoted as Q_{oc}.
A regression on the SN ratio was performed and the results are
in Tables G-1 and G-2, Appendix G. A graph of the contours

associated with constant values of the t$_r$ SN ratio are shown in Figure 5-4. The results, show as expected, that the larger total compensator gain gives the largest SN ratio.
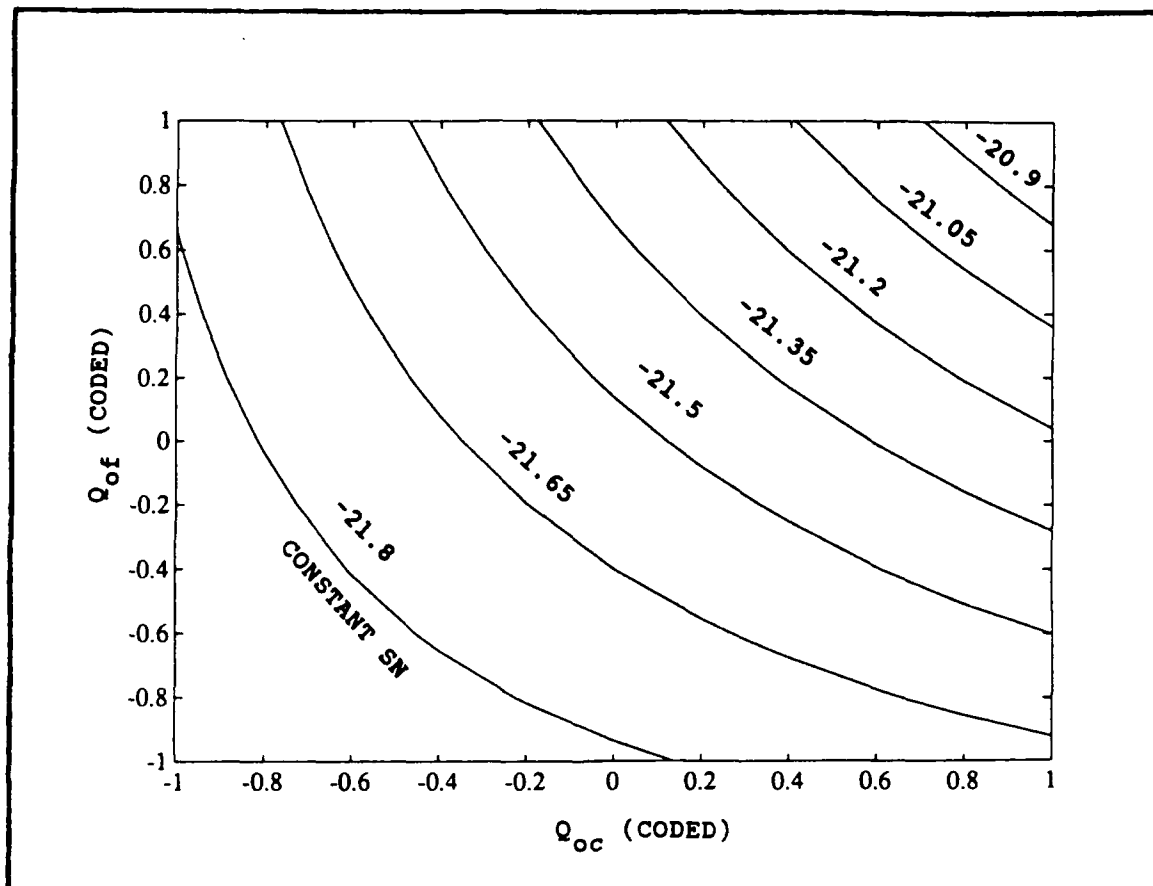
Figure 5-4 Estimator vs Controller State Weighting

It was originally hoped that Figure 5-4 would show a clear stationary ridge. If this had been the case, it could have been concluded that the estimator and controller gain were only measures of a more fundamental variable, namely compensator gain. However, this was not evident, but in order to reduce the number of inputs, Q_{of} was fixed at a coded 1 (uncoded value of 20), to coincide with the maximum signal-to-noise ratio. In all subsequent experiments Q_{of} was 20. Also R_{of} was set to an identity matrix for reasons

explained below.

After it was decided to investigate the controller gain
effects, Kc, the inputs to Kc were further restricted by only
varying Q_o, and not R_o. A small 3^2 experiment was performed
varying the diagonal elements of Q_o and R_o denoting these as
single variables Q_{oc} and R_{oc}. The regression analysis on the
t_r SN ratio is provided in Tables G-2 and G-3, Appendix G.
Again the contours for constant values of SN ratio are
plotted in Figure 5-5.
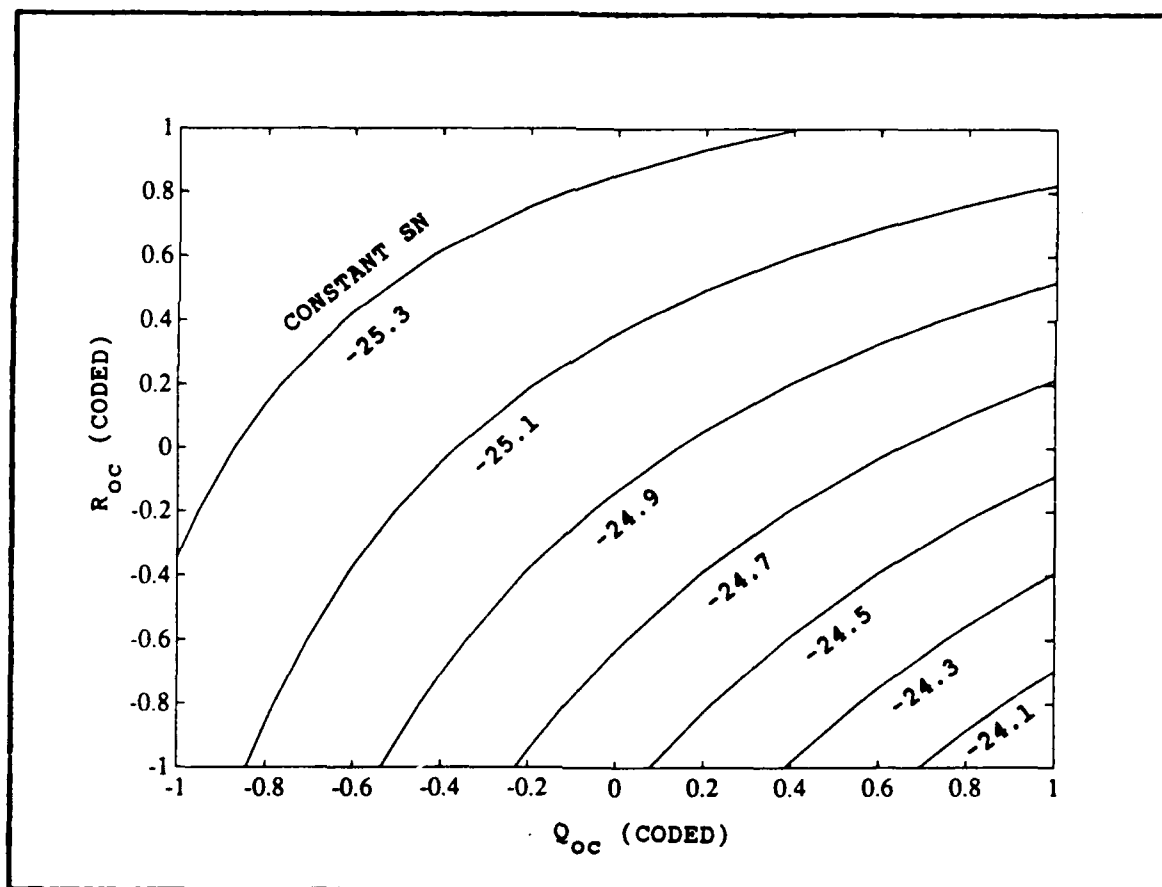
Figure 5-5 Control vs State Weighting

It was expected that the contours would show a stationary
ridge since the controller gain Kc is directly a function of
R_{oc} and Q_{oc} as described by Eqs (3.9) and (3.10). Again this

was not evident, but in order to reduce the number of inputs, R_{oc} was restricted to an identity matrix. While the regression analysis indicated that the effects of Q_{oc} and R_{oc} are very similar, Q_o was chosen as a design parameter because its matrix dimension is larger than the R_o matrix. The larger dimension allows for a more detailed adjustment on the states associated with the natural frequencies.

It is interesting to note that by examining Eq (3.8) the above results could have been deduced for the response time, but not necessarily the t_r SN ratio (the response time is a function of the size of gain). In Eq (3.8) it can be seen that a small R_o compared to a large Q_o simply means that the most performance improvement comes from reducing the amount of time to dampen the structure. The size of the control effort becomes a less important factor. This is the the same result (i.e. small R_o, large Q_o) that was experimentally determined for the t_r SN ratio. While this investigation didn't treat actuator energy as a response metric it is important and should be mentioned. If actuator energy had , en chosen as an output, a strictly small R_o and large Q_o would not have been the best setting. A good range of values for R_o and Q_o could have been selected by using both t_r and actuator energy in an initial screening type experiment. If a second response metric of total actuator or maximum actuator energy contour plot was overlaid on Figure 5-5, a region defining appropriate values of R_o and Q_o would have been defined. This region would represent the compromise

between quickly dampening system and the actuator energy. This side-point emphasizes the fact that simply maximizing the relationship shown in Figure 5-5 would not always be a wise decision since extremely large Q_o would over burden the actuators.

In summary, the response time, t_r, and signal-to-noise ratio of t_r were chosen as the response metrics. The noise inputs were sensor noise variation and modal truncation of the highest four modes. The design parameters included the 16 diagonal components of the Q_o matrix used in calculating the controller gain matrix Kc, and the particular arrangement of the lowest eight modes into a 3-2-3 decoupled controller. While this seems like a narrow slice of the total design problem, the possible combinations required to investigate is still quite astounding. This choice of variables represents a possible $3^6 \times 2^{16} \times 560$ or $2.7(10^6)$ combinations. Add to this the fact, the mathematical modeling requires three possible representative impulses, the design space grows to $8.03(10^6)$ combinations. The CSDL-I program written for this investigation required approximately 30 seconds CPU time to generate the time history necessary to compute t_r and t_r SN ratio. This equates to 76,354 years of CPU time to generate a complete data set. The power of RSM is utilized in the next section to intelligently probe and screen the design space to arrive at a good design.

Experiment

In order to find the best combinations of design

parameters out of the enormous possibilities, two functions must be accomplished; screen design parameters, and develop a relationship for only the important parameters. The following subsections will first examine the subcontroller mode arrangement then the controller gain.

Mode Arrangements. The first parameter screened was the arrangement of the eight highest modes in the 3-2-3 controller. Traditional RSM screening requires continuous independent variables. This makes it impossible to investigate each subcontroller separately as an independent parameter. For example, when different modes are assigned to subcontroller one, another subcontroller's modes must also change. This means the assignment of modes to subcontrollers must be treated as a single qualitative parameter consisting of 560 possible combinations. While it would be possible to investigate all 560 combinations for the CSDL-I, a larger more realistic model would require too much computational effort. This lead to the development of a heuristic to screen the design space without investigating all 560 design points.

In decoupled control the individual subcontrollers don't exercise the same amount of control over their particular assigned modes. Some of the subcontrollers must expend actuator energy to maintain orthogonality between subcontrollers so as to not destabilize each other. The condition used in Eq (3.34) enforces maximum controllability in subcontroller one, and minimum controllability in

subcontroller three. Likewise, it enforces maximum observability in subcontroller three and minimum observability in subcontroller one. It is also known that the lower frequency modes are more effective in controlling the structure than the higher modes. This logic leads to placing the lowest modes (i.e. 1,2,3) into subcontroller one, the next lowest (i.e. 4,5) into subcontroller two, etc. This ascending order (AO) design is usually a good design based on traditional practices. The important information it doesn't use is that certain modes tend to be aligned and prefer to be controlled together rather than in separated subcontrollers, Calico (3:43). The following rules determine a controller arrangement that keeps modes that are aligned together grouped in the same subcontroller.

Arrangement Heuristic. These rules are also shown in a flow chart type format in Figure 5-6.

1) Always place mode one in subcontroller one.

note: This rule is based on the fact that it is desirable to place the most controllable mode into the subcontroller able to enforce the most control.

2) Place the lowest modes into subcontrollers one (i.e. 1,2,3). Generate all possible combinations in subcontroller two while keeping subcontroller one modes fixed. Exercise model for a single impulse input and select the arrangements with the two shortest time of responses. For book keeping purposes designate the two controller arrangements as 2A and 2B. The 2A arrangement having the shorter response time.

note: See note for rule 3, page 5-14.

5-13

3) Place the highest modes into subcontroller one while still observing rule one (i.e. 1,7,8). Generate all possible combinations in subcontroller two while keeping subcontroller one modes fixed. Exercise model for the same impulse input as rule 2 and select the arrangements with the two shortest time of responses. For book keeping purposes designate the two controller arrangements as 3A and 3B. The 3A arrangement having the shorter response time.

note: The above two rules investigate the design space at two extremes. In rule two the most controllable modes are placed in subcontroller one and in three two the least controllable modes are assigned to subcontroller one.

4) If 2A and 3A contain different mode groups in subcontroller two fix these subcontroller two combinations and generate all possible arrangements for subcontroller one and three. If 2A and 3A contain the same mode groups in subcontroller two replace the longer response time arrangement, either 2A or 3A, with 2B or 3B respectively. Generate all possible combinations in subcontroller one and three. Exercise the model for a single impulse input and select the three shortest time responses for each unique controller two combination.

note: The above rule has made use of the fact that the two modes in subcontroller two had superior performance at the extreme ends of the design space. The modes prefer to be in the same controller.

5) Take the six arrangements selected from rule 4 and exercise the model for a different impulse direction. Select the three best arrangements from this second impulse.

note: The above rule tries to select arrangements that are robust to impulse direction. While impulse direction wasn't a noise variable in this investigation rule 5 is essential to selecting a good arrangement. It

5-14

is possible that an arrangement may have superior performance to a particular impulse by supplying control energy to a single mode that is especially sensitive to that particular impulse. An impulse from a different direction will reveal this situation as the controller arrangement will have significantly degraded performance for the different impulse.

The above heuristic was applied to the CSDL-I model yielding top three arrangements of 125-47-368, 126-47-358, and 158-47-236. A flow chart showing this process for the CSDL-I example is given in Figure 5-7. The heuristic required exercising the model a total of 43 times. A full factorial experiment was also performed on the model verifing the heuristic.

It would seem logical to select only one best arrangement from the heuristic, but this could lead to some problems. The CSDL-I model was exercised with all parameters fixed except the subcontroller arrangement. It could be possible that there are interaction effects between controller gain and subcontroller arrangement. By carrying forward at least three possible arrangements into the next screening experiment these second order effects may be revealed, but there is no guarantee. The final design cannot be called the "best" possible design, but only a "good" design.
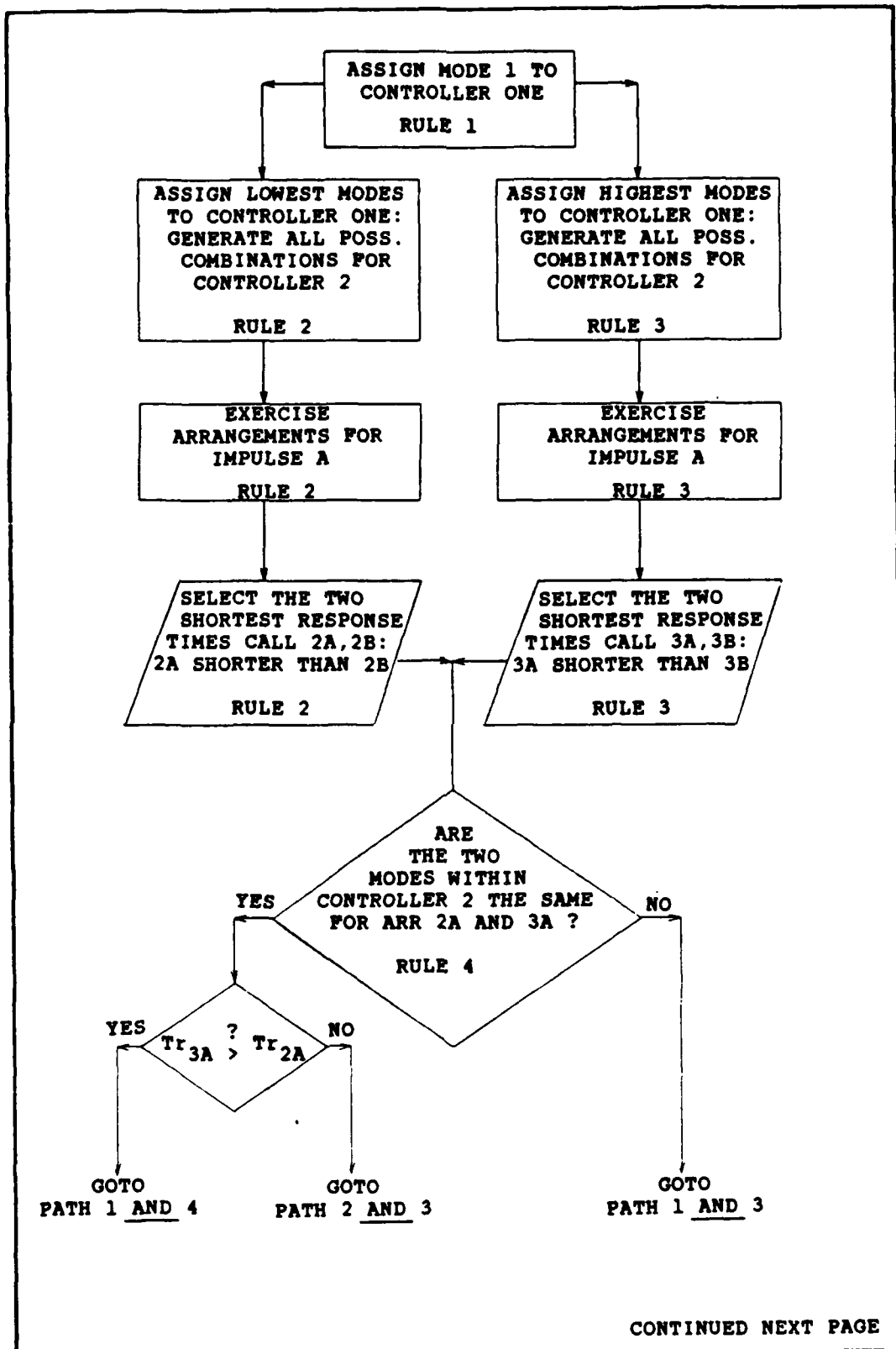
Figure 5-6 Modal Arrangement Heuristic
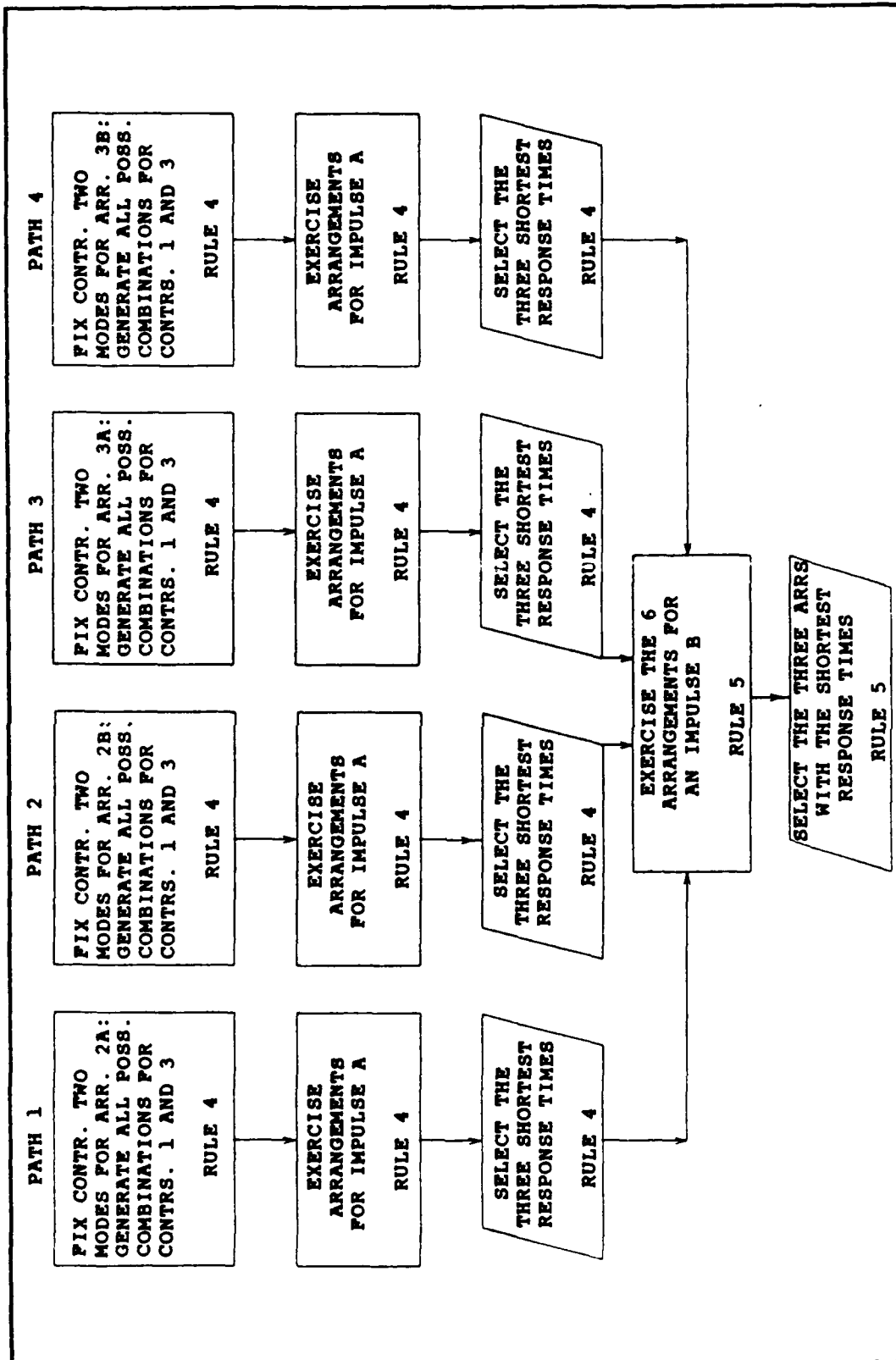
Figure 5-6 Modal Arrangement Heuristic (continued)
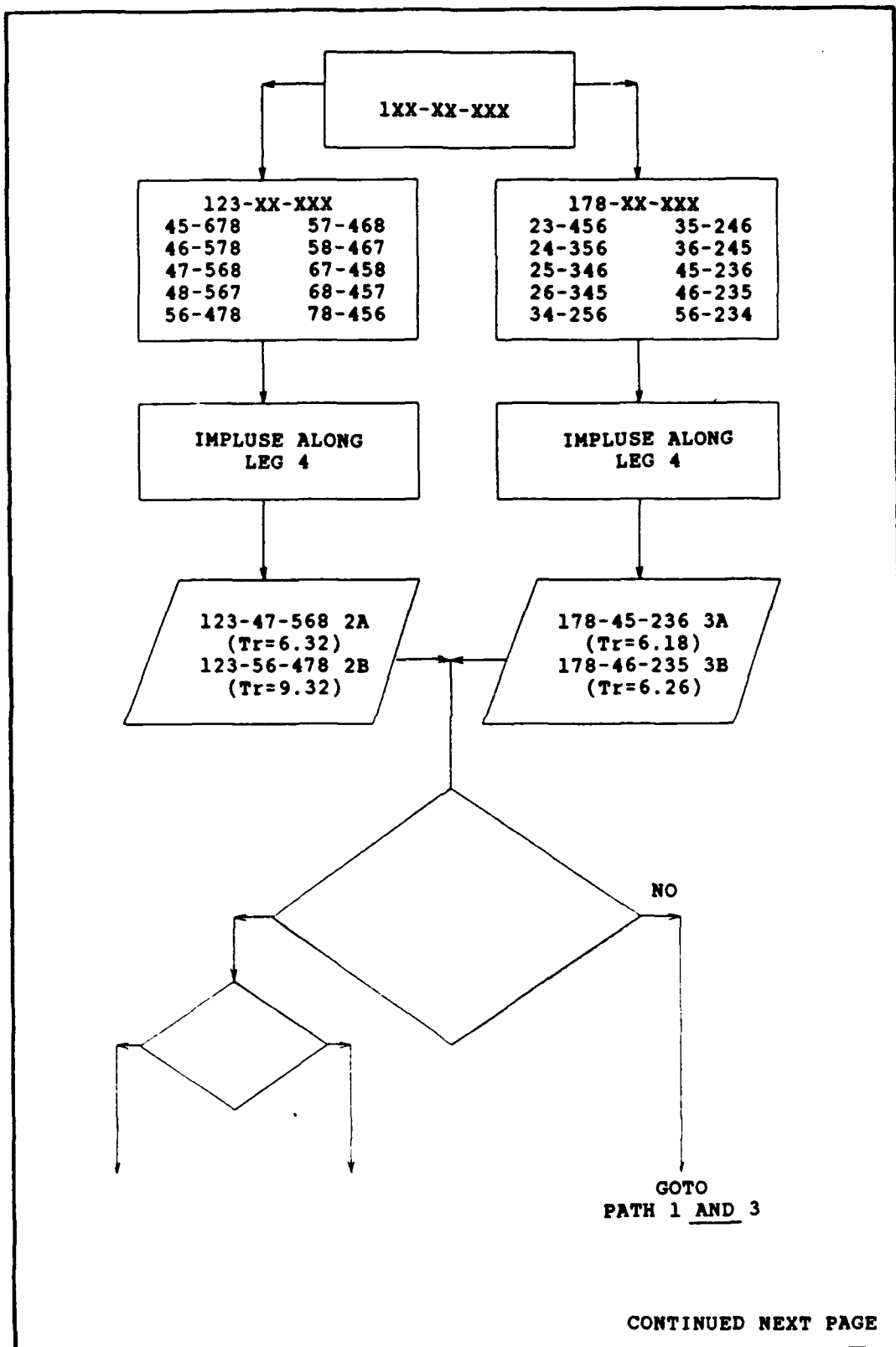
Figure 5-7 Modal Arrangement Heuristic Example

PATH 3

XXX-45-XXX (3A)
123-678 137-268
126-378 138-267
127-368 167-238
128-367 168-237
136-278 178-236

IMPLUSE ALONG
LEG 4

178-45-236
127-45-368
167-45-238

PATH 1

XXX-47-XXX (2A)
123-568 136-258
125-368 138-256
126-358 156-238
128-356 158-236
135-268 168-235

IMPLUSE ALONG
LEG 4

158-47-236
125-47-368
126-47-358

IMPLUSE ALONG
LEG 2

158-47-236 (Tr=4.30)
125-47-368 (Tr=7.52)
126-47-358 (Tr=7.56)
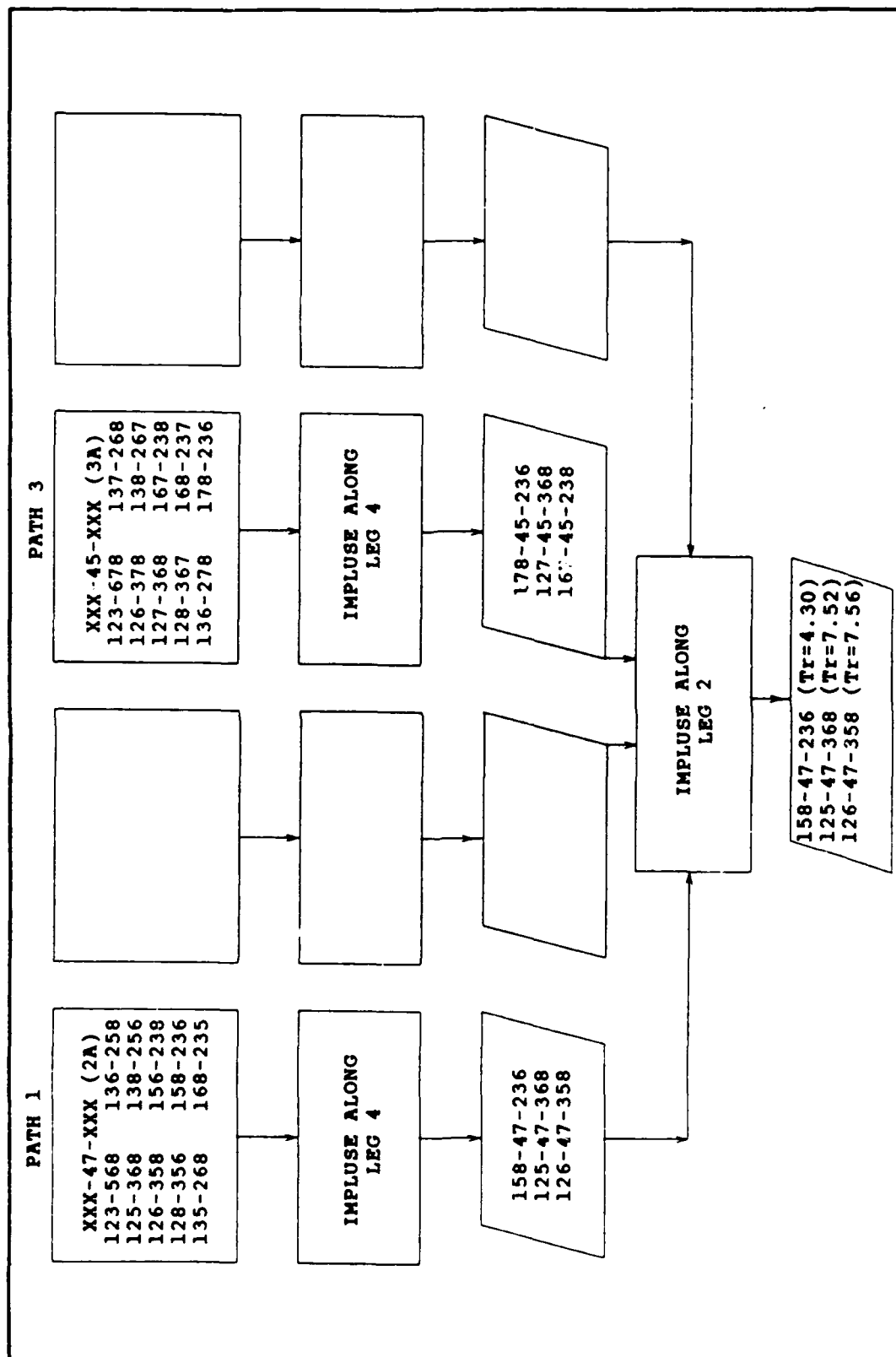
Figure 5-7 Modal Arrangement Heuristic Example (continued)

Controller Gains. The next design parameters screened were the 16 diagonal components of the Q_0 matrix used to calculate controller gains, Kc, as defined in Eq (3.8).

A group screening experiment was performed on the 16 factors. A group screening experiment logically arranges the individual factors into groups and then varies the groups as a whole to determine which groups are statistically significant. A basic assumption is that the important individual factors will be contained in the significant groups. The logical grouping of variables consisted of sorting the Q_0 elements by subcontroller and by velocity or position state. The six groups were varied from 20 for a low value to 40 for a high value using a 2^{6-2}_{IV} fractional experiment The experimental design matrix taken from Box and Draper (1:164) is listed in Appendix G. Three output variables were calculated, time of response, variance of time of response, and signal-to-noise ratio for time of response. The standard 3^{6-3}_{III} fractional design previously mentioned was used for the noise variable. The experiment was run for all three possible arrangements and the summary of results is contained in Tables G-5 and G-6, Appendix G for arrangement 126-47-358. This experiment was used to identify important groupings of the 16 Q_0 elements and to identify which of the three arrangements to carry forward for further experimentation.

Arrangement 126-47-358 was chosen as the best overall arrangement based on the average SN ratio and the average

variance of the time response. Arrangement 125-47-368 had an average SN ratio of -28.3 and an average variance of time response of 1.043. Arrangement 126-47-358 had an average SN ratio of -29.2 and an average variance of time response of .0467. Arrangement 158-47-236 had an average SN ratio of -29.4 and an average variance of time response of .096. The actual performance of the three arrangements was really quite similar. The SN ratio which was the primary output metric for designing a robust controller had a spread of only 4%. If the SN ratio had been strictly used, arrangement 125-47-368 would have been chosen since it had the largest SN ratio. By examining the results a little closer a better choice was made. The actual time response of all three arrangements was already determined as adequate by meeting an objective standard. Arrangement 126-47-358 had the lowest variance of all three, therefore, it was selected as the best arrangement based on its robustness to sensor error. Its signal-to-noise ratio wasn't superior only because its mean response time was slightly higher than the mean for arrangement 125-47-368, but as previously mentioned, this was already adequate and could be reduced by increasing feedback gain.

By examining the analysis of variance Table G-6 for t_r and SN in Appendix G it can be seen that the statistically significant groups for arrangement 126-47-358 were the Q_o groups for velocity state for modes in subcontroller one and the Q_o groups for velocity state for modes in subcontroller three. It seems reasonable that the velocity states should

be the most significant since in Eq (2.25) modal damping is associated with velocity states. These two significant groups represent six individual elements of the Q_o matrix.

The six elements or factors were then investigated to determine which of the six were significant, since the previous experiment only determined that the groupings were significant. The six factors were varied from a 20 for a low value to a 40 for a high value using a 2_{IV}^{6-2} fractional experiment. The factors from the insignificant groups were set to either the high or low value, whichever maximized the SN ratio. For example, the three Q_o elements for position states of the modes in subcontroller one were all set to the low value of 20 since the SN equation coefficient of this group was -.0113. It is important to set all the individual factors within the group to the same value so that the effects of the insignificant groups are aliased only with the mean. Design points at the center were used to check for any quadratic terms.

By examining the analysis of variance, Table G-7 and G-8 Appendix G, for t_r and SN it can be seen that the only significant factors were the Q_o elements for the velocity state of mode 3 in subcontroller three, and the velocity state of mode 8 in subcontroller three. These were the only statistically significant factors, but velocity state of mode 2 in subcontroller one was almost an order of magnitude more significant than any other factor, therefore it was carried forward into another experiment. It is interesting to note

that this result is not what would have been expected. Subcontroller one has the most control authority available, thus it would be expected that the modes in subcontroller one would be the significant modes in regulating the system. Evidently, the synergistic effect of modal grouping and the particular LOS requirement made the Q_o elements associated with the velocity states of modes 3 and 8 the most important. This result would have been difficult to determine without using RSM.

The final three significant factors, velocity state mode 3, velocity state mode 8, and velocity state mode 2 were further investigated for interaction terms using a 2^3 full-factorial experiment. It was found that only the velocity state mode 3, velocity state mode 8, and their interaction terms were significant as shown in Table G-9 and G-10, Appendix G. A final functional form was determined as:

$$SN = -29.2 + .086Q_{v3} + .071Q_{v8} + .059Q_{v3}Q_{v8} \qquad (5.1)$$

$$t_r = 5.57 - .057Q_{v3} - .047Q_{v8} - .04Q_{v3}Q_{v8} \qquad (5.2)$$

where

Q_{v3} = diagonal element of Q_o associated with velocity state of mode 3 in subcontroller three

Q_{v8} = diagonal element of Q_o associated with velocity state of mode 8 in subcontroller three

In Eq (5.1) there is no replication of the design points since the SN ratio is calculated across all of the noise settings. The absence of replications prevents the

computation of MS_e (pure error, Eq (4.8)) for the SN ratio regression. In Eq (5.2) there is replication of the design points associated with noise. The estimation of the standard deviation is $(MS_e)^{1/2}$ which is .1547. Typically, this large value of $(MS_e)^{1/2}$ would suggest that the coefficients in Eq (5.1) are of little use because of such a large underlying error. In this particular case the error that the $(MS_e)^{1/2}$ is measuring is the $\pm$ 20% sensor readings induced by the noise matrix. This large deviation may or may not be representative of real errors in a physical system, thus the coefficients may actually be larger than physical underlying error. The important observation to be made from Eq (5.1) is that the SN ratio is maximized by setting Q_{v3} and Q_{v8} to their high levels. It is also instructive to observe that even at the high levels of Q_{v3} and Q_{v8} the final SN ratio is changed very little. The Q_o factors had minimal effect on robustness of the system over the ranges of Q_o selected. A different range for Q_o might yield different results. Most of the increase in SN ratio was due to selecting a robust arrangement.

The error distribution of noise in the sensors can be further investigated by plotting the residuals of Eq (5.2). A residual plot is the graph of differences between the actual data points and the predicted values versus the predicted values. If the errors have constant variance and the model is specified correctly, the plot should have a

random scattering of points. The residual plot is shown in
Figure 5-8.
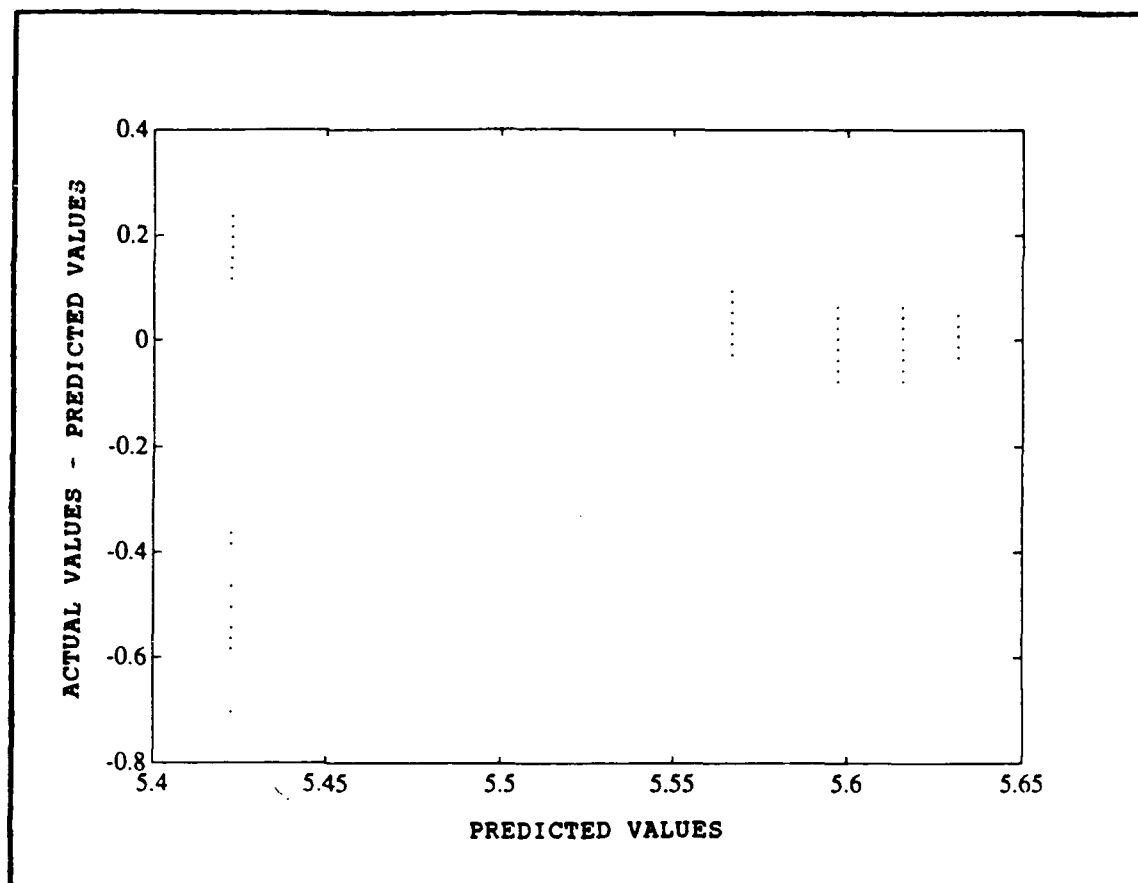
Figure 5-8 Residual Plot

It can be seen that the range of errors becomes smaller as
the magnitude of the response increases. This would suggest
a transformation of the output variable. A possible
transform might be $\log(t_r(max) - t_r)$. This was not actually
done since the range of differences between actual data
points and predicted points was so small, but other
situations may require such transforms.

At the end of the experiment the final design determined
consisted of:

1) A 3-2-3 controller arrangement with modal arrangement of 126-47-358.

2) An identity matrix for each of the R_o matrices used in calculating the control gains Kc and estimator gains Kf

3) A diagonal matrix of 20 for each of the Q_o matrices used in calculating the estimator gains Kf.

4) The following Q_o matrices used in calculating the controller gains Kc.

subcontroller one:
$$\begin{bmatrix} 20 & 0 & 0 & 0 & 0 & 0 \\ 0 & 20 & 0 & 0 & 0 & 0 \\ 0 & 0 & 20 & 0 & 0 & 0 \\ 0 & 0 & 0 & 20 & 0 & 0 \\ 0 & 0 & 0 & 0 & 40 & 0 \\ 0 & 0 & 0 & 0 & 0 & 40 \end{bmatrix}$$

subcontroller two:
$$\begin{bmatrix} 40 & 0 & 0 & 0 \\ 0 & 40 & 0 & 0 \\ 0 & 0 & 40 & 0 \\ 0 & 0 & 0 & 40 \end{bmatrix}$$

subcontroller three:
$$\begin{bmatrix} 40 & 0 & 0 & 0 & 0 & 0 \\ 0 & 40 & 0 & 0 & 0 & 0 \\ 0 & 0 & 40 & 0 & 0 & 0 \\ 0 & 0 & 0 & 40 & 0 & 0 \\ 0 & 0 & 0 & 0 & 40 & 0 \\ 0 & 0 & 0 & 0 & 0 & 40 \end{bmatrix}$$

After the final design was determined, a verification of the adequacy of the performance was accomplished. In the next chapter the performance of this design is compared to other designs.

VI. <u>Results</u>

The final robust design as described in the previous chapter was evaluated against three additional structural control conditions. The first additional condition was the structure with no-control representing the worst possible stable decoupled controller performance. The next condition was a full-order controller designed using total knowledge of the system. A control system based upon all twelve modes using LQR/LQE theory was implemented. All of the weighting matrices except for Q_o, used to compute Kc, were the same for the full-order controller as for the decoupled controller. The Q_o matrix was a diagonal matrix of 35 representing the center of the design space used in investigating the decoupled controller. This full-order design represents the best possible decoupled controller performance. The full-order controller doesn't have any residual modes and doesn't have to expend actuator energy to maintain subcontroller orthogonality. The last additional condition was an ascending order decoupled controller based on the first eight modes. The ascending order design represents the traditional design methodology. The ascending order design was constructed using LQR/LQE theory as previously developed with the same weighting matrices except Q_o, used to calculate Kc. The Q_o matrix was again a diagonal matrix of 35 to represent the center of the design.

In Figure 6-1 the moving average time history of all
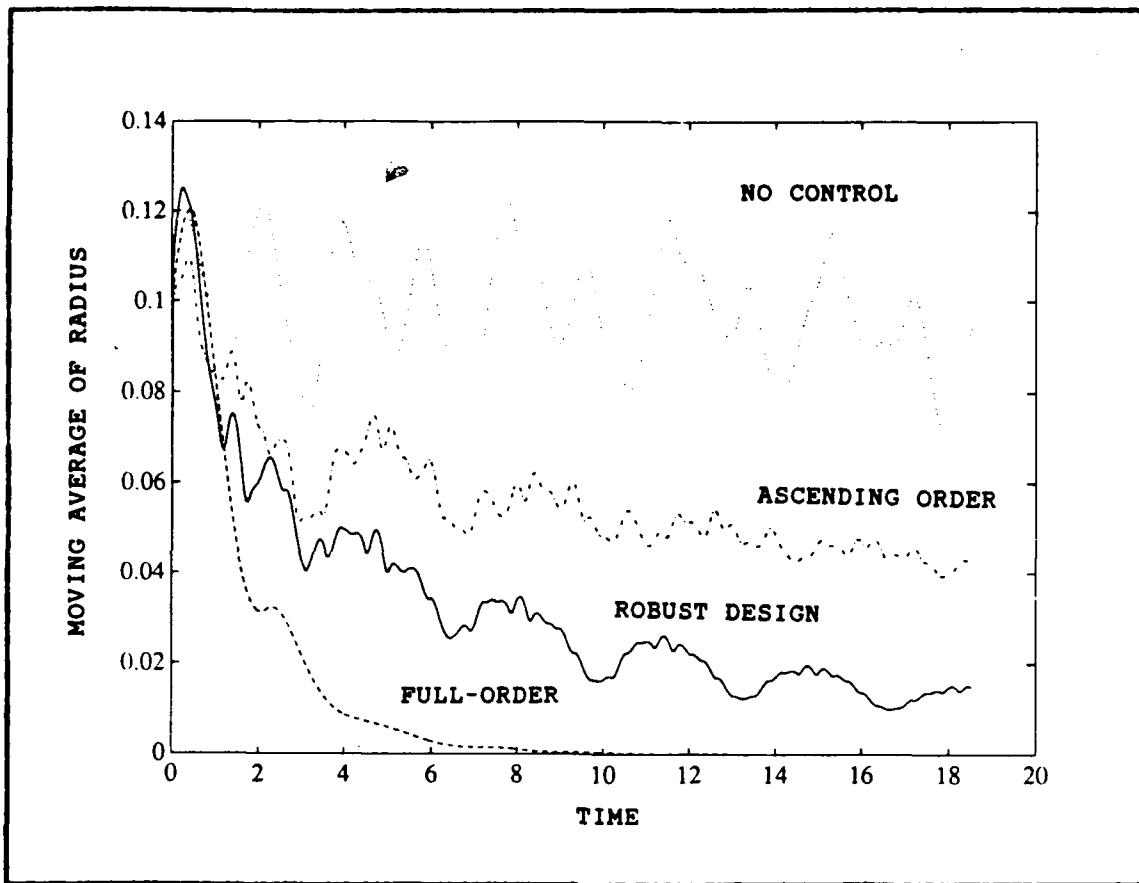
Figure 6-1 Moving Average of Radius vs Time

four conditions are plotted. It is clear to see that the
uncontrolled CSDL-I is extremely lightly damped as the moving
average decreases very little over the 20 second interval.
The full-order controller displays superior performance as
would be expected. This model has perfect knowledge of the
system, therefore, it is capable of enacting efficient
actuator authority. The ascending order design and robust
design, overall displayed fair performance. The robust
design is significantly better than the ascending order
design at long durations. While one cannot call the robust
design the optimum design due to numerous assumptions
preventing rigorous proof of optimallity, the robust design

can be considered a "good" design based upon the results of Figure 6-1.

In Figure 6-2 t_r is plotted against the 27 different sensor noise settings for the robust design, ascending order design, and the full-order design.
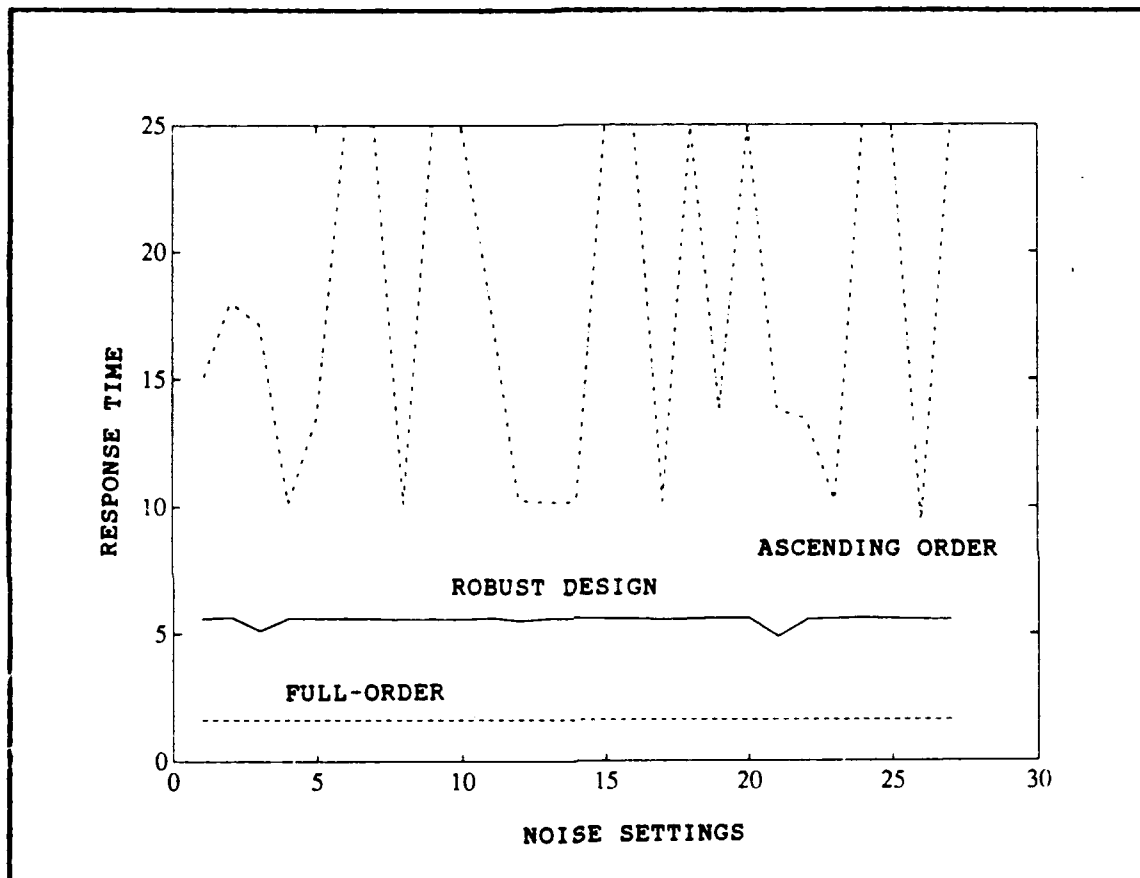
Figure 6-2 Reponse Time vs Noise Settings

The no-control design was obviously not plotted since it used no sensors or actuators. This figure demonstrates the robustness of each design. The full-order design is extremely robust to sensor error as shown in the graph. The ability to perfectly know the model allowed the system to drive the error states to zero very quickly. The sensor error gain multiplied by a zero displacement is still zero.

6-3

The robust decoupled design is also extremely robust to sensor noise. In fact, the only major disadvantage of the robust, decoupled design over a full-order design based upon Figure 6-1 and 6-2 is that the decoupled controller is slower in dampening the structure. The ascending order design is not a robust design. The particular settings of noise caused wild fluctuations in performance. This figure shows that modal grouping in decoupled control has a dramatic affect on sensitivity to sensor noise. The design techniques in this investigation produced a decoupled controller exhibiting more robustness than those of traditional design practices.

Before deciding to implement any controller design the performance required of the physical actuators must be known. In Figure 6-3 a plot of the time history of leg 9 actuator force is plotted. The plot was created from the state vector data for an impulse input with no sensor noise applied. The decoupled controller design's force time history was computed by summing the individual subcontroller actuator inputs as described in Eq (3.40). The full-order force time history was computed using Eq (3.6). As expected the full-order model is very efficient in using actuator energy to control the structure as it doesn't have to expend energy to maintain subcontroller orthogonality. It was surprising to see that the robust design was inputting significantly more energy into the actuators than the ascending order design. The gain matrices were computed using essentially the same weighting matrices. The different arrangements observe the system and

6-4
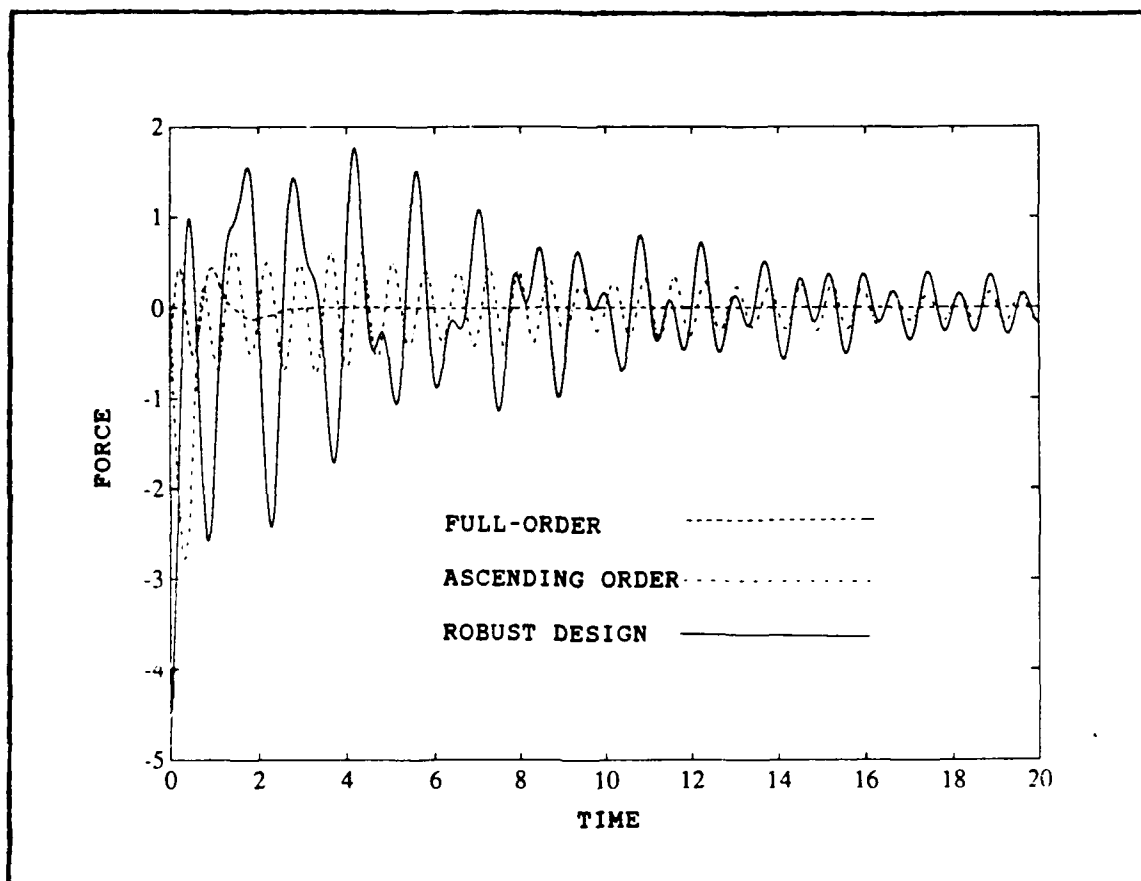
Figure 6-3 Leg 9 Actuator Force Time History

try to enforce control on the system differently, thus the
LQR/LQE theory computes different Kc and Kf matrices. It is
probable that the ascending order design has subcontroller
actuator inputs that are canceling each other out. This
would also explain the inability of the ascending design to
dampen the structure. From Figure 6-3 it can be seen that
the price paid for decoupled control in the robust design is
a larger actuator force requirement. As noted earlier if
actuator energy had been a response parameter it may be
possible to find a subcontroller arrangement that was less
robust, but also used less actuator authority.

VII. Conclusions and Recommendations

In conclusion, the statistical design methods developed in this investigation have produced a new decoupled controller design superior to a traditional design, namely the ascending order design. The statistical design mehtods employed signal-to-noise ratios, orthogonal numerical experiments, linear regression and a modal arrangement heuristic to efficiently explore the large design space. These methods reduced the computational efforts from a possible 76,354 years of CPU time for a global search method to only 16.5 Hrs of CPU time for the CSDL-I model. All of the design techniques used were general enough to apply to any size of structural control. It should be noted that the modal arrangement heuristic was only demonstrated on an eight mode 3-2-3 subcontroller arrangement and needs to be further investigated on other models, but should still be applicable to these other cases.

The first recommendation for further study is obviously to try the modal arrangement heuristic on other subcontroller arrangements. The 3-2-3 arrangement was very convenient since the middle controller contained only two modes. This allowed the screening techniques to directly generate pairs of modes that preferred to be together. For a larger subcontroller system, say 20-15-20, the exact procedure should yield good results, except the screening techniques would generate a set of 15 modes that prefer to be grouped

together. For a larger and more divided subcontroller system, say 30-15-10-30, the heuristic should still apply by simply grouping the 30 and 15 mode subcontrollers together and treating them as the first subcontroller. The 10 and 30 mode subcontroller would then be treated as the second and third subcontroller, respectively. Since the heuristic isn't based upon strict application of theory these possibilities should be exercised on other models and compared to the full factorial results.

The second recommendation for further study is to develop a response metric for actuator force output. As mentioned previously the performance of a control system must be implemented with real actuators that have a limited ability to apply control energy. A metric based upon either maximum force of any one actuator or, possibly, average energy supplied by an actuator could be used to screen modal arrangements and select controller gain. This second metric should be used in conjunction with the response time metric and the signal-to-noise type metric. This second metric may also be of benefit in selecting the range of weighting matrices, R_o and Q_o used in calculating gains. The important decision as to what range to investigate the system affects the final results since the techniques employed search for a local optimum and not a global optimum.

The third additional recommendation for further study is to investigate other sources of noise in the design process. The effects of perturbing the structural elements should be

examined. A change to the stiffness of an element will change the location of the natural frequencies, thus inducing noise to the system. Calico (3:44) investigated structural perturbations on the CSDL-I by examining open loop criteria in the form of reintroduction of coupling within the control and observation matrices. His preferred modal arrangement, 345-12-678, was robust to structural perturbations, but not extremely robust to sensor noise. This would indicate that a good design would be a comprise in robustness to various types of noise like sensor noise and structural miss-specification noise. This investigation could easily be accomplished by including the last lines of code from STIFF.M, Appendix B into the beginning of DECOUPLE.M, Appendix F and writing additional code to mesh the two together.

The final additional recommendation for further study is to build and exercise a control system based upon the proposed design techniques. The true test of a good design must be done in the lab. The design procedures only used knowledge of the first eight modes. The four residual modes represent all uncontrolled, unknown modes. It is asserted that if the controller doesn't destabilize the four residual modes it will probably not destabilize any other uncontrolled modes present. To verify this and other principles an actual experiment should be performed.

Appendix A

Global Coordinate Martrices K and D

Extended Stiffness Matrix for Element 3 in s Frame

Columns

1	2	3	4	5	6	7	8	9	10-30
0.2500	-0.1443	-0.4082	0	0	0	-0.2500	0.1443	0.4082	0...0
-0.1443	0.0833	0.2357	0	0	0	0.1443	-0.0833	-0.2357	:
-0.4082	0.2357	0.6667	0	0	0	0.4082	-0.2357	-0.6667	:
0	0	0	0	0	0	0	0	0	:
0	0	0	0	0	0	0	0	0	:
0	0	0	0	0	0	0	0	0	:
-0.2500	0.1443	0.4082	0	0	0	0.2500	-0.1443	-0.4082	:
0.1443	-0.0833	-0.2357	0	0	0	-0.1443	0.0833	0.2357	:
0.4082	-0.2357	-0.6667	0	0	0	-0.4082	0.2357	0.6667	:
0	0	0	0	0	0	0	0	0	:
0	0	0	0	0	0	0	0	0	:
0	0	0	0	0	0	0	0	0	:
0	0	0	0	0	0	0	0	0	:
0	0	0	0	0	0	0	0	0	:
0	0	0	0	0	0	0	0	0	:
0	0	0	0	0	0	0	0	0	:
0	0	0	0	0	0	0	0	0	:
0	0	0	0	0	0	0	0	0	:
0	0	0	0	0	0	0	0	0	:
0	0	0	0	0	0	0	0	0	:
0	0	0	0	0	0	0	0	0	:
0	0	0	0	0	0	0	0	0	:
0	0	0	0	0	0	0	0	0	:
0	0	0	0	0	0	0	0	0	:
0	0	0	0	0	0	0	0	0	:
0	0	0	0	0	0	0	0	0	:
0	0	0	0	0	0	0	0	0	:
0	0	0	0	0	0	0	0	0	:
0	0	0	0	0	0	0	0	0	:
0	0	0	0	0	0	0	0	0	0...0

Input Location Matrix, D in s Frame

Columns

1	2	3		5	6
0	0	0	0	0	0
0	0	0	0	0	0
0	0	0	0	0	0
-0.3536	0.3536	0	0	0	0
0.6124	-0.6124	0	0	0	0
-0.7071	-0.7071	0	0	0	0
0	0	-0.3536	0.3536	0	0
0	0	-0.6124	0.6124	0	0
0	0	-0.7071	-0.7071	0	0
0	0	0	0	0.7071	-0.7071
0	0	0	0	0	0
0	0	0	0	-0.7071	-0.7071

A-2

Total Stiffness Matrix K in s Frame with Boundry Conditions

Columns

1	2	3	4	5	6
13.7500	6.4952	18.3712	-12.5000	-7.2169	-20.4124
6.4952	6.2500	10.6066	-7.2169	-4.1667	-11.7851
18.3712	10.6066	40.0000	-20.4124	-11.7851	-33.3333
-12.5000	-7.2169	-20.4124	79.4194	21.2129	20.4124
-7.2169	-4.1667	-11.7851	21.2129	54.9249	11.7851
-20.4124	-11.7851	-33.3333	20.4124	11.7851	51.0110
-1.2500	0.7217	2.0412	-50.0000	0	0
0.7217	-0.4167	-1.1785	0	0	0
2.0412	-1.1785	-3.3333	0	0	0
0.0000	0.0000	0.0000	-12.5000	-21.6506	0
0.0000	-1.6667	2.3570	-21.6506	-37.5000	0
0.0000	2.3570	-3.3333	0	0	0

Columns Continued

7	8	9	10	11	12
-1.2500	0.7217	2.0412	0.0000	0.0000	0.0000
0.7217	-0.4167	-1.1785	0.0000	-1.6667	2.3570
2.0412	-1.1785	-3.3333	0.0000	2.3570	-3.3333
-50.0000	0	0	-12.5000	-21.6506	0
0	0	0	-21.6506	-37.5000	0
0	0	0	0	0	0
68.1694	-14.7177	-2.0412	-12.5000	21.6506	0
-14.7177	51.1749	1.1785	21.6506	-37.5000	0
-2.0412	1.1785	21.0110	0	0	0
-12.5000	21.6506	0	42.6777	0.0000	0.0000
21.6506	-37.5000	0	0.0000	76.6667	-2.3570
0	0	0	0.0000	-2.3570	21.0110

Appendix B

Listing of STIFF.M

```
%THIS IS A COMMAND FILE FOR FINDING THE STIFFNESS MATRIX
%INITIAL VARIABLES
%ZR-ZERO ROW,ZC-ZERO COLUMN,L-ROTATION MATRICES,K-STIFFNESS
ZR=[0,0,0,0,0,0;0,0,0,0,0,0;0,0,0,0,0,0];
ZC=[ZR,ZR,ZR,ZR,ZR];
ZC=ZC';
K=[1,0,0,-1,0,0;ZR((1:2),:);-1,0,0,1,0,0;ZR((1:2),:)];
%FIRST FIND THE INDIVIDUAL ROTATION MATRICES
%DEFINE MACROS
R2='[cos(B),0,-sin(B);0,1,0;sin(B),0,cos(B)]';
R3='[cos(C),sin(C),0;-sin(C),cos(C),0;0,0,1]';
%FINDING ROTATION MATRIX FOR ELEMENT ONE, B AND C ARE ANGLES
B=-.95531661830;
C=5*pi/6;
L1=eval(R3)*eval(R2);
L1=[L1',ZR(:,(1:3));ZR(:,(1:3)),L1'];
%FINDING ROTATION MATRIX FOR ELEMENT TWO
L2=[1,0,0;0,1,0;0,0,1];
L2=[L2',ZR(:,(1:3));ZR(:,(1:3)),L2'];
%FINDING ROTATION MATRIX FOR ELEMENT THREE
C=pi/6;
L3=eval(R3)*eval(R2);
L3=[L3',ZR(:,(1:3));ZR(:,(1:3)),L3'];
%FINDING REMAINING ROTATION MATRICES
C=-pi/2;
L4=eval(R3)*eval(R2);
L4=[L4',ZR(:,(1:3));ZR(:,(1:3)),L4'];
C=-pi/3;
L5=eval(R3);
L5=[L5',ZR(:,(1:3));ZR(:,(1:3)),L5'];
C=-2*pi/3;
L6=eval(R3);
L6=[L6',ZR(:,(1:3));ZR(:,(1:3)),L6'];
B=-pi/4;
L7=eval(R3)*eval(R2);
L7=[L7',ZR(:,(1:3));ZR(:,(1:3)),L7'];
C=pi/3;
L8=eval(R3)*eval(R2);
L8=[L8',ZR(:,(1:3));ZR(:,(1:3)),L8'];
C=2*pi/3;
L9=eval(R3)*eval(R2);
L9=[L9',ZR(:,(1:3));ZR(:,(1:3)),L9'];
C=-pi/3;
L10=eval(R3)*eval(R2);
L10=[L10',ZR(:,(1:3));ZR(:,(1:3)),L10'];
L11=eval(R2);
L11=[L11',ZR(:,(1:3));ZR(:,(1:3)),L11'];
C=pi;
L12=eval(R3)*eval(R2);
L12=[L12',ZR(:,(1:3));ZR(:,(1:3)),L12'];
%FIND THE ROTATED STIFFNES MATRICES FOR EACH ELEMENT
K1=L1'*K*L1;
K2=L2'*K*L2;
```

```
K3=L3'*K*L3;
K4=L4'*K*L4;
K5=L5'*K*L5;
K6=L6'*K*L6;
K7=L7'*K*L7;
K8=L8'*K*L8;
K9=L9'*K*L9;
K10=L10'*K*L10;
K11=L11'*K*L11;
K12=L12'*K*L12;
%FIND EXTENDED STIFFNESS MATRICES FOR GLOBAL COORDINATES
K1E=[K1;ZR;ZR;ZR;ZR;ZR;ZR;ZR;ZR];
K1E=[K1E,ZC,ZC,ZC,ZC,ZC,ZC,ZC,ZC];
K2E=[ZR;K2;ZR;ZR;ZR;ZR;ZR;ZR;ZR];
K2E=[ZC,K2E,ZC,ZC,ZC,ZC,ZC,ZC,ZC];
K3E=[K3((1:3),:);ZR;K3((4:6),:);ZR;ZR;ZR;ZR;ZR;ZR;ZR];
K3E=[K3E(:,(1:3)),ZC,K3E(:,(4:6)),ZC,ZC,ZC,ZC,ZC,ZC,ZC];
K4E=[K4((1:3),:);ZR;ZR;K4((4:6),:);ZR;ZR;ZR;ZR;ZR;ZR];
K4E=[K4E(:,(1:3)),ZC,ZC,K4E(:,(4:6)),ZC,ZC,ZC,ZC,ZC,ZC];
K5E=[ZR;K5((1:3),:);ZR;K5((4:6),:);ZR;ZR;ZR;ZR;ZR;ZR];
K5E=[ZC,K5E(:,(1:3)),ZC,K5E(:,(4:6)),ZC,ZC,ZC,ZC,ZC,ZC];
K6E=[ZR;ZR;K6;ZR;ZR;ZR;ZR;ZR;ZR];
K6E=[ZC,ZC,K6E,ZC,ZC,ZC,ZC,ZC,ZC];
K7E=[ZR;K7((1:3),:);ZR;ZR;K7((4:6),:);ZR;ZR;ZR;ZR;ZR];
K7E=[ZC,K7E(:,(1:3)),ZC,ZC,K7E(:,(4:6)),ZC,ZC,ZC,ZC,ZC];
K8E=[ZR;K8((1:3),:);ZR;ZR;ZR;K8((4:6),:);ZR;ZR;ZR;ZR];
K8E=[ZC,K8E(:,(1:3)),ZC,ZC,ZC,K8E(:,(4:6)),ZC,ZC,ZC,ZC];
K9E=[ZR;ZR;K9((1:3),:);ZR;ZR;ZR;K9((4:6),:);ZR;ZR;ZR];
K9E=[ZC,ZC,K9E(:,(1:3)),ZC,ZC,ZC,K9E(:,(4:6)),ZC,ZC,ZC];
K10E=[ZR;ZR;K10((1:3),:);ZR;ZR;ZR;ZR;K10((4:6),:);ZR;ZR];
K10E=[ZC,ZC,K10E(:,(1:3)),ZC,ZC,ZC,ZC,K10E(:,(4:6)),ZC,ZC];
K11E=[ZR;ZR;ZR;K11((1:3),:);ZR;ZR;ZR;ZR;K11((4:6),:);ZR];
K11E=[ZC,ZC,ZC,K11E(:,(1:3)),ZC,ZC,ZC,ZC,K11E(:,(4:6)),ZC];
K12E=[ZR;ZR;ZR;K12((1:3),:);ZR;ZR;ZR;ZR;ZR;K12((4:6),:)];
K12E=[ZC,ZC,ZC,K12E(:,(1:3)),ZC,ZC,ZC,ZC,ZC,K12E(:,(4:6))];
%COMBINE THE STIFFNESS MATRICES TOGETHER,THEN APPLY BOUNDRY
%COND. THE BOUNDRY CONDITONS ARE U13-U30 = 0
%SINCE ONLY INTERESTED IN DYNAMIC RESPONSE APPLY BOUNDRY
%COND THEN ADD STIFFNESS TOGETHER, THIS CREATES THE FORM
%K TOTAL= EA/L*K1E + EA/L*K2E ETC. WHERE EACH EA/L COULD BE
%DIFFERENT FOR EACH ELEMENT, APPLY NOISE TO THE EA/L TERM
K1D=K1E((1:12),(1:12));
K2D=K2E((1:12),(1:12));
K3D=K3E((1:12),(1:12));
K4D=K4E((1:12),(1:12));
K5D=K5E((1:12),(1:12));
K6D=K6E((1:12),(1:12));
K7D=K7E((1:12),(1:12));
K8D=K8E((1:12),(1:12));
K9D=K9E((1:12),(1:12));
K10D=K10E((1:12),(1:12));
K11D=K11E((1:12),(1:12));
K12D=K12E((1:12),(1:12));
%COMBINE TO TOTAL FINAL STIFFNESS
C1=100;
```

```
C2=10;
C3=100/sqrt(8);
LEGS=C3*(K7D+K8D+K9D+K10D+K11D+K12D);
KD=C1*K1D+C1*K2D+C2*K3D+C2*K4D+C1*K5D+C1*K6D+LEGS;
```

Appendix C

Listing of SENSOR.M

.

```
%THIS IS A COMMAND FILE FOR FINDING THE SENSOR MATRIX D
%INITIAL VARIABLES
%ZR-ZERO ROW,ZC-ZERO COLUMN,L-ROTATION MATRICES
ZR=[0,0,0,0,0,0;0,0,0,0,0,0;0,0,0,0,0,0];
ZC=[ZR,ZR,ZR,ZR,ZR];
ZC=ZC';
K=[1,0,0, 0,0,0;ZR((1:2),:); 0,0,0,0,0,0;ZR((1:2),:)];
%FIRST FIND THE INDIVIDUAL ROTATION MATRICES
%DEFINE MACROS
R2='[cos(B),0,-sin(B);0,1,0;sin(B),0,cos(B)]';
R3='[cos(C),sin(C),0;-sin(C),cos(C),0;0,0,1]';
C=-2*pi/3;
B=-pi/4;
L7=eval(R3)*eval(R2);
L7=[L7',ZR(:,(1:3));ZR(:,(1:3)),L7'];
C=pi/3;
L8=eval(R3)*eval(R2);
L8=[L8',ZR(:,(1:3));ZR(:,(1:3)),L8'];
C=2*pi/3;
L9=eval(R3)*eval(R2);
L9=[L9',ZR(:,(1:3));ZR(:,(1:3)),L9'];
C=-pi/3;
L10=eval(R3)*eval(R2);
L10=[L10',ZR(:,(1:3));ZR(:,(1:3)),L10'];
L11=eval(R2);
L11=[L11',ZR(:,(1:3));ZR(:,(1:3)),L11'];
C=pi;
L12=eval(R3)*eval(R2);
L12=[L12',ZR(:,(1:3));ZR(:,(1:3)),L12'];
K7=L7'*K;
K8=L8'*K;
K9=L9'*K;
K10=L10'*K;
K11=L11'*K;
K12=L12'*K;
K7E=[ZR;K7((1:3),:);ZR;ZR;K7((4:6),:);ZR;ZR;ZR;ZR;ZR];
K7E=[ZC,K7E(:,(1:3)),ZC,ZC,K7E(:,(4:6)),ZC,ZC,ZC,ZC,ZC];
K8E=[ZR;K8((1:3),:);ZR;ZR;ZR;K8((4:6),:);ZR;ZR;ZR;ZR];
K8E=[ZC,K8E(:,(1:3)),ZC,ZC,ZC,K8E(:,(4:6)),ZC,ZC,ZC,ZC];
K9E=[ZR;ZR;K9((1:3),:);ZR;ZR;ZR;K9((4:6),:);ZR;ZR;ZR];
K9E=[ZC,ZC,K9E(:,(1:3)),ZC,ZC,ZC,K9E(:,(4:6)),ZC,ZC,ZC];
K10E=[ZR;ZR;K10((1:3),:);ZR;ZR;ZR;ZR;K10((4:6),:);ZR;ZR];
K10E=[ZC,ZC,K10E(:,(1:3)),ZC,ZC,ZC,ZC,K10E(:,(4:6)),ZC,ZC];
K11E=[ZR;ZR;ZR;K11((1:3),:);ZR;ZR;ZR;ZR;K11((4:6),:);ZR];
K11E=[ZC,ZC,ZC,K11E(:,(1:3)),ZC,ZC,ZC,ZC,K11E(:,(4:6)),ZC];
K12E=[ZR;ZR;ZR;K12((1:3),:);ZR;ZR;ZR;ZR;ZR;K12((4:6),:)];
K12E=[ZC,ZC,ZC,K12E(:,(1:3)),ZC,ZC,ZC,ZC,ZC,K12E(:,(4:6))];
K7D=K7E((1:12),(1:12));
K8D=K8E((1:12),(1:12));
K9D=K9E((1:12),(1:12));
K10D=K10E((1:12),(1:12));
K11D=K11E((1:12),(1:12));
K12D=K12E((1:12),(1:12));
```

```
%COMBINING INTO FINAL MATRIX
D=[K7D(:,4),K8D(:,4),K9D(:,7),K10D(:,7),..
K11D(:,10),K12D(:,10)];
```

Appendix D

State-space Matrices A,B and C

State-space Plant Matrix A Full-order System
Columns

1	2	3	4	5	6	7
0	0	0	0	0	0	0
0	0	0	0	0	0	0
0	0	0	0	0	0	0
0	0	0	0	0	0	0
0	0	0	0	0	0	0
0	0	0	0	0	0	0
0	0	0	0	0	0	0
0	0	0	0	0	0	0
0	0	0	0	0	0	0
0	0	0	0	0	0	0
0	0	0	0	0	0	0
0	0	0	0	0	0	0
-1.8010	0	0	0	0	0	0
0	-2.7714	0	0	0	0	0
0	0	-8.3562	0	0	0	0
0	0	0	-8.7462	0	0	0
0	0	0	0	-11.5474	0	0
0	0	0	0	0	-17.6777	0
0	0	0	0	0	0	-21.7349
0	0	0	0	0	0	0
0	0	0	0	0	0	0
0	0	0	0	0	0	0
0	0	0	0	0	0	0
0	0	0	0	0	0	0

8	9	10	11	12	13	14
0	0	0	0	0	1.0000	0
0	0	0	0	0	0	1.0000
0	0	0	0	0	0	0
0	0	0	0	0	0	0
0	0	0	0	0	0	0
0	0	0	0	0	0	0
0	0	0	0	0	0	0
0	0	0	0	0	0	0
0	0	0	0	0	0	0
0	0	0	0	0	0	0
0	0	0	0	0	0	0
0	0	0	0	0	0	0
0	0	0	0	0	-0.0134	0
0	0	0	0	0	0	-0.0166
0	0	0	0	0	0	0
0	0	0	0	0	0	0
0	0	0	0	0	0	0
0	0	0	0	0	0	0
-22.6127	0	0	0	0	0	0
0	-72.9227	0	0	0	0	0
0	0	-85.5732	0	0	0	0
0	0	0	-105.7785	0	0	0
0	0	0	0	-166.5441	0	0

15	16	17	18	19	20	21
0	0	0	0	0	0	0
0	0	0	0	0	0	0
1.0000	0	0	0	0	0	0
0	1.0000	0	0	0	0	0
0	0	1.0000	0	0	0	0
0	0	0	1.0000	0	0	0
0	0	0	0	1.0000	0	0
0	0	0	0	0	1.0000	0
0	0	0	0	0	0	1.0000
0	0	0	0	0	0	0
0	0	0	0	0	0	0
0	0	0	0	0	0	0
0	0	0	0	0	0	0
-0.0289	0	0	0	0	0	0
0	-0.0296	0	0	0	0	0
0	0	-0.0340	0	0	0	0
0	0	0	-0.0420	0	0	0
0	0	0	0	-0.0466	0	0
0	0	0	0	0	-0.0476	0
0	0	0	0	0	0	-0.0854
0	0	0	0	0	0	0
0	0	0	0	0	0	0
0	0	0	0	0	0	0

22	23	24
0	0	0
0	0	0
0	0	0
0	0	0
0	0	0
0	0	0
0	0	0
0	0	0
0	0	0
1.0000	0	0
0	1.0000	0
0	0	1.0000
0	0	0
0	0	0
0	0	0
0	0	0
0	0	0
0	0	0
0	0	0
0	0	0
-0.0925	0	0
0	-0.1028	0
0	0	-0.1291

State-space Input Matrix B

Columns

1	2	3	4	5	6
0	0	0	0	0	0
0	0	0	0	0	0
0	0	0	0	0	0
0	0	0	0	0	0
0	0	0	0	0	0
0	0	0	0	0	0
0	0	0	0	0	0
0	0	0	0	0	0
0	0	0	0	0	0
0	0	0	0	0	0
0	0	0	0	0	0
0	0	0	0	0	0
0.0621	-0.0621	-0.0948	-0.0327	0.0327	0.0948
-0.0976	-0.0976	-0.0236	0.1582	0.1582	-0.0236
-0.0651	-0.0651	-0.3838	0.1095	0.1095	-0.3838
-0.3518	0.3518	0.0843	-0.2674	0.2674	-0.0843
0.4969	0.4969	-0.0686	0.2200	0.2200	-0.0686
-0.4082	0.4082	-0.4082	0.4082	-0.4082	0.4082
0.0689	-0.0689	-0.5217	-0.4528	0.4528	0.5217
0.0978	0.0978	-0.4232	-0.5162	-0.5162	-0.4232
0.3266	0.3266	0.3539	-0.3238	-0.3238	0.3539
0.4483	-0.4483	-0.2123	0.2360	-0.2360	0.2123
-0.3117	-0.3117	0.2067	-0.2049	-0.2049	0.2067
-0.1611	-0.1611	0.0187	-0.0351	-0.0351	0.0187

State-space Output Matrix, C

Columns

1	2	3	4	5	6	7
0.0621	-0.0976	-0.0651	-0.3518	0.4969	-0.4082	0.0689
-0.0621	-0.0976	-0.0651	0.3518	0.4969	0.4082	-0.0689
-0.0948	-0.0236	-0.3838	0.0843	-0.0686	-0.4082	-0.5217
-0.0327	0.1582	0.1095	-0.2674	0.2200	0.4082	-0.4528
0.0327	0.1582	0.1095	0.2674	0.2200	-0.4082	0.4528
0.0948	-0.0236	-0.3838	-0.0843	-0.0686	0.4082	0.5217

Columns Continued

8	9	10	11	12	13-24
0.0978	0.3266	0.4483	-0.3117	-0.1611	0...0
0.0978	0.3266	-0.4483	-0.3117	-0.1611	.
-0.4232	0.3539	-0.2123	0.2067	0.0187	.
-0.5162	-0.3238	0.2360	-0.2049	-0.0351	.
-0.5162	-0.3238	-0.2360	-0.2049	-0.0351	.
-0.4232	0.3539	0.2123	0.2067	0.0187	0...0

Appendix E

Total Plant Matrix of Decoupled Control

State-space Closed Looped Plant Matrix, Ae, Suppressed
for Arrangement 123-45-678 $Q_o=20$, $R_o=1$

Columns

1	2	3	4	5	6	7
0	0	0	1.0000	0	0	0
0	0	0	0	1.0000	0	0
0	0	0	0	0	1.0000	0
-1.9495	0.0000	0.0000	-0.9242	0.0000	0.0000	-0.1485
0.0000	-2.8973	-0.4290	0.0000	-1.3451	-0.4175	0.0000
0.0000	0.3469	-9.0286	0.0000	-0.7197	-2.6710	0.0000
0	0	0	0	0	0	0.0000
0	0	0	0	0	0	0.0000
0	0	0	0	0	0	0.0000
0	0	0	0	0	0	-1.8010
0	0	0	0	0	0	0.0000
0	0	0	0	0	0	0.0000
0	0	0	0	0	0	0
0	0	0	0	0	0	0
0.2250	0.0000	0.0000	1.3797	0.0000	0.0000	0.2250
0.0000	0.1455	0.0873	0.0000	0.5705	-0.3528	0.0000
-0.4261	0.0000	0.0000	0	0	0	0
0.0000	-0.2210	0.3103	0	0	0	0
-0.0513	0.0000	0.0000	0	0	0	0
0.0000	-0.0238	0.0334	0	0	0	0
0	0	0	0	0	0	0
0	0	0	0	0	0	0
0	0	0	0	0	0	0
0.0000	0.0000	0.0000	0.0000	0.0000	0.0000	0.0000
-0.7314	0.0000	0.0000	-4.4856	0.0000	0.0000	-0.7314
0.0000	0.9032	0.6338	0.0000	3.7579	-2.0031	0.0000
0.0000	0.0000	0.0000	0	0	0	0
0.6323	0.0000	0.0000	0	0	0	0
0.0000	-0.7694	0.9432	0	0	0	0
0.0000	0.0000	0.0000	0	0	0	0
0.0331	0.0000	0.0000	0	0	0	0
0.0000	-0.0348	0.0426	0	0	0	0
0	0	0	0	0	0	0
0	0	0	0	0	0	0
0	0	0	0	0	0	0
0	0	0	0	0	0	0
0.0000	-0.0464	1.3373	0.0000	3.0425	2.9039	0.0000
-0.4294	0.0000	0.0000	-2.6332	0.0000	0.0000	-0.4294
0.0000	-0.2373	0.2378	0.0000	-0.0323	1.3528	0.0000
0.0000	-0.0684	-0.0992	0.0000	-0.4055	0.0468	0.0000

8	9	10	11	12	13	14
0	0	0	0	0	0	0
0	0	0	0	0	0	0
0	0	0	0	0	0	0
0.0000	0.0000	-0.9108	0.0000	0.0000	0.0000	0.0000
-0.1259	-0.4290	0.0000	-1.3284	-0.4175	0.0000	0.0000
0.3469	-0.6724	0.0000	-0.7197	-2.6421	0.0000	0.0000
0.0000	0.0000	1.0000	0	0	0.0000	0.0000
-0.9230	-2.4710	0	1.0000	0	0.0000	0.0000
-0.8526	-2.2825	0	0	1.0000	0.0000	0.0000
0.0000	0.0000	-0.0134	0	0	0.0000	0.0000
-2.1047	1.7849	0	-0.0166	0	0.0000	0.0000
-0.9802	-10.9804	0	0	-0.0289	0.0000	0.0000
0	0	0	0	0	0	0
0	0	0	0	0	0	0
0.0000	0.0000	1.3797	0.0000	0.0000	-9.1275	0.0000
0.1455	0.0873	0.0000	0.5705	-0.3528	0.0000	-12.0382
0	0	0	0	0	0	0
0	0	0	0	0	0	0
0	0	0	0	0	0	0
0	0	0	0	0	0	0
0	0	0	0	0	0	0
0	0	0	0	0	0	0
0	0	0	0	0	0	0
0.0000	0.0000	0.0000	0.0000	0.0000	0.0000	0.0000
0.0000	0.0000	-4.4856	0.0000	0.0000	-0.3508	0.0000
0.9032	0.6338	0.0000	3.7579	-2.0031	0.0000	0.1737
0	0	0	0	0	0.0000	0.0000
0	0	0	0	0	0.4875	0.0000
0	0	0	0	0	0.0000	-0.3407
0	0	0	0	0	0.0000	0.0000
0	0	0	0	0	0.0255	0.0000
0	0	0	0	0	0.0000	-0.0154
0	0	0	0	0	0	0
0	0	0	0	0	0	0
0	0	0	0	0	0	0
0	0	0	0	0	0	0
-0.0464	1.3373	0.0000	3.0425	2.9039	0.0000	-0.1001
0.0000	0.0000	-2.6332	0.0000	0.0000	0.3978	0.0000
-0.2373	0.2378	0.0000	-0.0323	1.3528	0.0000	0.3391
-0.0684	-0.0992	0.0000	-0.4055	0.0468	0.0000	0.1418

Columns

15	16	17	18	19	20	21
0	0	0	0	0	0	0
0	0	0	0	0	0	0
0	0	0	0	0	0	0
0.0000	0.0000	0.0000	0.0000	0.0000	0.0000	0.0000
0.0000	0.0000	0.0000	0.0000	0.0000	0.0000	0.0000
0.0000	0.0000	0.0000	0.0000	0.0000	0.0000	0.0000
0	0	0	0	0	0	0.0000
0	0	0	0	0	0	0.0000
0	0	0	0	0	0	0.0000
0	0	0	0	0	0	0.0000
0	0	0	0	0	0	0.0000
0	0	0	0	0	0	0.0000
1.0000	0	0	0	0	0	0
0	1.0000	0	0	0	0	0
-2.7531	0.0000	-0.3814	0.0000	-2.7236	0.0000	0.0000
0.0000	-3.5440	0.0000	-0.4909	0.0000	-3.5101	0.0000
0	0	-2.9269	0.0000	1.0000	0	0.0000
0	0	0.0000	-3.5573	0	1.0000	0.0000
0	0	-9.0985	0.0000	-0.0296	0	0.0000
0	0	0.0000	-11.9308	0	-0.0340	0.0000
0	0	0	0	0	0	0
0	0	0	0	0	0	0
0	0	0	0	0	0	0
0.0000	0.0000	0.0000	0.0000	0.0000	0.0000	-18.2346
-2.5054	0.0000	-0.3508	0.0000	-2.5054	0.0000	0.0000
0.0000	1.2424	0.0000	0.1737	0.0000	1.2424	0.0000
0	0	0	0	0	0	0
0	0	0	0	0	0	0
0	0	0	0	0	0	0
0	0	0	0	0	0	0
0	0	0	0	0	0	0
0	0	0	0	0	0	0
0	0	0	0	0	0	0
0	0	0	0	0	0	0
0	0	0	0	0	0	0
0	0	0	0	0	0	0
0.0000	-0.7155	0.0000	-0.1001	0.0000	-0.7155	0.0000
2.8408	0.0000	0.3978	0.0000	2.8408	0.0000	0.0000
0.0000	2.4249	0.0000	0.3391	0.0000	2.4249	0.0000
0.0000	1.0139	0.0000	0.1418	0.0000	1.0139	0.0000

22	23	24	25	26	27	28
0	0	0	0	0	0	0
0	0	0	0	0	0	0
0	0	0	0	0	0	0
0.0000	0.0000	0.0000	0.0000	0.0000	0.0000	0.0000
0.0000	0.0000	0.0000	0.0000	0.0000	0.0000	0.0000
0.0000	0.0000	0.0000	0.0000	0.0000	0.0000	0.0000
0.0000	0.0000	0	0	0	0	0
0.0000	0.0000	0	0	0	0	0
0	0.0000	0	0	0	0	0
0	0.0000	0	0	0	0	0
0.0000	0.0000	0	0	0	0	0
0	0.0000	0	0	0	0	0
0	0	0	0	0	0	0
0	0	0	0	0	0	0
0.0000	0.0000	0.0000	0.0000	0.0000	0.0000	0.0000
0.0000	0.0000	0.0000	0.0000	0.0000	0.0000	0.0000
0.0000	0.0000	0	0	0	0	0
0.0000	0.0000	0	0	0	0	0
0.0000	0.0000	0	0	0	0	0
0.0000	0.0000	0	0	0	0	0
0	0	1.0000	0	0	0	0
0	0	0	1.0000	0	0	0
0	0	0	0	1.0000	0	0
0.0000	0.0000	-4.5952	0.0000	0.0000	-0.5569	0.0000
-21.7349	0.0000	0.0000	-0.0466	0.0000	0.0000	0.0000
0.0000	-22.6127	0.0000	0.0000	-0.0476	0.0000	0.0000
0	0	0	0	0	-4.5533	0.0000
0	0	0	0	0	0.0000	-4.4433
0	0	0	0	0	0.0000	0.0000
0	0	0	0	0	-18.0441	0.0000
0	0	0	0	0	0.0000	-21.9678
0	0	0	0	0	0.0000	0.0000
0	0	0	0	0	0	0
0	0	0	0	0	0	0
0	0	0	0	0	0	0
0	0	0	0	0	0	0
0.0000	0.0000	0.0000	0.0000	0.0000	0.0000	0.0000
0.0000	0.0000	0.0000	0.0000	0.0000	0.0000	0.0000
0.0000	0.0000	0.0000	0.0000	0.0000	0.0000	0.0000
0.0000	0.0000	0.0000	0.0000	0.0000	0.0000	0.0000

29	30	31	32	33	34	35
0	0	0	0	0	0	0
0	0	0	0	0	0	0
0	0	0	0	0	0	0
0.0000	0.0000	0.0000	0.0000	0	0	0
0.0000	0.0000	0.0000	0.0000	0	0	0
0.0000	0.0000	0.0000	0.0000	0	0	0
0	0	0	0	0.0000	0.0000	0.0000
0	0	0	0	-3.7106	0.0000	-1.0634
0	0	0	0	-3.4276	0.0000	-0.9823
0	0	0	0	0.0000	0.0000	0.0000
0	0	0	0	2.6804	0.0000	0.7682
0	0	0	0	-3.9408	0.0000	-1.1294
0	0	0	0	0	0	0
0	0	0	0	0	0	0
0.0000	0.0000	0.0000	0.0000	0	0	0
0.0000	0.0000	0.0000	0.0000	0	0	0
0	0	0	0	0.0000	-3.6116	0.0000
0	0	0	0	0.8460	0.0000	-2.5745
0	0	0	0	0.0000	-0.4347	0.0000
0	0	0	0	0.0912	0.0000	-0.2775
0	0	0	0	0	0	0
0	0	0	0	0	0	0
0	0	0	0	0	0	0
0.0000	-4.5531	0.0000	0.0000	0	0	0
0.0000	0.0000	0.0000	0.0000	0	0	0
0.0000	0.0000	0.0000	0.0000	0	0	0
0.0000	1.0000	0	0	0.0000	0.0000	0.0000
0.0000	0	1.0000	0	0.0000	0.3205	0.0000
-4.3123	0	0	1.0000	0.4677	0.0000	-0.1155
0.0000	-0.0420	0	0	0.0000	0.0000	0.0000
0.0000	0	-0.0466	0	0.0000	0.0168	0.0000
-22.8076	0	0	-0.0476	0.0211	0.0000	-0.0052
0	0	0	0	0	0	0
0	0	0	0	0	0	0
0	0	0	0	0	0	0
0	0	0	0	0	0	0
0.0000	0.0000	0.0000	0.0000	-72.9227	0	0
0.0000	0.0000	0.0000	0.0000	0	-85.5732	0
0.0000	0.0000	0.0000	0.0000	0	0	-105.7785
0.0000	0.0000	0.0000	0.0000	0	0	0

		Columns		
36	37	38	39	40
0	0	0	0	0
0	0	0	0	0
0	0	0	0	0
0	0	0	0	0
0	0	0	0	0
0	0	0	0	0
0.0000	0	0	0	0
0.1506	0	0	0	0
0.1391	0	0	0	0
0.0000	0	0	0	0
-0.1088	0	0	0	0
0.1599	0	0	0	0
0	0	0	0	0
0	0	0	0	0
0	0	0	0	0
0	0	0	0	0
0.0000	0	0	0	0
-1.0712	0	0	0	0
0.0000	0	0	0	0
-0.1155	0	0	0	0
0	0	0	0	0
0	0	0	0	0
0	0	0	0	0
0	0	0	0	0
0	0	0	0	0
0	0	0	0	0
0.0000	0	0	0	0
0.0000	0	0	0	0
-0.0526	0	0	0	0
0.0000	0	0	0	0
0.0000	0	0	0	0
-0.0024	0	0	0	0
0	1.0000	0	0	ʋ
0	0	1.0000	0	0
0	0	0	1.0000	0
0	0	0	0	1.0000
0	-0.0854	0	0	0
0	0	-0.0925	0	0
0	0	0	-0.1028	0
166.5441	0	0	0	-0.1291

Appendix F

Listing of DECOUPLE.M

```
%THIS M-FILE CALCULATES A TIME HISTORY RESPONSE METRIC FOR 3
%DECOUPLED LQR CONTROLLERS APPLIED TO THE CSDL1
%THE VARIABLES REQUIRED IN THE WORK SPACE ARE:
%THE IMPORTANT OUTPUT VARIABLES ARE:
load input.mat
chdir ga90m:[jbrewer.matlab.output]
for i=1:length(n(1,:))
CON1M1=n(1,i);
CON1M2=n(2,i);
CON1M3=n(3,i);
CON2M1=n(4,i);
CON2M2=n(5,i);
CON3M1=n(6,i);
CON3M2=n(7,i);
CON3M3=n(8,i);
RESM1=n(9,i);
RESM2=n(10,i);
RESM3=n(11,i);
RESM4=n(12,i);
%FORMING THE INDIVIDUAL A MATRICES FOR EACH CONTROLLER,
%A MODAL DAMPING OF .005 IS USED
W=[V(CON1M1,1),0,0;0,V(CON1M2,1),0;0,0,V(CON1M3,1)];
ZW=-2*.005*sqrt(W);
W=-W;
A1=[zeros(3),eye(3);W,ZW];
W=[V(CON2M1,1),0;0,V(CON2M2,1)];
ZW=-2*.005*sqrt(W);
W=-W;
A2=[zeros(2),eye(2);W,ZW];
W=[V(CON3M1,1),0,0;0,V(CON3M2,1),0;0,0,V(CON3M3,1)];
ZW=-2*.005*sqrt(W);
W=-W;
A3=[zeros(3),eye(3);W,ZW];
%FIND THE RESIDUAL A MATRIX
W=[V(RESM1,1),0,0,0;0,V(RESM2,1),0,0;0,0,V(RESM3,1),0;..
  0,0,0,V(RESM4,1)];
ZW=-2*.005*sqrt(W);
W=-W;
AR=[zeros(4),eye(4);W,ZW];
%FIND THE INDIVIDUAL CONTROLLER'S Bj MATRIX USING THE ORG
%STATESPACE MODEL D MATRIX (INPUT MATRIX)
B=U'*D;
B1=[zeros(3,6);B(CON1M1,:);B(CON1M2,:);B(CON1M3,:)];
B2=[zeros(2,6);B(CON2M1,:);B(CON2M2,:)];
B3=[zeros(3,6);B(CON3M1,:);B(CON3M2,:);B(CON3M3,:)];
%FIND THE RESDUAL MODE'S B MATRIX
BR=[zeros(4,6);B(RESM1,:);B(RESM2,:);B(RESM3,:);B(RESM4,:)];
%DIVIDE THE UNPRETURBED  C MATRIX INTO CORRECT Cj MATRIX
%FOR EACH CONTROLLER
C=(U'*D)';
C1=[C(:,CON1M1),C(:,CON1M2),C(:,CON1M3)];
C1=[C1,zeros(6,3)];
C2=[C(:,CON2M1),C(:,CON2M2)];
```

F-2

```
C2=[C2,zeros(6,2)];
C3=[C(:,CON3M1),C(:,CON3M2),C(:,CON3M3)];
C3=[C3,zeros(6,3)];
CR=[C(:,RESM1),C(:,RESM2),C(:,RESM3),C(:,RESM4)];
CR=[CR,zeros(6,4)];
%CONVERT INDIVIDUAL CONTROLLER MATRICES TO A DECOUPLED SUB-
%SPACE,USING THE RELATIONSHIP BiTj=0 AND GAMiCj=0 i=1,2 j=2,3
T1=eye(6,6);
T2=null(B1);
T3=null([B1;B2]);
GAM1=null([C2,C3]');
GAM2=null(C3');
GAM3=eye(6,6);
B1STAR=B1*T1;
B2STAR=B2*T2;
B3STAR=B3*T3;
C1STAR=GAM1'*C1;
C2STAR=GAM2'*C2;
C3STAR=GAM3'*C3;
%DESIGN A LINEAR QUADRATIC REGULATOR AND ESTIMATOR FOR EACH
%CONTROLLER, Rc-CONROL WEIGHTING, QcL AND QcL STATE WT.
%NOTE THE SIX DIFFERENT SIZES OF THE CONTROL WEIGHTING
%GAINS. Rc1 IS USED TO FIND CON1 CONTROLLER GAINS, WHILE
%Rf1 IS USED TO FIND CON1 ESTIMATOR GAINS
eval(['COMB',int2str(i),'=zeros(length(Qc(1,:)),..
length(NOISE(1,:))); '])
for qc=1:length(Qc(1,:))
Rc1=eye(length(T1'*T1));
Rc2=eye(length(T2'*T2));
Rc3=eye(length(T3'*T3));
Rf1=eye(length(GAM1'*GAM1));
Rf2=eye(length(GAM2'*GAM2));
Rf3=eye(length(GAM3'*GAM3));
%ASSUME NOISE IS DECOUPLED IN THE MODAL STATES
GAML=eye(6,6);
GAMS=eye(4,4);
%STATE CONTROLL WEIGHTING VARIATION
%eval(['COMB',int2str(i),'= zeros(length(Qc(1,:)),..
length(NOISE(1,:))); '])
%for qc=1:length(Qc(1,:))
Qcf1=20*eye(6,6);
Qcf2=20*eye(4,4);
Qcf3=20*eye(6,6);
%Qc1=diag(Qc((1:3),qc),0);
Qc1=[20*eye(3,3),zeros(3,3);zeros(3,3),..
diag([20,Qc(1,qc),35])];
%Qc1=Qc(qc)*eye(6,6);
%Qc2=diag(Qc((4:5),qc),0);
Qc2=[35*eye(2,2),zeros(2,2);zeros(2,2),35*eye(2,2)];
%Qc2=Qc(qc)*eye(4,4);
%Qc3=diag(Qc((4:6),qc),0);
Qc3=[35*eye(3,3),zeros(3,3);zeros(3,3),..
diag([Qc(2,qc),35,Qc(3,qc)])];
%Qc3=Qc(qc)*eye(6,6);
%FIND GAINS FOR CONTROLLER AND ESTIMATOR USING lqr, lge
```

```
%A NEG SIGN IS REQUIRED ON CONTROLLER GAIN DUE TO THE WAY
%MATLAB DEFINES FEEDBACK, AND THE WAY THE THESIS EQUATIONS
%DEFINE IT.ALSO NOTE GAINS ARE CALCULATED FOR UNPRETURBED
%STATES
Kc1=-lqr(A1,B1STAR,Qc1,Rc1);
Kf1=lqe(A1,GAML,C1STAR,Qcf1,Rf1);
Kc2=-lqr(A2,B2STAR,Qc2,Rc2);
Kf2=lqe(A2,GAMS,C2STAR,Qcf2,Rf2);
Kc3=-lqr(A3,B3STAR,Qc3,Rc3);
Kf3=lqe(A3,GAML,C3STAR,Qcf3,Rf3);
%USE ORGINAL INPUT MATRIX B WITH ADDTIIONAL ERROR STATES ADD
%AS THE REFERENCE INPUT MATRIX TO CONVERT AN IMPULSE AT ONE
%OF THE LEGS INTO THE MODAL COORDINATE SYSTEM
Btotal=[B;zeros(28,6)];
%
%THE ABOVE Btotal WAS THE REFERENCE INPUT MATRIX USED TO
%GENERATE ALL OF THE THESIS DATA. IT ACTUALLY APPLIES INITIAL
%VELOCITY CONDITIONS INSTEAD OF DISPLACEMENT CONDITIONS. THE
%FINAL SELECTED COMBINATION CHANGES VERY LITTLE SINCE ALL
%COMBINATIONS ARE COMPARED TO THE SAME REF. INPUT. IF FURTHER
%WORK IS DONE I WOULD SUGGEST CHANGING THE ABOVE LINE TO
% [zeros(12,6);B;zeros(16,6)]; AS THIS MATCHES EQ 3.19
%ALSO CHANGING THE MOVING AVERAGE CUT OF FROM .05 TO .01 IS
%NECESSARY SINCE THE NEW Btotal INPUTS LESS ENERGY
%
%EXTRACT NOISE VARIABLES FROM INPUT MATRIX NOISE
%THREE LEVELS OF NOISE ARE .8 1.0 AND 1.2 MULTIPLIERS
%NOISE7 IS NOISE APPLIED TO THE SENSOR ON LEG 7, ETC
for  j=1:length(NOISE(1,:))
NOISE7=NOISE(1,j);
NOISE8=NOISE(2,j);
NOISE9=NOISE(3,j);
NOISE10=NOISE(4,j);
NOISE11=NOISE(5,j);
NOISE12=NOISE(6,j);
%THIS FINDS THE C MATRIX AFTER APPLYING THE NOISE TO THE
%SENSORS IN LOCAL COORDINATE FRAME AND ROTATING INTO MODAL CD
%ZR-ZERO ROW,ZC-ZERO COLUMN,L-ROTATION MATRICES,K-INPUT LOCAL
ZR=[0,0,0,0,0,0;0,0,0,0,0,0;0,0,0,0,0,0];
ZC=[ZR,ZR,ZR,ZR,ZR];
ZC=ZC';
K=[1,0,0, 0,0,0;ZR((1:2),:); 0,0,0,0,0,0;ZR((1:2),:)];
%FIRST FIND THE INDIVIDUAL ROTATION MATRICES
%DEFINE MACROS
R2='[cos(Ba),0,-sin(Ba);0,1,0;sin(Ba),0,cos(Ba)]';
R3='[cos(Ca),sin(Ca),0;-sin(Ca),cos(Ca),0;0,0,1]';
Ca=-2*pi/3;
Ba=-pi/4;
L7=eval(R3)*eval(R2);
L7=[L7',ZR(:,(1:3));ZR(:,(1:3)),L7'];
Ca=pi/3;
L8=eval(R3)*eval(R2);
L8=[L8',ZR(:,(1:3));ZR(:,(1:3)),L8'];
Ca=2*pi/3;
L9=eval(R3)*eval(R2);
```

```
L9=[L9',ZR(:,(1:3));ZR(:,(1:3)),L9'];
Ca=-pi/3;
L10=eval(R3)*eval(R2);
L10=[L10',ZR(:,(1:3));ZR(:,(1:3)),L10'];
L11=eval(R2);
L11=[L11',ZR(:,(1:3));ZR(:,(1:3)),L11'];
Ca=pi;
L12=eval(R3)*eval(R2);
L12=[L12',ZR(:,(1:3));ZR(:,(1:3)),L12'];
K7=L7'*(NOISE7*K);
K8=L8'*(NOISE8*K);
K9=L9'*(NOISE9*K);
K10=L10'*(NOISE10*K);
K11=L11'*(NOISE11*K);
K12=L12'*(NOISE12*K);
K7E=[ZR;K7((1:3),:);ZR;ZR;K7((4:6),:);ZR;ZR;ZR;ZR;ZR];
K7E=[ZC,K7E(:,(1:3)),ZC,ZC,K7E(:,(4:6)),ZC,ZC,ZC,ZC,ZC];
K8E=[ZR;K8((1:3),:);ZR;ZR;ZR;K8((4:6),:);ZR;ZR;ZR;ZR];
K8E=[ZC,K8E(:,(1:3)),ZC,ZC,ZC,K8E(:,(4:6)),ZC,ZC,ZC,ZC];
K9E=[ZR;ZR;K9((1:3),:);ZR;ZR;ZR;K9((4:6),:);ZR;ZR;ZR];
K9E=[ZC,ZC,K9E(:,(1:3)),ZC,ZC,ZC,K9E(:,(4:6)),ZC,ZC,ZC];
K10E=[ZR;ZR;K10((1:3),:);ZR;ZR;ZR;ZR;K10((4:6),:);ZR;ZR];
K10E=[ZC,ZC,K10E(:,(1:3)),ZC,ZC,ZC,ZC,K10E(:,(4:6)),ZC,ZC];
K11E=[ZR;ZR;ZR;K11((1:3),:);ZR;ZR;ZR;ZR;K11((4:6),:);ZR];
K11E=[ZC,ZC,ZC,K11E(:,(1:3)),ZC,ZC,ZC,ZC,K11E(:,(4:6)),ZC];
K12E=[ZR;ZR;ZR;K12((1:3),:);ZR;ZR;ZR;ZR;ZR;K12((4:6),:)];
K12E=[ZC,ZC,ZC,K12E(:,(1:3)),ZC,ZC,ZC,ZC,ZC,K12E(:,(4:6))];
K7D=K7E((1:12),(1:12));
K8D=K8E((1:12),(1:12));
K9D=K9E((1:12),(1:12));
K10D=K10E((1:12),(1:12));
K11D=K11E((1:12),(1:12));
K12D=K12E((1:12),(1:12));
Dn=[K7D(:,4),K8D(:,4),K9D(:,7),K10D(:,7),K11D(:,10),..
K12D(:,10)];
Ctotal=[(U'*Dn)',zeros(6,28)];
%DIVIDE THE PRETURBED C MATRIX INTO CORRECT Cj MATRIX
%FOR EACH CONTROLLER
Ce1=[Ctotal(:,CON1M1),Ctotal(:,CON1M2),Ctotal(:,CON1M3)];
Ce1=[Ce1,zeros(6,3)];
Ce2=[Ctotal(:,CON2M1),Ctotal(:,CON2M2)];
Ce2=[Ce2,zeros(6,2)];
Ce3=[Ctotal(:,CON3M1),Ctotal(:,CON3M2),Ctotal(:,CON3M3)];
Ce3=[Ce3,zeros(6,3)];
CeR=[Ctotal(:,RESM1),Ctotal(:,RESM2),Ctotal(:,RESM3),..
Ctotal(:,RESM4)];
CeR=[CeR,zeros(6,4)];
%COMBINING THE DECOUPLED CONTROLLERS BACK INTO A SINGLEPLANT
%MATRIX INCLUDING THE ERROR STATES (MODES NOT IN ORDER !)
%NOTE PRETURBED C MATRICES ARE USED IN FEEDBACK!
Atotal=[(A1+B1STAR*Kc1),B1STAR*Kc1,B1*T2*Kc2,B1*T2*Kc2,..
        B1*T3*Kc3,B1*T3*Kc3,zeros(6,8);..
zeros(6,6),(A1-Kf1*GAM1'*Ce1),Kf1*GAM1'*Ce2,zeros(6,4),..
        Kf1*GAM1'*Ce3,zeros(6,6),Kf1*GAM1'*CeR];
Atotal=[Atotal;B2*T1*Kc1,B2*T1*Kc1,(A2+B2STAR*Kc2),B2STAR*Kc2,..
```

```
              B2*T3*Kc3,B2*T3*Kc3,zeros(4,8);..
     Kf2*GAM2'*Cel,zeros(4,6),zeros(4,4),(A2-Kf2*GAM2'*Ce2),..
              Kf2*GAM2'*Ce3,zeros(4,6),Kf2*GAM2'*CeR];
     Atotal=[Atotal;B3*T1*Kcl,B3*T1*Kcl,B3*T2*Kc2,B3*T2*Kc2,..
              (A3+B3STAR*Kc3),B3STAR*Kc3,zeros(6,8);..
     Kf3*GAM3'*Cel,zeros(6,6),Kf3*GAM3'*Ce2,zeros(6,4),zeros(6,6)..
              (A3-Kf3*GAM3'*Ce3),Kf3*GAM3'*CeR];
     Atotal=[Atotal;BR*T1*Kcl,BR*T1*Kcl,BR*T2*Kc2,BR*T2*Kc2,..
              BR*T3*Kc3,BR*T3*Kc3,AR];
     %SORT Atotal MATRIX INTO MODAL SEQ BY ROWS FIRST
     Ahold=zeros(48,40);
     POSCON=n(1:8,i);
     POSRES=n(9:12,i);
     RM=POSRES;
     MIXED=[1 2 3 13 14 21 22 23];
     MIXEDR=[33 34 35 36];
     CTY=[3 3 3 2 2 3 3 3];
     for h=1:1:4
     Ahold(POSCON,:)=Atotal(MIXED,:);
     POSCON=POSCON + 12;
     MIXED=MIXED+CTY;
     end
     for g=1:1:2
     Ahold(POSRES,:)=Atotal(MIXEDR,:);
     POSRES=POSRES+12;
     MIXEDR=MIXEDR+4;
     end
     %REMOVING ROWS CORRESPONDING TO NONEXISTANT RESIDUAL ERROR
     %STATES
     RM=[(RM+24),(RM+36)];
     Ahold(RM,:)=[];
     %SORT Atotal INTO MODAL SEQ BY COLUMNS USING Ahold
     Asort=zeros(40,48);
     POSCON=n(1:8,i);
     POSRES=n(9:12,i);
     RM=POSRES;
     MIXED=[1 2 3 13 14 21 22 23];
     MIXEDR=[33 34 35 36];
     CTY=[3 3 3 2 2 3 3 3];
     for h=1:1:4
     Asort(:,POSCON)=Ahold(:,MIXED);
     POSCON=POSCON + 12;
     MIXED=MIXED+CTY;
     end
     for g=1:1:2
     Asort(:,POSRES)=Ahold(:,MIXEDR);
     POSRES=POSRES+12;
     MIXEDR=MIXEDR+4;
     end
     %REMOVING COLUMNS CORRESPONDING TO NONEXISTANT RESIDUAL ERROR
     %STATES
     RM=[(RM+24),(RM+36)];
     Asort(:,RM)=[];
     %REDUCING MEMORY REQUIREMENTS BY CLEARING VARIABLES
     clear W ZW;
```

```
clear ZR ZC K L7 L8 L9 L10 L11 L12;
clear K7 K8 K9 K10 K11 K12 K7E K8E K9E K10E K11E K12E;
clear K7D K8D K9D K10D K11D K12D Dn;
clear Atotal C Ce1 Ce2 Ce3 CeR;
clear Ahold POSCON POSRES RM MIXED CTY MIXEDR;
%SIMULATE SYSTEM RESPONSE TO AN IMPULSE AT LEG10 (4th ACTOR)
%NOTE DUE TO SYMMETRY ONLY AN INPUT AT ANY ONE OF THE SIX
%LEGS PRODUCES SIMILAR OUTPUT ONLY IN DIFFERENT DIRECTIONS
% x IS THE STATE TIME HISTORY, y IS WHAT THE SENSORS SEE
%T IS THE TIME INCREMENT AND INTERVAL SPECIFIED, Dtotal IS
%THE FEEDFORWARD PORTION
T=0:.02:20;
Dtotal=[0 0 0 0 0 0]';
[y,x]=impulse(Asort,Btotal,Ctotal,Dtotal,4,T);
%CONVERT THE TIME HISTORY STATE MATRIX x TO GENERALIZED COORD
%Q1 AND Q2 ASSOCIATED WITH THE LOS OF NODE 1
COUNTER=1:length(T);
WW=[1 0 0 0 0 0 0 0 0 0 0 0];
WX=[0 1 0 0 0 0 0 0 0 0 0 0];
Q1=WW*U*(x(COUNTER,(1:12)))';
Q2=WX*U*(x(COUNTER,(1:12)))';
V1=WW*U*(x(COUNTER,(13:24)))';
V2=WX*U*(x(COUNTER,(13:24)))';
VELOCITY=sqrt(V1.^2 + V2.^2);
RADIUS=sqrt(Q1.^2 + Q2.^2);
ANGLE=atan2(Q2,Q1);
%INITIAL SCREENING CALCULATIONS, FIRST TWO MOMENTS OF
%RAD AND ANGLE ACROSS TOTAL TIME (NOT ERGODIC) APPLIED ONLY
%WHEN NO NOISE APPLIED
%RADMEAN=mean(RADIUS);
%RADSTD=std(RADIUS);
%FOLLOWING CODE HELPS RELATE SPATIAL EVECTS OF VARIANCE
%CONVERTING POSITION ANGLE TO BE BETWEEN 0 AND 2PI
%for p=1:length(ANGLE)
%   if ANGLE(p)<0
%       ANGLE(p)=ANGLE(p) + 2*pi;
%   end
%end
%ANGMEAN=mean(ANGLE);
%ANGSTD=std(ANGLE);
%%INITIALIZES COUNTER TO ZERO
%%   if j==1
%%      RAD1=zeros(4,length(RADIUS));
%%      ANG1=zeros(4,length(ANGLE));
%%      QUAD1=zeros(4,length(ANGLE));
%%      RADTOTAL=zeros(RAD1);
%%      ANGTOTAL=zeros(ANG1);
%%      QUADTOTAL=zeros(QUAD1);
%%      RADSQUARED=zeros(RAD1);
%       zero out the tr(j) used for each noise setting
%%   end
%%DIVIDING THE ANGLE AND RADIUS INTO QUADRANTS 1 THRU 4
%%   for k=1:LENGTH(ANGLE)
%%      if ANGLE(k)>3*pi/2
%%          RAD1(4,k)=RADIUS(k);
```

F-7

```
%%          ANG1(4,k)=ANGLE(k);
%%          QUAD1(4,k)=1;
%%      else if ANGLE(k)>pi
%%          RAD1(3,k)=RADIUS(k);
%%          ANG1(3,k)=ANGLE(k);
%%          QUAD1(3,k)=1;
%%      else if ANGLE(k)>pi/2
%%          RAD1(2,k)=RADIUS(k);
%%          ANG1(2,k)=ANGLE(k);
%%          QUAD1(2,k)=1;
%%          else
%%            RAD1(1,k)=RADIUS(k);
%%            ANG1(1,k)=ANGLE(k);
%%            QUAD1(1,k)=1;
%%          end
%%      end
%% end
%%RADTOTAL=RADTOTAL+RAD1;
%%RADSQUARED=RADSQUARED+RAD1.^2;
%%ANGTOTAL=ANGTOTAL+ANG1;
%%QUADTOTAL=QUADTOTAL+QUAD1;
%CALCULATE A MOVING AVERAGE FOR EACH CONRTOLLER AT
%EACH NOISE LEVEL. STATISTIC ARE THEN CALCULATED FOR
%THE MOVING AVERAGE
flag=0;
if flag==0
for k=927:-1:2
  ma(k)=mean(RADIUS(:,(k:k+74)));
if flag==0 & .05-ma(k)<=.002 ,%criteria
%
%IF THE NEW Btotal IS USED CHANGE THE ABOVE .05 TO SOME
%NUMBER BEWTEEN .01 AND .005 AS LESS ENERGY IS APPLIED
%
    if k<=926
      tr=(k+38)*.02;   ,%midpoint
%      Vavg=mean(VELOCITY(:,(k:k+74)));
    else
      tr=25;
%      Vavg=25;
    end
      flag=1;
end
end
end
eval(['COMB',int2str(i),'(qc,j)=tr;'])
%THIS end GOES BACK TO THE NOISE LOOP COUNTER j
end
%THIS end GOES BACK TO THE Qc LOOP COUNTER qc
end
%SAVES SEPARATE VARIABLE FOR EACH COMBINATION
eval(['save ','COMB',int2str(i),' COMB',int2str(i)])
%INITIALIZING AN OVERALL VARIABLE SCREEN210
%TO HOLD ALL OF THE INFORMATION GENERATED
%if i==1
```

```
%   SCREEN210=zeros(6,210);
%end
%eval(['SCREEN210(1,',int2str(i),')= tr ;'])
%eval(['SCREEN210(2,',int2str(i),')= Vavg ;'])
%eval(['SCREEN210(3,',int2str(i),')= RADMEAN ;'])
%eval(['SCREEN210(4,',int2str(i),')= RADSTD ;'])
%eval(['SCREEN210(5,',int2str(i),')= ANGMEAN ;'])
%eval(['SCREEN210(6,',int2str(i),')= ANGSTD ;'])
%%SETTING ANY ZERO ENTRIES OF QUADTOTAL TO 1 SO AS TO
%%AVOID DIVIDING BY ZERO. QUOTIENT STILL ZERO SINCE NUM WILL
%%BE ZERO. ALSO MUST AVOID TAKING THE LOG OF ZERO
%%for p=1:4
%%   for k=1:length(QUADTOTAL)
%%     if QUADTOTAL(p,k)==0
%%       QUADTOTAL(p,k)=1;
%%       RAD_SN(p,k)=0;
%%     else
%%       RAD_SN(p,k)=-10*log(RADSQUARED(p,k)/QUADTOTAL(p,k));
%%     end
%%   end
%%end
%%FINDING MEASURE OF PERFORMANCE
%%ANG_MEAN=ANGTOTAL./QUADTOTAL;
%%RAD_MEAN=RADTOTAL./QUADTOTAL;
%%RAD_VAR=RADSQUARED./QUADTOTAL -RAD_MEAN.^2;
%%eval(['save ','RAD_MEAN',int2str(i),' RAD_MEAN']);
%%eval(['save ','RAD_VAR',int2str(i),' RAD_VAR']);
%%eval(['save ','RAD_SN',int2str(i),' RAD_SN']);
%%eval(['save ','ANG_MEAN',int2str(i),' ANG_MEAN']);
%clear RAD_MEAN RAD_VAR RAD_SN ANG_MEAN
%clear ANGTOTAL QUADTOTAL RADTOTAL RADSQUARED RAD1 ANG1 QUAD1
%clear Ctotal Asort x y Q1 Q2 V1 V2 ANGLE RADIUS
%%THIS end GOES BACK TO SELECT ANOTHER CONTROLLER ARRANGEMENT
end
%save SCREEN210 SCREEN210
```

Appendix G

Regression Results

Table G-1

SCREENING DESIGN FOR Q_{of} and Q_{oc} ARR 126-47-358

GROUP 1	ξ_1	STATE WEIGHTING COEFF. CONTROLLER GAIN
GROUP 2	ξ_2	STATE WEIGHTING COEFF. ESTIMATOR GAIN
GROUP 1^2	ξ_{11}	
GROUP 12	ξ_{12}	
GROUP 2^2	ξ_{22}	
GROUP $1^2 2$	ξ_{112}	
GROUP 12^2	ξ_{122}	
GROUP $1^2 2^2$	ξ_{1122}	

USED 3^2 FULL FACTORIAL   9 RUNS x NOISE

SIGNIFICANT GROUPS 1, 2 AND 12   (F=159,120,37)

LACK OF FIT $(F = 1.4(10^{-26}))$

EXPERIMENTAL DESIGN MATRIX Z

ξ_1	ξ_2	$3\xi_{11}-2$	ξ_{12}	$3\xi_{22}-2$	$(3\xi_{11}-2)\xi_2$	$(3\xi_{22}-2)\xi_1$	$(3\xi_{22}-2)\times(3\xi_{11}-2)$
-1	-1	1	1	1	-1	-1	1
0	-1	-2	0	1	2	0	-2
1	-1	1	-1	1	-1	1	1
-1	0	1	0	-2	0	2	-2
0	0	-2	0	-2	0	0	4
1	0	1	0	-2	0	-2	-2
-1	1	1	-1	1	1	-1	1
0	1	-2	0	1	-2	0	-2
1	1	1	1	1	1	1	1

ANOVA FOR Q_{of} AND Q_{oc} SCREENING
MEAN RESPONSE ARR 126-47-358

	MEAN	GROUP 1	GROUP 2	GROUP 1^2
SS	6.7030e+03	2.1942e+01	1.6653e+01	1.1574e-01
df	1.0000e+00	1.0000e+00	1.0000e+00	1.0000e+00
MS	6.7030e+03	2.1942e+01	1.6653e+01	1.1574e-01
F	4.8628e+04	1.5918e+02	1.2081e+02	8.3965e-01
θ	5.2521e+00	-3.6802e-01	-3.2062e-01	1.5432e-02

	GROUP 12	GROUP 2^2	GROUP $1^2 2$	GROUP 12^2
SS	5.0700e+00	8.4807e-02	1.2346e+00	1.9753e-03
df	1.0000e+00	1.0000e+00	1.0000e+00	1.0000e+00
MS	5.0700e+00	8.4807e-02	1.2346e+00	1.9753e-03
F	3.6781e+01	6.1524e-01	8.9563e+00	1.4330e-02
θ	-2.1667e-01	-1.3210e-02	6.1728e-02	2.4691e-03

	GROUP $1^2 2^2$	LACK FIT	PURE ERROR	TOTAL
SS	2.8624e-01	1.9382e-27	3.2255e+01	6.7807e+03
df	1.0000e+00	1.0000e+00	2.3400e+02	2.4300e+02
MS	2.8624e-01	1.9382e-27	1.3784e-01	2.7904e+01
F	2.0765e+00	1.4061e-26	0	0
θ	1.7160e-02	0	0	5.2521e+00

SIGNAL-TO-NOISE ARR 126-47-358

	MEAN	GROUP 1	GROUP 2	GROUP 1^2
SS	4.1609e+03	5.7928e-01	4.5764e-01	2.0349e-03
df	1.0000e+00	1.0000e+00	1.0000e+00	1.0000e+00
MS	4.1609e+03	5.7928e-01	4.5764e-01	2.0349e-03
F	not applicable: 9 coefficients for 9 data points			
θ	-2.1502e+01	3.1072e-01	2.7618e-01	-1.0633e-02

	GROUP 12	GROUP 2^2	GROUP $1^2 2$	GROUP 12^2
SS	1.5193e-01	4.0050e-03	2.8526e-02	1.5059e-05
df	1.0000e+00	1.0000e+00	1.0000e+00	1.0000e+00
MS	1.5193e-01	4.0050e-03	2.8526e-02	1.5059e-05
F	**	**	**	**
θ	1.9489e-01	1.4916e-02	-4.8756e-02	1.1202e-03

	GROUP $1^2 2^2$	LACK FIT	TOTAL
SS	7.9895e-03	**	4.1621e+03
df	1.0000e+00	**	9.0000e+00
MS	7.9895e-03	**	4.6245e+02
F	**	**	0
θ	-1.4897e-02	**	-2.1502e+01

Table G-3

SCREENING DESIGN FOR Q_{oc} and R_{oc} ARR 126-47-358

GROUP 1	ξ_1	STATE WEIGHTING COEFF. CONTROLLER GAIN
GROUP 2	ξ_2	CONTROL WEIGHTING COEFF. CONTROLLER GAIN
GROUP 1^2	ξ_{11}	
GROUP 12	ξ_{12}	
GROUP 2^2	ξ_{22}	
GROUP $1^2 2$	ξ_{112}	
GROUP 12^2	ξ_{122}	
GROUP $1^2 2^2$	ξ_{1122}	

USED 3^2 FULL-ORDER   9 RUNS x NOISE

SIGNIFICANT GROUPS 1, 2 AND 12   (F=1371,1407,345)

LACK OF FIT   (F=2.3(10^{-25}))

EXPERIMENTAL DESIGN MATRIX Z

ξ_1	ξ_2	$3\xi_{11}-2$	ξ_{12}	$3\xi_{22}-2$	$(3\xi_{11}-2)\xi_2$	$(3\xi_{22}-2)\xi_1$	$(3\xi_{22}-2)\times(3\xi_{11}-2)$
-1	-1	1	1	1	-1	-1	1
0	-1	-2	0	1	2	0	-2
1	-1	1	-1	1	-1	1	1
-1	0	1	0	-2	0	2	-2
0	0	-2	0	-2	0	0	4
1	0	1	0	-2	0	-2	-2
-1	1	1	-1	1	1	-1	1
0	1	-2	0	1	-2	0	-2
1	1	1	1	1	1	1	1

Table G-4

ANOVA FOR Q_{oc} AND R_{oc} SCREENING
MEAN RESPONSE ARR 126-47-358

	MEAN	GROUP 1	GROUP 2	GROUP 1^2
SS	3.3169e+04	2.0299e+02	2.0826e+02	3.0658e-02
df	1.0000e+00	1.0000e+00	1.0000e+00	1.0000e+00
MS	3.3169e+04	2.0299e+02	2.0826e+02	3.0658e-02
F	2.2407e+05	1.3713e+03	1.4069e+03	2.0710e-01
θ	1.1683e+01	-1.1194e+00	1.1338e+00	7.9424e-03

	GROUP 12	GROUP 2^2	GROUP $1^2 2$	GROUP 12^2
SS	5.1143e+01	3.2253e-01	1.9497e+01	1.7269e+01
df	1.0000e+00	1.0000e+00	1.0000e+00	1.0000e+00
MS	5.1143e+01	3.2253e-01	1.9497e+01	1.7269e+01
F	3.4549e+02	2.1788e+00	1.3171e+02	1.1666e+02
θ	6.8815e-01	-2.5761e-02	-2.4531e-01	2.3086e-01

	GROUP $1^2 2^2$	LACK FIT	PURE ERROR	TOTAL
SS	4.3506e+01	3.3312e-26	3.4639e+01	3.3747e+04
df	1.0000e+00	1.0000e+00	2.3400e+02	2.4300e+02
MS	4.3506e+01	3.3312e-26	1.4803e-01	1.3888e+02
F	2.9390e+02	2.2504e-25	0	0
θ	2.1156e-01	0	0	1.1683e+01

SIGNAL-TO-NOISE ARR 126-47-358

	MEAN	GROUP 1	GROUP 2	GROUP 1^2
SS	5.6030e+03	1.1375e+00	1.1774e+00	1.0033e-04
df	1.0000e+00	1.0000e+00	1.0000e+00	1.00C0e+00
MS	5.6030e+03	1.1375e+00	1.1774e+00	1.0033e-04
F	not applicable: 9 coefficients for 9 data points			
θ	-2.4951e+01	4.3542e-01	-4.4298e-01	-2.3609e-03

	GROUP 12	GROUP 2^2	GROUP $1^2 2$	GROUP 12^2
SS	3.1281e-01	2.4659e-03	1.0867e-01	9.2076e-02
df	1.0000e+00	1.0000e+00	1.0000e+00	1.0000e+00
MS	3.1281e-01	2.4659e-03	1.0867e-01	9.2076e-02
F	**	**	**	**
θ	-2.7965e-01	1.1705e-02	9.5163e-02	-8.7596e-02

	GROUP $1^2 2^2$	LACK FIT	TOTAL
SS	2.5324e-01	**	5.6061e+03
df	1.0000e+00	**	9.0000e+00
MS	2.5324e-01	**	6.2290e+02
F	**	**	0
θ	-8.3872e-02	**	-2.4951e+01

Table G-5

GROUP SCREEN DESIGN FOR CONTROLLER GAIN

GROUP 1 ξ_1 SUBCONTROLLER 1 POSITION   3 MODES

GROUP 2 ξ_2 SUBCONTROLLER 1 VELOCITY   3 MODES

GROUP 3 ξ_3 SUBCONTROLLER 2 POSITION   2 MODES

GROUP 4 ξ_4 SUBCONTROLLER 2 VELOCITY   2 MODES

GROUP 5 ξ_5 SUBCONTROLLER 3 POSITION   3 MODES

GROUP 6 ξ_6 SUBCONTROLLER 3 VELOCITY   3 MODES

USED 2^{6-2}_{iv} FRACTIONAL   3x16 RUNS x NOISE

BEST COMBINATION 126-45-358

SIGNIFICANT GROUPS 2 AND 6   (F=10,110)

LACK OF FIT   (F=.88)

EXPERIMENTAL DESIGN MATRIX Z

ξ_1	ξ_2	ξ_3	ξ_4	ξ_5	ξ_6
-1	-1	-1	-1	-1	-1
1	-1	-1	-1	1	-1
-1	1	-1	-1	1	1
1	1	-1	-1	-1	1
-1	-1	1	-1	1	1
1	-1	1	-1	-1	1
-1	1	1	-1	-1	-1
1	1	1	-1	1	-1
-1	-1	-1	1	-1	1
1	-1	-1	1	1	1
-1	1	-1	1	1	-1
1	1	-1	1	-1	-1
-1	-1	1	1	1	-1
1	-1	1	1	-1	-1
-1	1	1	1	-1	1
1	1	1	1	1	1

Table G-6

ANOVA FOR CONTROLLER GAIN GROUP SCREEN
MEAN RESPONSE ARR 126-47-358

	MEAN	GROUP 1	GROUP 2	GROUP 3
SS	1.3343e+04	2.9668e-02	4.8669e-01	2.0833e-04
df	1.0000e+00	1.0000e+00	1.0000e+00	1.0000e+00
MS	1.3343e+04	2.9668e-02	4.8669e-01	2.0833e-04
F	2.7478e+05	6.1094e-01	1.0022e+01	4.2901e-03
θ	5.5576e+00	8.2870e-03	-3.3565e-02	-6.9444e-04

	GROUP 4	GROUP 5	GROUP 6
SS	4.1565e-03	1.2245e-02	5.3734e+00
df	1.0000e+00	1.0000e+00	1.0000e+00
MS	4.1565e-03	1.2245e-02	5.3734e+00
F	8.5593e-02	2.5217e-01	1.1065e+02
θ	-3.1019e-03	-5.3241e-03	-1.1153e-01

	LACK FIT	PURE ERROR	TOTAL
SS	3.8628e-01	2.0201e+01	1.3370e+04
df	9.0000e+00	4.1600e+02	4.3200e+02
MS	4.2920e-02	4.8561e-02	3.0949e+01
F	8.8384e-01	0	0
θ	0	0	5.5576e+00

SIGNAL-TO-NOISE ARR 126-47-358

	MEAN	GROUP 1	GROUP 2	GROUP 3
SS	1.3657e+04	2.0579e-03	4.4054e-02	4.0439e-05
df	1.0000e+00	1.0000e+00	1.0000e+00	1.0000e+00
MS	1.3657e+04	2.0579e-03	4.4054e-02	4.0439e-05
F	3.5846e+06	5.4013e-01	1.1563e+01	1.0614e-02
θ	-2.9216e+01	-1.1341e-02	5.2473e-02	1.5898e-03

	GROUP 4	GROUP 5	GROUP 6
SS	3.0570e-04	1.2396e-03	4.5181e-01
df	1.0000e+00	1.0000e+00	1.0000e+00
MS	3.0570e-04	1.2396e-03	4.5181e-01
F	8.0236e-02	3.2534e-01	1.1859e+02
θ	4.3711e-03	8.8018e-03	1.6804e-01

	LACK FIT	TOTAL
SS	3.4290e-02	1.3658e+04
df	9.0000e+00	1.6000e+01
MS	3.8100e-03	8.5362e+02
F	0	0
θ	0	-2.9216e+01

Table G-7

INDIVIDUAL SCREEN DESIGN FOR CONTROLLER GAIN

(1 ARRANGEMENT, SET GROUPS TO MIN VARIANCE)

FACTOR 1	ξ_1	SUBCONTROLLER 1 VELOCITY MODE 1
FACTOR 2	ξ_2	SUBCONTROLLER 1 VELOCITY MODE 2
FACTOR 3	ξ_3	SUBCONTROLLER 1 VELOCITY MODE 6
FACTOR 4	ξ_4	SUBCONTROLLER 3 VELOCITY MODE 3
FACTOR 5	ξ_5	SUBCONTROLLER 3 VELOCITY MODE 5
FACTOR 6	ξ_6	SUBCONTROLLER 3 VELOCITY MODE 8

USED 2_{iv}^{6-2} FRACTIONAL $\qquad$ 16 RUNS x NOISE

WITH CENTER POINTS

SIGNIFICANT FACTORS 4 AND 6 $\qquad$ (F=50,56)

NOT SIGNIFICANT, BUT INCLUDED FACTOR 2 $\qquad$ (F=1.6)

LACK OF FIT CROSS TERMS $(F_{.10} = 1.63)$ $\qquad$ (F=3.4)

LACK OF FIT QUADRATIC TERMS $(F_{.10} = 2.71)$ $\qquad$ (F=1.8)

EXPERIMENTAL DESIGN MATRIX Z

ξ_1	ξ_2	ξ_3	ξ_4	ξ_5	ξ_6
-1	-1	-1	-1	-1	-1
1	-1	-1	-1	1	-1
-1	1	-1	-1	1	1
1	1	-1	-1	-1	1
-1	-1	1	-1	1	1
1	-1	1	-1	-1	1
-1	1	1	-1	-1	-1
1	1	1	-1	1	-1
-1	-1	-1	1	-1	1
1	-1	-1	1	1	1
-1	1	-1	1	1	-1
1	1	-1	1	-1	-1
-1	-1	1	1	1	-1
1	-1	1	1	-1	-1
-1	1	1	1	-1	1
1	1	1	1	1	1
0	0	0	0	0	0

Table G-8

ANOVA FOR CONTROLLER GAIN INDIVIDUAL SCREEN
MEAN RESPONSE ARR 126-47-358 .

CONTROLLER 1 VELOCITY

	MEAN	MODE 1	MODE 2	MODE 6
SS	1.3392e+04	1.0800e-02	5.1570e-02	8.1815e-03
df	1.0000e+00	1.0000e+00	1.0000e+00	1.0000e+00
MS	1.3392e+04	1.0800e-02	5.1570e-02	8.1815e-03
F	4.1637e+05	3.3578e-01	1.6033e+00	2.5437e-01
θ	5.5678e+00	5.0000e-03	-1.0926e-02	-4.3519e-03

CONTROLLER 3 VELOCITY

	MODE 3	MODE 5	MODE 8
SS	1.6084e+00	3.0000e-04	1.8148e+00
df	1.0000e+00	1.0000e+00	1.0000e+00
MS	1.6084e+00	3.0000e-04	1.8148e+00
F	5.0007e+01	9.3271e-03	5.6423e+01
θ	-6.1019e-02	-8.3333e-04	-6.4815e-02

LACK OF FIT

	CROSS PROD	PURE QUAD	PURE ERROR	TOTAL
SS	9.9502e-01	5.8008e-02	1.4217e+01	1.3411e+04
df	9.0000e+00	1.0000e+00	4.4200e+02	4.5900e+02
MS	1.1056e-01	5.8008e-02	3.2164e-02	2.9218e+01
F	3.4373e+00	1.8035e+00	0	0
θ	0	0	0	5.5678e+00

SIGNAL-TO-NOISE ARR 126-47-358

CONTROLLER 1 VELOCITY

	MEAN	MODE 1	MODE 2	MODE 6
SS	1.3671e+04	7.9481e-04	5.1101e-03	9.8009e-04
df	1.0000e+00	1.0000e+00	1.0000e+00	1.0000e+00
MS	1.3671e+04	7.9481e-04	5.1101e-03	9.8009e-04
F	1.4216e+06	8.2649e-02	5.3139e-01	1.0192e-01
θ	-2.9231e+01	-7.0481e-03	1.7871e-02	7.8266e-03

CONTROLLER 3 VELOCITY

	MODE 3	MODE 5	MODE 8
SS	1.3469e-01	8.9692e-05	1.5108e-01
df	1.0000e+00	1.0000e+00	1.0000e+00
MS	1.3469e-01	8.9692e-05	1.5108e-01
F	1.4006e+01	9.3267e-03	1.5710e+01
θ	9.1752e-02	2.3676e-03	9.7173e-02

	LACK FIT	TOTAL
SS	8.6550e-02	1.3671e+04
df	9.0000e+00	1.6000e+01
MS	9.6166e-03	8.5445e+02
F	0	0
θ	0	-2.9231e+01

Table G-9

CONTROLLER GAIN INTERACTION DESIGN

(OTHER FACTOR SET TO MINIMIZE VARIANCE)

FACTOR 1 ξ_1 SUBCONTROLLER 1 VELOCITY MODE 2

FACTOR 2 ξ_2 SUBCONTROLLER 3 VELOCITY MODE 3

FACTOR 3 ξ_3 SUBCONTROLLER 3 VELOCITY MODE 8

FACTOR 12 ξ_{12}

FACTOR 13 ξ_{13}

FACTOR 23 ξ_{23}

USED FULL FACTORIAL   8 RUNS x NOISE

SIGNIFICANT TERMS 2 3 AND 23 $(F=29,20,14)$

LACK OF FIT $(F=.64)$

$$\text{TIME}_R = 5.5669 - .05676 Q_{V3} - .0475 Q_{V8} - .0397 Q_{V3} Q_{V8}$$

EXPERIMENTAL DESIGN MATRIX Z

ξ_1	ξ_2	ξ_3	ξ_{12}	ξ_{13}	ξ_{23}
-1	-1	-1	1	1	1
1	-1	-1	-1	-1	1
-1	1	-1	-1	1	-1
1	1	-1	1	-1	-1
-1	-1	1	1	-1	-1
1	-1	1	-1	1	-1
-1	1	1	-1	-1	1
1	1	1	1	1	1

Table G-10

ANOVA FOR CONTROLLER GAIN INTERACTION
MEAN RESPONSE ARR 126-47-358

	MEAN	MODE ?	MODE 3	MODE 8
SS	6.6940e+03	4.0017e-02	6.9587e-01	4.8735e-01
df	1.0000e+00	1.0000e+00	1.0000e+00	1.0000e+00
MS	6.6940e+03	4.0017e-02	6.9587e-01	4.8735e-01
F	2.7969e+05	1.6720e+00	2.9075e+01	2.0363e+01
θ	5.5669e+00	-1.3611e-02	-5.6759e-02	-4.7500e-02

		CROSS 2-3	CROSS 2-8	CROSS 3-8
SS		1.6713e-02	1.8150e-02	3.4082e-01
df		1.0000e+00	1.0000e+00	1.0000e+00
MS		1.6713e-02	1.8150e-02	3.4082e-01
F		6.9831e-01	7.5836e-01	1.4240e+01
θ		-8.7963e-03	-9.1667e-03	-3.9722e-02

		LACK FIT	PURE ERROR	TOTAL
SS		1.5335e-02	4.9781e+00	6.7006e+03
df		1.0000e+00	2.0800e+02	2.1600e+02
MS		1.5335e-02	2.3933e-02	3.1021e+01
F		0	0	0
θ		0	0	5.5669e+00

SIGNAL-TO NOISE ARR 126-47-358

	MEAN	MODE 2	MODE 3	MODE 8
SS	6.8344e+03	3.6282e-03	5.8972e-02	4.0888e-02
df	1.0000e+00	1.0000e+00	1.0000e+00	1.0000e+00
MS	6.8344e+03	3.6282e-03	5.8972e-02	4.0888e-02
F	4.8434e+06	2.5712e+00	4.1793e+01	2.8977e+01
θ	-2.9228e+01	2.1296e-02	8.5858e-02	7.1492e-02

		CROSS 2-3	CROSS 2-8	CROSS 3-8
SS		1.5391e-03	1.6650e-03	2.8344e-02
df		1.0000e+00	1.0000e+00	1.0000e+00
MS		1.5391e-03	1.6650e-03	2.8344e-02
F		1.0908e+00	1.1799e+00	2.0087e+01
θ		1.3871e-02	1.4426e-02	5.9523e-02

			LACK FIT	TOTAL
SS			1.4111e-03	6.8345e+03
df			1.0000e+00	8.0000e+00
MS			1.4111e-03	8.5431e+02
F			0	0
θ			0	-2.9228e+01

Bibliography

1. Box, George E.P. and Norman R. Draper. <u>Empirical Model-Building and Response Surfaces</u>. New York: John Wiley and Sons, 1987.

2. Calico, Robert A. and Eastep, Franklin E. "Structural Design and Decoupled Control," <u>Acta Astronautica</u>, 19: 9-15 (1989).

3. Calico, Robert A. and Hinrichsen, R.L. "The Effects of Structural Pertubations on Decoupled Control," <u>Proceedings of the Second International Symposium on Space Flight Dynamics</u>. ESA-SP-255. Netherlands, 1987

4. Carignan, Craig R. and Wallace E. Vander Velde. "Number and Placement of Control System Components Considering Possible Failures," March 1982. NASA-CR-168988. Massachusetts Institute of Technology (N82-25277).

5. Connor, W.S. and Zelen, M. "Fractional Factorial Experiment Designs for Experiments with Factors at Three Levels," National Bureau of Standards, Applied Math Series No. 54. May 1959

6. Franklin, Gene F. and others. <u>Feedback Control of Dynamic Systems</u>. Reading Massachusetts: Addison-Wesley Publishing Company, 1986.

7. Meirovitch, Leonard. <u>Elements of Vibration Analysis</u> (Second Edition). New York: McGraw-Hill Book Company, 1986.

8. Mercadal, Mathieu. "Survey on Large Scale System Control Methods," 25 November 1987. NASA-CR-181556. Massachusetts Institute of Technology (N88-13374).

9. Ridgely, Capt Brent D. and Siva S. Banda. <u>Introduction to Robust Multivariable Control</u>. Report AFWAL-TR-85-3102. Air Force Wright Aeronautical Laboratories, Wright-Patterson AFB OH, February 1986 (AD-A165891).

10. Ross, Phillip J. <u>Taguchi Techniques for Quality Engineering</u>. New York: McGraw-Hill Book Company, 1988.

11. Sumner, Jonathan B. <u>Modal Assignment Effects on Decentralized Control of a Large Space Structure</u>. MS Thesis, AFIT/GA/AA/85D-9. School of Engineering, Air Force Institute of Technology (AU), Wright-Patterson AFB OH, December 1985.

Vita

Jeb Ewell Brewer ██.
██

I████████████████████ He graduated from Ames Senior High

School, Ames, Iowa in 1980 and attended Iowa State University

from which he received the degree of Bachelor of Science in

Civil Engineering in May 1985. Upon graduation, he received

a reserve commission in the United States Air Force through

Air Force ROTC. After commissioning he was assigned to the

44th Civil Engineering Squadron, Ellsworth AFB, South Dakota

as a design engineer and later as Chief of Readiness. In

June 1988 he entered the School of Engineering, Air Force

Institute of Technology. He is married to the former████

████████████ and together they have two children,

████████████████

████████████████████

████ Iowa 50010.

REPORT DOCUMENTATION PAGE

1a. REPORT SECURITY CLASSIFICATION UNCLASSIFIED	1b. RESTRICTIVE MARKINGS		
2a. SECURITY CLASSIFICATION AUTHORITY	3. DISTRIBUTION/AVAILABILITY OF REPORT Approved for public release; distribution unlimited		
2b. DECLASSIFICATION/DOWNGRADING SCHEDULE			
4. PERFORMING ORGANIZATION REPORT NUMBER(S) AFIT/GA/ENY/90M-1	5. MONITORING ORGANIZATION REPORT NUMBER(S)		

6a. NAME OF PERFORMING ORGANIZATION School of Engineering	6b. OFFICE SYMBOL (If applicable) AFIT/EN	7a. NAME OF MONITORING ORGANIZATION
6c. ADDRESS (City, State, and ZIP Code) Air Force Institue of Technology Wright-Patterson AFB, OH 45433		7b. ADDRESS (City, State, and ZIP Code)

8a. NAME OF FUNDING/SPONSORING ORGANIZATION	8b. OFFICE SYMBOL (If applicable)	9. PROCUREMENT INSTRUMENT IDENTIFICATION NUMBER		

8c. ADDRESS (City, State, and ZIP Code)	10. SOURCE OF FUNDING NUMBERS			
	PROGRAM ELEMENT NO.	PROJECT NO.	TASK NO	WORK UNIT ACCESSION NO.

11. TITLE (Include Security Classification)
Statistical Techniques for Designing a Decoupled Controller to be Robust to Model and Sensor Noise

12. PERSONAL AUTHOR(S)
Jeb E. Brewer, Capt USAF

13a. TYPE OF REPORT MS Thesis	13b. TIME COVERED FROM _____ TO _____	14. DATE OF REPORT (Year, Month, Day) 1990 March	15. PAGE COUNT 139

16. SUPPLEMENTARY NOTATION

17. COSATI CODES			18. SUBJECT TERMS (Continue on reverse if necessary and identify by block number)
FIELD	GROUP	SUB-GROUP	large flexible space structures, CSDL I, modal analysis, signal-to-noise ratios, orthogonal experiments, decoupled control
13	13		

19. ABSTRACT (Continue on reverse if necessary and identify by block number)

see reverse

Title: Statistical Techniques for Designing a Decoupled Controller to be Robust
to Model and Sensor Noise

Advisor: Major David G. Robinson, PhD

20. DISTRIBUTION/AVAILABILITY OF ABSTRACT ☒ UNCLASSIFIED/UNLIMITED ☐ SAME AS RPT ☐ DTIC USERS	21. ABSTRACT SECURITY CLASSIFICATION UNCLASSIFIED	
22a. NAME OF RESPONSIBLE INDIVIDUAL Major David G. Robinson, USAF	22b. TELEPHONE (Include Area Code) 513-255-2362	22c. OFFICE SYMBOL AFIT/ENY

DD Form 1473, JUN 86 Previous editions are obsolete.

Block 19.(continued) Abstract

This investigation developed and tested statistical design methods for configuring a robust decoupled controller on a lightly damped structure. The test model used was a lumped mass finite element representation of the Charles Stark Draper Laboratory Model I (CSDL-I). The decoupled control methods consisted of a system of three individual subcontrollers designed on the basis of a subset of plant dynamics with control authority enacted through the total system of structural actuators. Transforms were applied to the subcontrollers to insure that dynamic coupling, called observation spillover and control spillover, didn't destabilize the global system. The decoupled controller system was designed based on only the first eight of the twelve natural frequencies (modes) for the CSDL-I. The remaining four high frequency modes were modeled as residuals.

This investigation used signal-to-noise ratios, orthogonal numerical experiments, and linear regression to efficiently probe the design space and to produce a robust control system. The measure of system performance was the structural alignment of a particular node referred to as line-of-sight (LOS). This LOS requirement simulated space vehicle requirements associated with aligning antennas, LASER beams, solar arrays, etc.

It was concluded that the techniques were efficient in configuring a decoupled controller to be robust to sensor noise and modal truncation while still maintaining adequate LOS performance. The techniques reduced the CPU time required from a possible 76,354 years for a global search to only 16.5 hours. It was also found that the robust controller used a significant amount of actuator authority and it was recommended that further work be done to expand the statistical design techniques to include actuator authority as an output metric.